NASA
National Aeronautics and
Space Administration

Lyndon B. Johnson Space Center
Houston, Texas 77058

NASA-CR-151765
19790008738

SPACE SHUTTLE
AEROTHERMODYNAMIC DATA REPORT

Data Management Services

SPACE DIVISION CHRYSLER CORPORATION

January, 1979

DMS-DR-2440
NASA CR-151,765

BASE PRESSURE AND HEAT TRANSFER TESTS OF THE 0.0225-SCALE SPACE SHUTTLE PLUME SIMULATION MODEL (19-OTS) IN YAWED FLIGHT CONDITIONS IN THE NASA-LEWIS 10x10-FOOT SUPERSONIC WIND TUNNEL (TEST IH83)

by

J. W. Foust
Shuttle Aerosciences
Rockwell International Space Systems Group

Prepared under NASA Contract Number NAS9-13247

by

Data Management Services
Chrysler Corporation Michoud Defense-Space Division
New Orleans, La. 70189

for

Engineering Analysis Division

Johnson Space Center
National Aeronautics and Space Administration
Houston, Texas

N79-16909 #

WIND TUNNEL TEST SPECIFICS:

Test Number:	LeRC 10SWT 044
NASA Series Number:	IH83
Model Number:	19-OTS
Test Dates:	January 9 through March 24, 1978
Occupancy Hours:	11 weeks

FACILITY COORDINATOR:

Paul Colarusso
Mail Stop 86-7
NASA-Lewis Research Center
21000 Brookpark Road
Cleveland, Ohio 44135

Phone: (216) 433-4000, Ext. 542

PROJECT ENGINEERS:

J. W. Foust, M. Quan
Mail Code AD38
Space Division
Rockwell International
12214 Lakewood Blvd.
Downey, CA. 90241

Phone: (213) 922-1451

Kenneth Baskin
Mail Stop 86-7
NASA-Lewis Research Center
21000 Brookpark Road
Cleveland, Ohio 44135

Phone: (216) 433-4000, Ext. 371

DATA MANAGEMENT SERVICES:

Prepared by: Operations--G. R. Lutz
Liaison--D. W. Hersey

Reviewed by: G. G. McDonald

Approved: J. L. Glynn (signature)
J. L. Glynn, Manager
Data Operations

Concurrence: J. L. Glynn (signature) FOR N. D. Kemp, Manager
Data Management Services

Chrysler Corporation Michoud Defense-Space Division assumes no responsibility for the data presented other than display characteristics.

BASE PRESSURE AND HEAT TRANSFER TESTS OF THE 0.0225-SCALE SPACE SHUTTLE PLUME SIMULATION MODEL (19-OTS) IN YAWED FLIGHT CONDITIONS IN THE NASA-LEWIS 10x10-FOOT SUPERSONIC WIND TUNNEL (TEST IH83)

by

J. W. Foust
Shuttle Aerosciences
Rockwell International Space Division

ABSTRACT

Test IH83 was conducted in the NASA-Lewis Research Center 10x10-foot Supersonic Wind Tunnel to determine pressures, heat transfer rates, and gas recovery temperatures in the base region of a rocket firing model of the Space Shuttle integrated vehicle during simulated yawed flight conditions. The objectives were (1) to measure heat transfer and pressure distributions about the orbiter, external tank (ET), and solid rocket booster (SRB) afterbody surfaces due to rocket plume recirculation and impingement and (2) to derive gas recovery temperatures in the base region using gas temperature probe measurements.

First and second stage flight of the Space Shuttle were simulated by firing the Space Shuttle main engines (SSME's) in conjunction with the SRB rocket motors or only the SSME's into the continuous tunnel airstream. The Space Shuttle model rocket engines operated at one-half of full-scale pressure due to design heating limitations; for the correct rocket plume environment, the simulated altitude pressures were halved

ABSTRACT (Concluded)

to maintain the rocket chamber/altitude pressure ratio. Tunnel freestream Mach numbers from 2.2 to 3.5 were simulated over an altitude range of 60 to 130 thousand feet with varying angle of attack, yaw angle, nozzle gimbal angle and SRB chamber pressure.

All objectives of test IH83 were fulfilled. Twenty-four runs were obtained to support the first objective, and nine runs were obtained to support the second objective.

Tabulated heat transfer and pressure data are not presented with this report; information for obtaining these data is in Appendix A.

Gas recovery temperature data derived from the nine gas temperature probe runs are presented in Appendix B.

The model configuration, instrumentation, test procedures, and data reduction are described in this report.

TABLE OF CONTENTS

TABLE OF CONTENTS (Concluded)

INDEX OF MODEL FIGURES

INDEX OF MODEL FIGURES (Continued)

INDEX OF MODEL FIGURES (Concluded)

INTRODUCTION

Not being a conventional rocket launch vehicle, the Space Shuttle, with its solid rocket boosters and/or orbiter main engines (SSME's) operating during first and second stage ascent, experiences complex heating and pressure conditions in the base regions due to rocket plume interaction in the presence of the surrounding airstream. These complex conditions are partly attributed to various yaw attitudes required along the Space Shuttle ascent flight trajectory. Since analytical methods are not available to adequately define these heating rates and pressures, they must be determined experimentally. The experimental data will assist the design of thermal protection for the Space Shuttle vehicle bases.

This investigation, test IH83, was undertaken to measure heating rates and pressures and to determine gas recovery temperatures on a scaled model of the Space Shuttle vehicle during yawed flight conditions with firing rocket engines, orbiter and SRB, simulating plume recirculation and impingement in an atmospheric environment. Thirty-three runs were obtained at various Mach numbers and altitudes with model yaw and other model parameters varying to simulate numerous Space Shuttle ascent flight trajectory conditions. The model parameters included angle of attack, SRB chamber pressure, and nozzle gimbal angle. The results of the investigation are presented in this report.

NOMENCLATURE

PLOT SYMBOL	MNEMONIC	DEFINITION
TUNNEL PARAMETERS (FREESTREAM)		
h	ALTITUDE or ALTB	model altitude, ft.
H_O	HOB	stagnation pressure, psfa
M	MACH NO. or MOB	Mach number
P	POB	static pressure, psfa
q	QOB	dynamic pressure, psf
R_e	REB	Reynolds number, 1/ft.
T	TOB	static temperature, °R
T_O	TTBMB	stagnation temperature, °R
ρ	DENSB	density, slugs/ft.^{3}
γ	GAMB	specific heat ratio
MODEL PARAMETERS		
α	ALPHA or ALPHAB	angle-of-attack, degrees
ψ	YAW ANGLE	model yaw angle, degrees
δ_{E_I}	ELEVON CONF.	inboard elevon deflection, degrees
δ_{E_O}	ELEVON CONF.	outboard elevon deflection, degrees
	S.S.M.E. CONF.	SSME gimbal angles, degrees
	S.R.B. CONF.	SRB gimbal angles, degrees

NOMENCLATURE (Continued)

PLOT SYMBOL	MNEMONIC	DEFINITION
DATA PARAMETERS		
a		curve fit coefficient
c		specific heat of the thin-film gauge substrate, BTU/lbm-°F
	E8XX	event market, milliseconds
	E901	autovalve marker, milliseconds
E_{AVD}		recording system voltage, volts
E_X		regulated power supply voltage, volts
ΔE		measured voltage change, volts
ΔEc		corrected voltage change, volts
GAIN		amplifier gain
i		iteration variable
k		thermal conductivity of the thin-film gauge substrate, BTU/ft-sec-°F
K_B		thin-film gauge sensitivity at elevated temperature, Ohms/°F
K_C		thin-film gauge calibration sensitivity, Ohms/°F
K_{70}		thin-film gauge sensitivity at 70°F, Ohms/°F
m		curve fit order
n		number of time intervals from o to t
P_A	P	absolute pressure, psia
P_G		measured gauge pressure, psi
P_R		steady state reference pressure psia

PLOT SYMBOL	MNEMONIC	DEFINITION
DATA PARAMETERS (continued)		
P_{7xx}	P7XX	absolute model operating pressure, psia
$\dot{q}_{AVG}$	Q	average heating rate, BTU/ft^2-sec
$\dot{q}$		variable heating rate, BTU/ft^2-sec
$\dot{q}_R$	QR	incident radiant heating rate, BTU/ft^2-sec
$\dot{q}'_R$		measured radiant heating rate, BTU/ft^2-sec
R_C		thin-film gauge calibration resistance, Ohms
R_{GA}		thin-film gauge resistance at ambient temperature, Ohms
R_{GB}		thin-film gauge resistance at elevated temperature, Ohms
R_L		circuit line resistance, Ohms
R_S		circuit series resistance, Ohms
R_{SS}		gas temperature probe steady state wire resistance, Ohms
R_{WIRE}	G7XXS,L	gas temperature probe absolute wire resistance, Ohms
ΔR		incremental resistance change, Ohms
S		Piezo-electric transducer sensitivity, mV/psi
t		time, seconds
Δt		time increment, seconds
T		temperature, °F
T_A		thin-film gauge ambient temperature, °F
T_B		thin-film gauge elevated temperature, °F

NOMENCLATURE (Continued)

PLOT SYMBOL	MNEMONIC	DEFINITION
DATA PARAMETERS (Continued)		
	T6XX	gas temperature probe thermocouple temperature, °C
ΔT		surface temperature change, °F
y		curve fit of the thin-film gauge substrate properties
π		constant
ρ		density of the thin-film gauge substrate, lbm/ft^3
τ		circuit time constant, seconds
GAS RECOVERY TEMPERATURE PARAMETERS		
A		wire cross sectional area, cm^2
D		wire diameter, cm
h		convective heat transfer coefficient, $cal/sec\text{-}cm^2\text{-}°K$
h_c	h	corrected convective heat transfer coefficient, $cal/sec\text{-}cm^2\text{-}°K$
K		wire thermal conductivity, cal/cm-sec-°K
ℓ		wire length, cm
q_c		heat input to the wire from the gas, cal/sec
q_j		heat due to current flow, cal/sec
q_k		heat conduction to wire supports, cal/sec
q_{rw}		heat loss by radiation from the wire, cal/sec
q_s		heat accumulated in the wire, cal/sec
q_{wg}		heat gained by radiation from the gas, cal/sec

NOMENCLATURE (Concluded)

PLOT SYMBOL	MNEMONIC	DEFINITION
GAS RECOVERY TEMPERATURE PARAMETERS (continued)		
R_o		wire resistance at T_o, Ohms
R_w		measured wire resistance, Ohms
T_o		initial wire temperature, °K (20°C)
T_r		gas recovery temperature, °K
T_{r_c}	Tr	corrected gas recovery temperature, °K
T_s		wire support temperature, °K
T_w		wire temperature, °K
$\bar{T}_w$		mean wire temperature, °K
x		distance along the wire, cm
α, β		R-T curve fit coefficients
γ		parameter $\sqrt{h/KD}$, $\frac{1}{cm}$
π		constant
σ_o		wire resistivity at T_o ($\sigma_o = R_oA/\ell$), Ohm-cm
Subscripts 1, 2		denotes long and short wires

REMARKS

Test Conditions and Run Schedule

The test conditions and test run schedule are presented in Tables I and II, respectively. Part 1 of the run schedule contains the steady-state reference base pressure runs; Part 2 contains the base pressure, heat transfer, and gas recovery temperature runs.

RSRB Chamber Pressure

During the first five combustion runs, runs 9 through 13, the right-hand solid rocket booster indicated a problem with the chamber pressure. The measured chamber pressure was erratic and low level; however, the nozzle exit plane pressure trace indicated that the chamber pressure was normal. Initial investigation revealed a faulty amplifier and a shorted cable as being the problems. The erratic behavior was solved, but the low level output continued. Further investigation revealed the Kistler pressure transducer measuring the chamber pressure as being the problem. The Kistler transducer had four puncture holes in its peripheral case just below the diaphragm. The four holes equalized pressure on both sides of the diaphragm causing the low output. In view of the damaged transducer, shorted cable, and faulty amplifier, and considering the normal nozzle exit plane pressure trace, it is felt that the SRB plume flow field was not abnormal in any way during these first five combustion runs.

CONFIGURATIONS INVESTIGATED

The model configuration for test IH83 was a 0.0225-scale version of the space shuttle integrated vehicle. Designated 19-OTS, the model employed short-duration, rocket firing techniques to simulate the vehicle rocket plumes during ascent. The space shuttle main engines (SSME's) burned hydrogen and oxygen gases, and the solid rocket boosters (SRB's) burned a solid propellant (ANB-3066B) to simulate either first-or second-stage rocket plumes.

The integrated vehicle model consisted of the orbiter, external tank (ET), and solid rocket boosters (SRB's) designed to outer mold line vehicle 5 specifications.

Orbiter

The wing, vertical tail, and body flap simulated planform, contour, and thickness distribution. Deflective split elevons were simulated on the wing. Inboard elevons deflect 0, +5, +10, and +15 degrees; outboard elevons deflect -5, 0, and +5 degrees. Elevons remained fixed throughout test IH83 at +10° inboard and 0° outboard. The rudder on the vertical tail was not simulated. The body flap remained fixed in the nominal position (zero deflection).

The base heat shield was divided into four segments to facilitate gimbal angle changes and to provide easy access to the instrumentation.

Nozzles

SSME and SRB nozzle internal surfaces were geometrically duplicated.

External surfaces were smooth except for one extra SSME nozzle which simulated the external hatbands; the hatband nozzle was used in the #1 SSME location during gas temperature probe runs. SSME and SRB nozzle walls were structurally thickened to withstand nozzle heating.

Both SSME and SRB nozzles had gimbaling capability. Gimbal angle blocks defined specific pitch and yaw nozzle displacements. When required, each gimbal block rotated about its central axis to simulate various gimbal configurations; all gimbal blocks were designed to be positioned at 45-degree intervals around the circumference. Null position for the SSME and SRB nozzles was as follows:

Left and Right SRB's: Pitch = 0, Yaw = 0

#1 SSME: Pitch = 16° up, Yaw = 0

#2 and #3 SSME: Pitch = 10° up, Yaw = 0

For both SSME and SRB nozzles, deflections were as shown in Figure 1.

Two non-firing SSME nozzles were provided with the model for simulating engine-out operation. Although the two non-firing nozzles could replace any of the three firing nozzles, they were not used for this test program.

OMS nozzles were non-functional. They were simulated internally and externally at their "stowed" ascent position which is six degrees pitch down from null and seven degrees yaw outboard from null.

External and Support Hardware

External and support hardware on the orbiter, ET, and SRB's were not simulated except for the aft support hardware on the ET consisting of struts, cross beam, diagonal cross strut, and LO_2 and LH_2 feed lines. These hardware were simulated to scale but were not detailed or capable of carrying support loads.

Support between the orbiter and external tank was provided by an adapter which contained propulsion supply gas lines, autovalve control gas lines, instrumentation wire routing, charge tube thermocouples, and cooling lines. The adapter also provided a mounting surface for the orbiter wing.

The SRB's were supported at the center of the external tank by mounting pads. A small strut also attached just aft of the SRB nose. The mounting pad provided for ignition gas passages to the SRB and a transducer installation to monitor chamber pressure.

Model Support

A thin-blade yaw strut was mounted to the bottom of the external tank to suspend the model inverted in the tunnel. A support sting linked the model strut to a tunnel ceiling strut.

Nomenclature

Nomenclature for model 19-OTS was as follows:

CONFIGURATIONS INVESTIGATED (Continued)

Component	Definition
B_{64}	fuselage body
C_{16}	canopy
E_{63}	elevon
F_{14}	body flap
M_{18}	OMS pod
N_{92}	OMS nozzle
N_{94}	SSME nozzle
V_{23}	vertical tail
W_{129}	wing
S_{22}	solid rocket booster
N_{106}	solid rocket booster nozzle
T_{33}	external tank

These components of the space shuttle vehicle are identified in Figures 2 and 3.

Dimensional Data

Dimensional data for model 19-OTS are presented in Table III.

Propulsion Systems

(Orbiter)

The orbiter propulsion system consisted of hydrogen and oxygen charge tubes, a fast-acting bipropellant valve (autovalve), hydrogen and oxygen venturis, an injector, a combustion chamber, and the SSME gimbal block/ nozzle assemblies.

The charge tubes were arranged spirally inside the external tank to supply hydrogen and oxygen at approximately 3000 psia through the autovalve to the venturis. When the autovalve opened, the gases were supplied to the venturis at constant conditions for the wave time of the charge tubes. The hydrogen charge tube, being larger, was located in the front of the external tank. The oxygen charge tube, in the back of the external tank, was separated from the hydrogen charge tube by a cavity used to route gas lines and wiring from the orbiter to the model strut.

The autovalve is a pneumatically operated piston-type valve. Two solenoid (Valcor) valves, when energized, emitted high-pressure nitrogen (approximately 3000 psia) to chambers within the autovalve for opening or closing. SSME nozzle flow time was controlled by the relative time between solenoid valve operation.

The venturis operated under choked flow conditions. They were designed for an O/F ratio of 6.0. Separate venturis were used for two-engine and three-engine SSME operation to simulate the proper mass flow at each condition.

The injector was composed of twelve doublets designed to impinge on a diameter equivalent to the combustion chamber area mean diameter. Doublet holes were of equal size and angled to balance the radial momentum of the hydrogen and oxygen streams.

The combustion chamber provided necessary volume for the gases to mix and burn. It was common to all three SSME nozzles. A pyrotechnic ignition source was located in the chamber.

The SSME gimbal block/nozzle assemblies were located downstream of the combustion chamber. The nozzles were scaled and contoured internally.

(Solid Rocket Booster)

Each solid rocket booster consisted of a propellant holder, an ignition gas system, a diaphragm, and a gimbal block/nozzle assembly. SRB flow was controlled by the amount of solid propellant used; propellant thickness determined the burn time while propellant surface area determined chamber pressure level.

The propellant holder was a cylindrical casing which fit inside the SRB. Solid propellant ($\approx$ 0.050 inch thick) was glued to a thin aluminum sheet ($\approx$ 0.011 inch thick) and rolled inside the holder. Both ends of the propellant holder were capped to enclose the holder during initial propellant burning. Cool nitrogen was flowed through the propellant holder to maintain the propellant at constant temperature before model firing during the run.

An ignition gas composition of ethylene and oxygen flowed through each SRB to provide a high-energy source for rapid ignition (<5 msec.) of the solid propellant. Ignition gas pressure was nominally 16.5 psia. The mixture was nominally O/F = 5.6. A pyrotechnic source in each SRB nose ignited the gas which, in turn, ignited the propellant.

The diaphragm was contained in the aft propellant holder end cap. It consisted of thin sheets of Mylar, 0.045 inch total thickness, sized to burst slightly above the desired chamber pressure. A 1/16 inch diameter hole at the center allowed ignition gas and cooling gas flow.

The gimbal block/nozzle assemblies were scaled and contoured internally.

The solid propellant, ANB-3066B, was a Class B explosive that functioned by rapid combustion rather than detonation. The burning rate was a function of pressure, temperature and humidity.

INSTRUMENTATION

Pressure and Heat Transfer

Pressure data on the model bases and sidewalls were measured with piezo-electric pressure transducers mounted inside the model close to each orifice. The transducers measured static pressure data.

Heat transfer data were measured with total heat transfer gauges, radiation heat transfer gauges, and gas temperature probes. Total and radiation heat transfer gauges were used to determine heating rates. Gas temperature probes were used to derive gas recovery temperatures.

Pressure and heat transfer instrumentation locations are shown on Figures 4a through 4t. The instrumentation is summarized below and itemized on each figure.

Total heat transfer gauges	188
Radiation heat transfer gauges	21
Piezo-electric pressure transducers	30
Gas temperature probes	7

The instrumentation numbering system used on Figures 4a through 4t is summarized in Table IV.

Reference

Sixteen static pressure taps located throughout the model base regions and on the orbiter sidewall provided steady-state reference pressures for the piezo-electric transducers. They are also shown on Figures 4a through 4t, identified by 500 series numbers. Model pressure orifices were joined to scanivalves by thin-walled stainless steel tubing (0.125

inch OD, 0.095 inch ID). Scanivalves were located on top of the test section.

Seven pressures monitoring the operation of the orbiter and solid rocket booster propulsion systems were also recorded with piezo-electric transducers. The pressures were hydrogen and oxygen venturi, hydrogen and oxygen injector, SSME chamber, and left and right SRB chamber.

Fourteen thermocouples, chromel-alumel and iron-constantan, monitored the temperature of the piezo-electric transducers, Valcor valve cavity, and hydrogen and oxygen charge gases.

Seven iron-constantan, Type "J", thermocouples, one in each gas temperature probe, recorded the probe temperature change during model firing.

Table V lists all thermocouple locations.

Sensor Description

Piezo-electric transducers responded only to pressure changes. Piezo-electric materials inside the transducer sensed pressure changes on the transducer diaphragm. Each transducer was compensated for acceleration by a diaphragm wired opposite to the active diaphragm. All transducers, except the venturis and injector, also had a heat shield mounted ahead of the diaphragm to minimize temperature and radiation effects. Piezo-electric transducers were either PCB or Kistler type. Kistler transducers, being less sensitive to temperature, were used for SSME and SRB chamber pressures; they were rated for 4000 psid maximum. PCB transducers were used for the model bases and sidewalls and for the venturis and injector. The venturi and injector transducers were rated for 5000 psid maximum. The model base and sidewall transducers were low-range, all were rated for 2 psid except the SSME and SRB nozzle exit plane transducers which were rated for 10 psid.

The total heat transfer gauge was a thin-film gauge consisting of a thin resistance film of platimum fused to a Pyrex substrate (#7740 Pyrex). Silver tabs were fused to the platinum film terminals. Electrical connections were made to the silver with soft solder. The platinum film was insulated from the airstream by a thin dielectric coating of magnesium fluoride. All thin-film gauges measured the change in local surface temperature. The total gauge responded to both convective and radiative heating.

The radiation heat transfer gauge was also a thin-film gauge. It consisted of thin coats of aluminum black deposited over the total gauge film/substrate composite and shielded by a synthetic sapphire window. The aluminum black preserved the response characteristics of the gauge.

The gas temperature probe was a thin-wire resistance thermometer. It consisted of two, thin platinum-rhodium wires, approximately 1 and 2 mm long, mounted parallel on the tips of four needles positioned 0.25 inch from the model surface. The wire diameter was 5.08×10^{-4} cm (0.2 mil). An iron-constantan "Type J" thermocouple was mounted in the tip of one needle to monitor probe temperature.

Thin-film gauges were contoured as required to match model curvature. Contouring was required on the aft external tank hardware and on the hat-band nozzle.

All thin-film gauges were bonded in place. Piezo-electric transducers were also bonded in place except for the high-pressure PCB's and Kistler's which were threaded. Gas temperature probes were mounted in unique probe holders. The probes were held in position by a setscrew which allowed various translational and rotational probe positions. As mentioned previously, the probe tips remained at 0.25 inch from the model surface.

Further descriptions of the piezo-electric transducer total heat transfer gauge, and radiation heat transfer gauge can be found in Reference 1. The design of the gas temperature probe is described in References 2, 3, and 4.

Figures 5 and 6 are various views of the base of the model showing excellent visualization of the heat transfer instrumentation. The small piezo-electric transducer pressure orifices and larger static pressure orifices are also visible on some views. Total and radiation heat transfer gauges are the primary instrumentation shown on Figures 5a through 5e, but they are also shown on Figures 6a through 6d. Gas temperature probes are shown on Figures 6a through 6d.

TEST FACILITY DESCRIPTION

The NASA Lewis 10 x 10-Foot Supersonic Wind Tunnel is capable of attaining test section flow in the Mach number range from 2.0 to 3.5 in increments of 0.1. The tunnel may be operated in either of two modes: aerodynamic cycle or propulsion cycle.

The floor of the test section can be lowered to the first floor level by means of screwjacks at each corner. Model installation is generally made through the resulting 10.067 m (33 ft. 4-1/8 in.) by 3.048 m (10 ft.) opening. A special model dolly can be used to move the model onto the floor plate. Two 22,700 kg (25 ton) traveling overhead cranes capable of running the length of the building housing the test section are available for model installation. These cranes have 4540 kg (5 ton) auxiliaries.

There are removable top and bottom plates in the test section which are available for installation of small model supports and auxiliary apparatus. The opening may vary up to 6.10 m (20 ft.) long by 1.07 m (3.5 ft.) wide depending upon the selection of insert plates. Model mountings are installed through these openings.

Three pairs of 0.84 m (33 in.) diameter windows are located in the side walls of the test section. Two pairs of these windows are mounted eccentrically in 1.52 m (5 ft.) diameter movable disks. The disks may be rotated to position the windows on a 0.267 m (10.5 in.) radius. The third pair of windows is located in a fixed position downstream of the movable windows.

The strut for sting-mounted models is extended through the tunnel floor when in use. The strut has a chord length of 1.22 m (4 ft.) and is 20.32 cm (8 in.) thick, and can be rotated in the vertical plane about a pin located 24.13 cm (9.5 in.) below the test section floor. The angle-of-attack can be remotely varied from -5° to +20°.

A ceiling strut assembly is available. This assembly consists of the strut proper to which the model is attached, and the anchoring structure and angle-of-attack mechanism which are outside the test section.

Strut thickness may vary up to 25.4 cm (10 in.) and the chord length up to 2.13 m (7 ft.). The maximum chord length is determined by the angle-of-attack requirement.

Angle-of-attack of the model is remotely controlled by a screwjack mechanism which rotates the strut around a 7.62 cm (3 in.) diameter pin located 17.78 cm (7 in.) above the inside surface of the tunnel top plate. The angle-of-attack range is determined by model size and strut attachment details. Electrical wiring from the strut is connected to terminal panels on top of the test section. Pressure tubing is connected to Scanivalves located on top of the test section.

An auxiliary strut is provided to hold a nozzle plug-actuating mechanism or tail rake when a suspended model is used. The strut is designed to rotate about the ceiling strut center of rotation at a radius of 3.73 m (12 ft. 3 in.).

All electrical and pressure connections on top of the test section are the same as those used with the ceiling strut.

TEST FACILITY DESCRIPTION (Concluded)

A high-pressure air storage facility is available with a capacity of 6120 m^3 (216,000 ft^3) of standard dry air at 1.83×10^7 N/m^2 (2650 psi) for use at the tunnel. Two other air storage facilities are interconnected with it. These are a 4110 m^3 (145,000 ft^3) system located at the 8 x 6 wind tunnel and a 17 600 m^3 (620,000 ft^3) system located at the 9 x 15 test section. The three facilities together provide a total capacity of 27 800 m^3 (981,000 ft^3) of standard dry air for use at the 10 x 10 wind tunnel. They are charged by a pump having a capacity of 0.24 m^3/sec (500 ft^3/min) of standard air. Total charging time from 2.76×10^6 N/m^2 (400 psi) to 1.83×10^7 N/m^2 (2650 psi) is approximately 28 hours for the combined systems. A variable pressure air supply system with a capacity of 45.4 kg/sec (100 lb/sec) is available at pressures up to 1.03×10^6 N/m^2 (150 psi). A service air system with a capacity of 0.91 kg/sec (2 lb/sec) continuous service is available at 8.62×10^5 N/m^2 (125 psi).

A hydraulic system is available for actuation or positioning of a model and/or its components. This system consists of three pumps each rated at 1.26×10^{-3} m^3/sec (20 gal/min). The pumps are connected in parallel and may be used in any combination. The maximum capacity of the system is 3.79×10^{-3} m^3/sec (60 gal/min) at 2.07×10^7 N/m^2 (3000 psi).

The liquid fuel system is made of stainless steel and has a total flow capacity of 4.42×10^{-3} m^3/sec (70 gal/min) at 2.76×10^5 N/m^2 (40 psi). The maximum pressure available is 6.55×10^6 N/m^2 (950 psi) at a flow of 1.89×10^{-3} m^3/sec.

TEST PROCEDURES

Installation

The model-strut-sting assembly was inverted to suspend from a tunnel ceiling strut positioned to locate the model base at the upstream Schlieren window. A thin-bladed strut, mounted to the bottom surface of the external tank, linked the model to a cantilevered sting attached to the tunnel ceiling strut. A schematic of the installation in the NASA-LeRC 10 x 10-foot Supersonic Wind Tunnel is shown in Figure 7.

A new thin-bladed strut to allow model yaw was designed for test IH83. It was identical to previous struts except for a horizontal splitter plate adjacent to the external tank and except for the trailing edge shroud. The horizontal plate had specific bolt hole patterns to set the desired yaw angles. The trailing edge shroud had to be flared into a diamond cross section to allow rotation of tubing and wiring as the model yawed. Figure 8 shows four views of the thin-bladed yaw strut during installation in the tunnel.

To make a yaw angle change, the thin-blade portion of the strut was separated from the horizontal splitter plate which was permanently attached to the external tank. The external tank could then be rotated to the desired yaw angle defined by a specific bolt hold pattern. In this way, only the Shuttle model was yawed; the thin-blade portion of the strut remained stationary.

All instrumentation wiring, model control wiring, model control pressure lines, cooling lines, and pressure tubing were routed through the model strut-sting-ceiling strut assembly to the top of the tunnel where they connected to wire connector panels, gas panels, or scanivalves. Due to limited space in the model component bases, pressure tubing and instrumentation wiring would not fit simultaneously in the model. Pressure tubing was installed first. Instrumentation wiring was routed through the top section of the sting, model control wiring was routed through the middle section, while all pressure lines and tubing were routed through the lower section of the sting.

Gas panels for regulating flow to the model propulsion systems were mounted at the top of the tunnel. The system panels were (1) gaseous oxygen, (2) gaseous hydrogen, (3) high-pressure control nitrogen for auto-valve operation, (4) oxygen/ethylene for SRB ignition, and (5) low-pressure purge and cooling nitrogen. Gas system panels are shown in Figure 9. Supply bottles for each gas system, except the cooling nitrogen, were located adjacent to the panels. Cooling nitrogen was supplied by tandem gaseous nitrogen-liquid nitrogen trailers located outside the building as shown in Figure 10. Electronic control panels for regulating each gas system panel were located in the tunnel control room.

Calibrations

New thin-film heat transfer gauges, total and radiation, were calibrated prior to installation in the model. Gauge resistance change with temperature was measured to determine a sensitivity factor, K. The temperature range for total and radiation gauges was nominally 70°F to 150°F;

three temperature points were measured.

All low-range PCB piezo-electric pressure transducers were calibrated prior to installation in the model to determine sensitivity variation with temperature. The transducers, 2 psid and 10 psid, were calibrated at nominal temperatures of 75°F and 125°F or 75°F and 150°F. For data reduction of all low range transducers, a linear variation of sensitivity between 100°F and 125°F or between 100°F and 150°F was assumed; sensitivity was assumed constant up to 100°F.

Kistler pressure transducers were not calibrated specifically for this test program since temperature had little effect on their sensitivity.

High-range PCB and Kistler transducers were check-calibrated before and as required during the test to determine effects of installation and prolonged use on sensitivity. They were replaced as required.

Prior to the test or installation in the model during the test, gas temperature probes were calibrated over their operating temperature range to determine resistance change with temperature.

Operating Procedure

Limited space in the model did not allow simultaneous installation of reference pressure tubing and instrumentation wiring. Reference pressure tubes were installed first to record static pressures as reference for the low-range PCB piezo-electric transducers. First-and second-stage model configuration data were recorded at each proposed test condition and model attitude. Reference pressure runs are Part 1, Runs 1 - 8 of Table II.

Following reference pressure runs, instrumentation wiring was installed. Also during this time period, the model propulsion systems were operationally checked to insure reliability and repeatability.

Base pressure and heat transfer runs were categorized according to the instrumentation being recorded. Instrumentation patterns were usually distinguished by model configuration or type of instrumentation. The general run sequence was:

1. First-stage configuration runs
2. Second-stage configuration runs
3. Gas temperature probe runs (second stage)
4. Gas temperature probe runs (first stage)

Procedure for all base pressure and heat transfer runs was similar. Gas temperature probe runs required additional monitoring to insure probe integrity. Runs 9 - 41 comprise this part of the test program; all are good data runs, listed in Part 2 of Table II.

The short duration of the model firing, approximately 60 milliseconds for the orbiter and 150 milliseconds for the SRB's, was contrary to the designed use of the continuous flow wind tunnel. Because the SRB solid propellant and pyrotechnic igniters required refurbishment after each model firing, only one firing was possible per tunnel run. Two to four runs were typical during a six-hour running shift (midnight to 6:00 AM).

Model refurbishment between runs consisted of replacing the SRB propellant and SRB and SSME igniters. At the same time before the tunnel was closed, an SRB ignition gas leak check procedure insured that the new propellant holders were installed correctly. Loss of ignition gas during a run would cause SRB misfire. To leak check, 30 psia nitrogen was loaded into the propellant holder. An acceptable leak rate was 0.2 psi per minute. For a good propellant holder installation, which was common, there would be no leak during the first minute.

All pre-and post-model firing events, before and during the tunnel run, were prescribed in a check list which was strictly adhered to. Abort procedures were also prescribed in the same check list. Coordination of the model, tunnel, and data recording systems was essential for the model firing. Model gas systems, except hydrogen and oxygen, were set to the desired pressures before the tunnel was started with final adjustment just before model firing. Due to the time required, the hydrogen and oxygen charge tubes were still being pressurized when the tunnel was started. Cooling nitrogen gas, used for limiting the low-range piezo-electric transducer temperatures to 80°F to 100°F, was initiated after the tunnel was started. Cooling gas was discontinued during data recording, both steady state CADDE recording and dynamic analog recording.

Model firing was controlled by a series of timing relays. The relays were set to initiate SRB flow slightly before SSME flow, allowing stabilization of the two flows at about the same time period. A single push button initiated the relay sequence. Typical model firing data are shown in Figures 11 and 12.

Four "data calls" were taken during a run: one before and after tunnel operation and one before and after model firing. A data call recorded steady-state data on digital tape (CADDE system). Data calls before and after tunnel operation were taken with the tunnel evacuated to about 1000 psf. The first and second data calls were used for data reduction. The third and fourth data calls were used to check instrumentation integrity only.

Data Acquisition

The type of data recorded dictated the data acquisition used. Steady-state data recorded during "data calls" were recorded by the CADDE system. Dynamic data recorded during model firing were recorded on analog tape and visicorders.

CADDE is a 200-channel Central Automatic Digital Data Encoder capable of immediate playback to the tunnel control room for inspection or analysis. Steady-state data recorded by CADDE included reference static base pressures, temperatures, thin-film gauge resistances, gas temperature probe resistances, gas system pressures, tunnel condition parameters, and tunnel configuration parameters. Temperature readings were recorded on CADDE through an automatic voltage digitizer (AVD).

The analog system consisted of 12 FM multiplex tape recorders with 15 channels each; however, only 150 channels were available for test IH83.

Full scale millivolt ranges were 5, 10, and 20 with amplifications of 1, 10, and 100. Dynamic data were recorded on analog tape from thin-film gauges, piezo-electric pressure transducers, gas temperature probes, and timing relays. Analog data were played back immediately onto visicorders in the data room for inspection.

Visicorders were high-speed oscillographs for on-line analysis of model operating pressures and timing events. Two, 9-channel visicorders were used in the control room. Data shown on Figures 11 and 12 plus a time code signal on each composed the visicorder data.

Model gas system pressures and model thermocouples were also displayed in the control room in engineering units for immediate analysis.

Four instrumentation patterns were developed for this test program. Each pattern was distinguished by type of instrumentation or model configuration. The four patterns were first-and second-stage model configurations, with and without gas temperature probes.

Instrumentation patterns only reflected changes in thin-film gauges or gas temperature probes; pressure transducers, timing relays, thermocouples, etc., did not change with each pattern. A block diagram showing the model instrumentation data acquisition is shown on Figure 13. Instrumentation patterns are listed in Table VI.

Pressure transducer, thermocouple, and timing relay wiring were "hard" wired in the model sting and remained so throughout the test program. Thin-film gauges and gas temperature probes were interchanged by a patchboard arrangement in the model sting. Jumper panels, connecting model thin-film gauge and gas temperature probe wiring to data system wiring at the patchboard, were used to switch instrumentation patterns; no other wiring in the data systems required changing.

SSME nozzle positions and instrumentation orientation varied with instrumentation. Specifically, they were based on whether or not gas temperature probes were being measured. Figure 14 shows the various positions and orientations for each run. The figures are viewed looking forward with the model inverted as installed in the 10 x 10-foot Supersonic Wind Tunnel.

Each type of model instrumentation went through signal conditioning in the tunnel control room before entering the data acquisition systems. Signal conditioning was selected to produce a circuit time constant of 2.0 or greater. Table VII lists the signal conditioning used for each type of instrumentation. Thin-film heat transfer gauges, grounded in the model, sting, or elsewhere, were routed through Preston amplifiers before entering the analog recording system; Preston amplifiers restored the signal otherwise lost by grounding.

DATA REDUCTION

Tunnel Conditions

Tunnel test conditions were reduced according to standard NASA-Lewis Research Center methods and presented in engineering units. They included:

Stagnation pressure, psfa

Static pressure, psfa

Dynamic pressure, psf

Model altitude, ft.

Reynolds number, 1/ft.

Stagnation temperature, °R

Static temperature, °R

Density, (slugs/ft.^{3})

Mach number

Thermocouple Data

Chromel-Alumel thermocouple data were converted to degrees Fahrenheit using standard methods for a 150° reference. Iron-constantan thermocouple data were either converted to degrees Fahrenheit or to degrees Centigrade (GTP thermocouples) using standard methods for a 150° reference.

Model Operating Pressures

Model operating pressures were reduced according to Equation (1).

$$P_{7xx}(t) = \left(\frac{\Delta E(t)}{GAIN}\right) \frac{1}{S} + P_R \tag{1}$$

where

$\Delta E(t)$ = voltage measured by the recording system at time, t

GAIN = net gain of the electronic system between the sensor and recording system

S = transducer sensitivity

P_R = steady-state reference pressure; P_R was negligible except for the SRB chamber pressure transducers where P_R = ignition gas pressure = 16.0 psi

Pressure Data

Absolute pressures were obtained using Equation (2).

$$P_A(t) = P_G(t) + P_R \tag{2}$$

where

$P_G(t)$ = pressure measured by the piezo-electric transducer at time, t

P_R = steady state reference pressure

$$P_G(t) = \frac{\Delta E(t)}{GAIN} \frac{1}{S} \tag{3}$$

where $\Delta E(t)$, GAIN, and S were defined earlier.

Sensitivity, S, of the low-range PCB transducers varied with temperature determined by surrounding thermocouples. A transducer/thermocouple correlation is given in Table VIII. Where more than one thermocouple is shown for a transducer, the temperatures were averaged. Pretest calibrations at approximately 75°F and 125°F or 150°F were used to determine a sensitivity. For data reduction, the sensitivity was assumed constant between 75°F and 100°F and assumed linear between 100°F and 125°F or between 100°F and 150°F.

Reference pressures, P_R, were reduced to engineering units using standard NASA-Lewis Research Center methods. Table IX lists the reference pressures used with each piezo-electric transducer for data reduction.

Heating Rate Data

Thin-film gauge output was a surface temperature-time history which is analogous to homogeneous one-dimensional, semi-infinite slab theory for unsteady heat conduction. The numerical technique used to extract heating rates from the surface temperature-time history, i.e., the solution to the unsteady, one-dimensional heat conduction equation for a semi-infinite body, is described in Reference 5. The solution is:

$$(4) \quad \dot{q}n(t) = \sqrt{\frac{\rho c k}{\pi}} \left[\frac{\Delta T(t_n)}{\sqrt{t_n}} + \sum_{i=2}^{n-1} \left\{ \frac{\Delta T(t_n)-\Delta T(t_i)}{\sqrt{t_n-t_i}} - \frac{\Delta T(t_n)-\Delta T(t_{i-1})}{\sqrt{t_n-t_{i-1}}} + 2\,\frac{\Delta T(t_i)-\Delta T(t_{i-1})}{\sqrt{t_n-t_i}+\sqrt{t_n-t_{i-1}}} \right\} \frac{\Delta T(t_n)-\Delta T(t_{n-1})}{\sqrt{\Delta t}} \right]$$

with t_1 = 0, $\Delta T(t_1) \neq 0$, and $t_n = (n-1)\,\Delta t$ for n = 1, 2, 3, ..n

and where ΔT = surface temperature change from the temperature time history

t = time at which the heating rate is being determined

n = number of time intervals from 0 to t

i = an iteration variable

Δt = t/n = time interval (Δt = 0.4 msec)

ρck = thin-film gauge substrate properties

One characteristic of Equation (4) is that the surface temperature-time history must be a smooth curve in order to produce a smooth heating rate-time history. A smooth temperature-time history was attained by applying Equations (5) and (6) three successive times to the thin-film gauge data before using Equation (4).

(5) $$\Delta T(t_1) = \frac{\Delta T(t_1) + \Delta T(t_2)}{2}$$

(6) $$\Delta T(t_2 \ldots . t_n) = \frac{\Delta T(t_{n-1}) + \Delta T(t_n) + \Delta T(t_{n+1})}{3}$$

The thin-film gauge substrate properties varied with gauge temperature. The properties, $\sqrt{\rho ck}$, were obtained by Equation (7) which is a curve fit of Figure 15.

(7) $$\sqrt{\rho ck} = \sqrt{\rho ck_{70}} \; [\text{curve fit } y = a + a_1 T + a_2 T^2 + \ldots . + a_m T^m]$$

where $y = \dfrac{\sqrt{\rho ck}}{\sqrt{\rho ck_{70}}}$ with $50°F \leq T \leq 300°F$

Thin-film radiation gauge heating rates calculated by Equation (4) required correction, due to spectral absorptivity characteristics of the radiation gauges, to obtain a true incident radiant heating rate. The correction used was:

(8) $$\dot{q}R(t) = \frac{\dot{q}'R(t)}{0.85}$$

where $\dot{q}R(t)$ = true incident heating rate at time, t.

$\dot{q}'R(t)$ = calculated incident heating rate at time, t.

The surface temperature change, ΔT, of the thin-film gauge was derived by Equation (9).

(9) $$\Delta T(t) = \frac{\Delta R(t)}{K_B}$$

$\Delta R(t)$ is the thin-film gauge resistance change at time, t, calculated by Equation (10).

(10) $$\Delta R(t) = \frac{\Delta E(t)}{E_X} R_S$$

$\Delta E(t)$ = voltage change at time, t

E_X = regulated power supply voltage

R_S = series resistance

K_B is the thin-film gauge sensitivity at elevated temperature, T_B calculated by Equation (11).

(11) $$K_B = K_{70}(1.018 - 2.59 \times 10^{-4} T_B)$$

where K_{70} = thin-film gauge sensitivity at 70°F

T_B = elevated thin-film gauge temperature

Elevated thin-film gauge temperature, T_B, was derived from steady-state data (data calls one and two) recorded prior to tunnel start and prior to model firing as opposed to pressures and heating rates derived from data recorded during model firing.

(12) $$T_B = \frac{1 - \left[1 - 5.18 \times 10^{-4} \left(\frac{\Delta R}{K_{70}}\right)\right]^{1/2}}{2.59 \times 10^{-4}} + T_A$$

where $\Delta R = R_{GB} - R_{GA}$

R_{GB} is the thin-film gauge resistance at elevated temperature, T_B.

(13) $$R_{GB} = \left[\left(\frac{E_{AVD}}{E_X - E_{AVD}}\right) R_S\right] - R_L$$

where E_{AVD} = voltage drop at the recording system

E_X = regulated power supply voltage

R_S = series resistance

R_L = measured signal line plus connector contact resistance

R_{GA} is the thin-film gauge resistance at ambient temperature, T_A, prior to each run.

(14) $$R_{GA} = \left[\left(\frac{E_{AVD}}{E_X - E_{AVD}}\right) R_S\right] - R_L$$

where E_{AVD}, E_X, R_S, and R_L are the same as above at condition, T_A.

K_{70} was derived by Equation (15).

(15) $$K_{70} = \frac{R_{GA}}{\frac{R_c}{K_c} + (T_A - 70)}$$

where R_C = thin-film gauge calibration resistance

K_C = thin-film gauge calibration sensitivity

T_A is the ambient model temperature prior to tunnel start; T_A was measured by thermocouple 601.

Gas Temperature Probe Data

Gas temperature probe data were reduced into the form of resistance versus time. Total resistance for each gas temperature probe wire was determined by Equation (16).

$$(16) \qquad R_{WIRE} = \Delta R(t)_{WIRE} + R_{SS}$$

$\Delta R(t)_{WIRE}$ is the wire resistance change at time, t.

$$(17) \qquad \Delta R(t)_{WIRE} = \frac{\Delta E(t)_{WIRE}}{E_X} R_S$$

where $\Delta E(t)$, E_X, and R_S are the same parameters as the thin-film gauge (see Equation 10). R_{SS} is the steady state wire resistance recorded prior to model firing.

$$(18) \qquad R_{SS} = \left[\left(\frac{E_{AVD_{WIRE}}}{E_X - E_{AVD_{WIRE}}}\right) R_S\right] - R_L$$

where E_{AVD}, E_X, R_S, and R_L are the same parameters as the thin-film gauge (see Equation 13).

Data Reduction Time

All data were averaged over a time interval corresponding to stable model operation and peak level of sensor output. The time to begin averaging and the number of data points to be averaged were determined from time histories of the SSME and SRB chamber pressures and manually input to the data reduction computer program. Normally, 40 to 50 data points were averaged (16 to 20 milliseconds).

Voltage Signal Correction

The various types of instrumentation used for test IH83 required different types of electronic circuitry signal conditioning to link the instrumentation to the analog tape and CADDE recording systems (see Table VII). Electronic circuitry to the analog recording system was characterized by a voltage signal decay with time depending on the time constant of the circuitry. Thin-film gauge and gas temperature probe circuit time constants were two seconds. Piezo-electric transducer circuit time constants were ten seconds. A two-second time constant will reduce an initial voltage response by approximately 5 percent in 100 milliseconds (SSME firing lasted approximately 60 milliseconds; SRB firing lasted approximately 150 milliseconds). To correct for any voltage loss due to the time constant, Equation (19) was applied to all analog instrumentation output signals.

(19) $$\Delta E_c(t_n) = \Delta E_c(t_{n-1}) + \Delta E(t_n) - \Delta E(t_{n-1})e^{-\Delta t/\pi}$$

ΔE_c = corrected voltage

ΔE = actual voltage output

t = time at which voltage is being corrected

n = t/n = time interval at which voltages are recorded (Δt = 0.4 msec)

π = circuit time constant

Recovery Temperature (Gas Temperature Probes)

Gas recovery temperature data reduction procedures, in general, remain unchanged from those used for previous impulse base heating tests. These procedures are documented in References 2 and 3. For test IH83, however, there were improvements to the data reduction program used for calculating gas recovery temperature. These improvements are detailed in Reference 4 and outlined briefly in the remainder of this section.

Previous data reduction required simultaneous solution of the complete heat balance equation for two thin wires. The equation is

(20) $$q_s = q_j + q_c - q_k - q_{rw} + q_{wg}$$

where q_s = heat accumulated in wire

q_j = heat due to current flow

q_c = heat input to the wire from gas

q_k = heat conduction to wire supports

q_{rw} = heat loss by radiation from wire

q_{wg} = heat gained by radiation from gas

This equation is non-linear in two unknowns, T_r and h, and required a numerical iteration scheme via a computer code called SNEBE 4 to obtain solutions. Improvements were made in Reference 3 where a linearized semi-closed form solution to the wire heat balance equation provided initial estimates of the recovery temperature and heat transfer coefficient for the non-linear numerical technique thereby saving considerable data reduction time.

Further modifications to the linearized semi-closed form solution have produced a complete linear solution which agrees very well with results of the non-linear numerical technique. The results are much more data in much less data reduction time; specifically, gas recovery temperature and heat transfer coefficient can now be obtained as a function of test time, instead of a single average value, allowing more detailed analysis.

Experience with previous gas temperature probe data has shown that most heat transfer associated with the wires is due to convective heat input and conduction. Eliminating other types of heat, Equation 20 simplifies to

(21) $$q_c = q_k$$

Substituting,

(22) $$h\pi D(T_r - T_w) = -A \frac{\partial^2 k\ T_w}{\partial X^2}$$

where

	h	=	heat transfer coefficient
	D	=	wire diameter
	T_r	=	gas recovery temperature
	T_w	=	wire temperature

A = wire cross-section area

k = wire thermal conductivity

X = distance along wire

Assuming k does not vary with temperature and substituting for A,

$$(23) \qquad h\pi D(T_r - T_w) = k \frac{\pi D^2}{4} \frac{d^2T_w}{dX^2}$$

Equation 23 can be transformed into a simple homogeneous differential equation (Reference 6) which has the solution

$$(24) \qquad T_w(X) = T_r - (T_r - T_s) \frac{\cos h\ (X\sqrt{4h/kD})}{\cos h\ (\ell\sqrt{4h/kD/2})}$$

where T_s = wire support temperature

ℓ = wire length

To obtain the average wire temperature for a finite length wire, Equation 24 is integrated over the wire length.

$$(25) \qquad \bar{T}_w = T_r - (T_r - T_s) \frac{\tan h\ (\ell\sqrt{h/kD})}{\ell\sqrt{h/kD}}$$

Solving for T_r and inserting parameter γ = h/kD,

$$(26) \qquad T_r = \frac{(\ell\gamma)\bar{T}_w - T_s \tan h\ (\ell\gamma)}{\ell\gamma - \tan h\ (\ell\gamma)}$$

Equation 26 is an explicit expression of finite length single wire heating with two unknowns, T_r and h. Two distinct equations can be written for the two different gas temperature probe wire lengths, denoted by subscripts 1 and 2, and solved simultaneously to obtain an equation of only one unknown, h.

(27) $$\frac{\ell_2\gamma - \tan h\,(\ell_2\gamma)}{\ell_1\gamma - \tan h\,(\ell_1\gamma)} = \frac{\ell_2\gamma\ \bar{T}_{w2} - T_s \tan h\,(\ell_2\gamma)}{\ell_1\gamma\ \bar{T}_{w1}\quad T_s \tan h\,(\ell_1\gamma)}$$

For practical use of the preceding equations, γ must first be obtained from Equation 27. From γ, h is calculated and used in Equation 26 to obtain T_r. Parameters T_s, $\bar{T}_w$, ℓ used in Equation 26 and 27 are obtained as follows: T_s, the wire support temperature, is measured by an iron-constantan thermocouple in the tip of one of the gas temperature probe short wire support needles. $\bar{T}_w$, the average wire temperature, is calculated by Equation 28.

(28) $$R_w = R_o\,[1 + \alpha(\bar{T}_w - T_o) + \beta(\bar{T}_w - T_o)^2]$$

where R_w = measured wire resistance

R_o = wire resistance at temperature T_o

T_o = 20°C = 293°K

α,β = R-T curve fit coefficients

Wire length, ℓ, is calculated by Equation 29.

(29) $$\sigma_o = R_o \frac{A}{\ell} = 1.853\text{x}10^{-5} \text{ ohm-cm for Platinum -10\% Rhodium wire}$$

where σ_o = manufacturers stated value of resistivity at T_o

With all parameters known, γ is still not directly obtained from Equation 27 due to the hyperbolic functions. An efficient method for obtaining accurate values of γ is known as the Fibonacci series search routine. It is an interval elimination search method which sets upper and lower bounds to an initial heat transfer coefficient estimate ($h_{initial} = 1 \times 10^{-2}$ cal/cm^2 - sec - °K) and then proceeds to reduce the interval in which the optimum value occurs until a final value is reached. If the final value is equivalent to the upper or lower bounds, it becomes the new initial estimate, and the procedure is repeated.

The final solutions to Equations 26 and 27, i.e., h and T_r, must satisfy the following boundary conditions; if not, the solutions are considered non-convergent.

$$T_r > \bar{T}_{w_1} > \bar{T}_{w_2} > T_s$$

$$T_r < 4000°K$$

$$1 \times 10^{-5} < h < 1.0 \quad \text{cal/cm}^2 - \text{sec} - °K$$

As gas temperature increases, the non-linear terms of the wire heat balance equation, ignored for the preceding simplified solution, cause the linear gas recovery temperature to diverge from the true non-linear solution. Correction Equations 30 and 31 are applied to the linear gas recovery temperature and heat transfer coefficient solutions to account for non-linearity.

(30) $$T_{r_c} = 4.6805 \times 10^{-7}\, T_r^3 - 9.4521 \times 10^{-4}\, T_r^2 + 1.6682\, T_r - 152.02$$

(31) $$h_c = 2.8598 \times 10^{-10}\, h^4 + 6.1589 \times 10^{-7}\, h^3 - 5.0279\, h^2 + 0.13456\, h + h$$

To use the simplified linear equations, the following assumptions must be made:

1. The gas temperature probe wires are at a steady state heating condition.
2. The convective heat transfer coefficient and gas recovery temperature are identical for both wires.
3. The wire supports do not significantly disturb the flow in which the measurement is made.

RESULTS AND DISCUSSION

The basic test IH83 data consisted of heating rates, pressures, and gas temperature probe resistances varying as a function of time during the model firing. By selecting a time interval to average data, as described in the preceding section, each sensor output during the firing was summarized by a single value. Only summary heating rate and pressure data were tabulated at the test site. Both types of gas temperature probe data, time varying and summary, were tabulated at the test site.

Plots of the time varying data were also received at the test site. Specifically, surface temperature change, heating rate, absolute pressure, and gas temperature probe resistance were plotted as a function of model firing time.

A computer tape containing all test data was supplied to Rockwell to allow easier manipulation and analysis of the data.

Analog data were of good quality with a high signal to noise ratio. Noisy channels were usually filtered to eliminate much of the noise. Some channels did experience transient signals from the model firing which could not be eliminated, but the signals were usually before the data period.

With normal model use, the SSME engine adapter inserts in the combustion chamber become worn. If not detected and replaced, the worn inserts will allow combustion chamber gas to slowly leak into the volume behind the base heat shield. It has been theorized that when leaks occur, the gas not only fills the volume but also escapes around the SSME nozzles causing erroneous heating rates in the SSME engine-mounted heat shield (SSME bulge) area, i.e., a low-pressure, supersonic, outward flow around the nozzles may be inhibiting the normal SSME plume recirculation and impingement. With a comparatively short test program (33 combustion runs), erosion of the engine adapter inserts was not a problem. A low-pressure leak check (200 psi) following run 18 verified that the engine adapter inserts were not leaking at that point. The leak check was initiated because of copper deposit in the throat area of the #2 SSME nozzle. A slow leak (2 psi/min) was detected at the marmon clamp holding the #2 SSME nozzle to the gimbal adapter. At that time, the leak was attributed to the marmon clamp. During the first gimbal change following run 24, the copper throat insert in the #2 SSME nozzle was discovered to be warped enough to be the source of the leak. The throat insert was replaced, and an added precaution was taken to prevent flow around the engine-mounted heat shield if leaks did occur. The precaution was to seal around the engine-mounted heat shield O-ring area with a putty-like substance. At that time, only the #2 SSME engine-mounted heat shield was sealed. The #1 and #3 SSME engine-mounted heat shields were sealed following run 28. It is felt that the slow leak, which was discovered after run 18 and repaired after run 24, did not adversely affect the base heating rate data. The leak was small compared with leaks that have occurred in the past with eroded engine adapter inserts.

Tabulated source data are not supplied with this document but are available through the Rockwell International, Shuttle Aero Sciences Department as shown in Appendix A.

Plotted source data are also available through Rockwell International Shuttle Aero Sciences Department as shown in Appendix A.

Gas recovery temperatures, derived from the gas temperature probe resistance and thermocouple time history data as described in the preceding section and Reference 4, are presented in Appendix B. An example of the gas temperature probe time history data is also presented in Appendix B. The data presented were extracted from Reference 4.

Reference base pressure data obtained during runs 1-8 and used in the data reduction as reference for the low-range piezo-electric pressure transducers are presented in Appendix C. These data were either selected from or are the average of several data points recorded at each test condition.

REFERENCES

1. L. Bogdan, "Instrumentation Techniques for Short Duration Test Facilities," CAL No. WTH-030, 31 March, 1967.

2. Charles E. Fuller, III and Dr. Carl D. Engel, "Gas Temperature Probe Development and Short Duration Space Shuttle Testing Support." REMTECH Incorporated RTR0151-1, December, 1974.

3. Charles E. Fuller, Michael W. Morrison, Robert T. Powell, and James K. Levie, III, "Utilization of a Gas Recovery Temperature Probe on Space Shuttle Short Duration Base Heating Model Tests OH-78 and IH-39," REMTECH Incorporated RTR019-2, July, 1977.

4. Charles E. Fuller, James K. Levie, III, Robert T. Powell, "Utilization of a Gas Recovery Temperature Probe on Space Shuttle Short Duration Base Heating Model Tests IH-75 and IH-83," REMTECH Incorporated RTR019-3, July, 1978.

5. W. T. Cook and E. J. Felderman, "Reduction of Data from Thin-Film Heat Transfer Gauges: A Concise Numerical Technique, " AIAA Journal, Vol. 4, No. 3, March, 1966.

6. V. A. Sandborn, "Resistance Temperature Transducers," Metrology Press, Fort Collins, Colorado, 1972.

TABLE I. TEST CONDITIONS

Mach No.	Model Altitude	Facility Altitude	P_∞	H_O	H_OB	q_∞	P_C (SSME)	P_C (SRB)	Notes
	k ft.	k ft.	psfa	psfa	psfa	psf	psia	psia	$P_\infty = P_{facility\ altitude} = \frac{1}{2} P_{model\ altitude}$
2.2	60	74.1	77.8	831.6	774	263.5	1500 ↓	290 ↓	∞ = Freestream Conditions
2.5	70	84.6	47.5	810.8	781	207.7			
2.9	80	95.1	29.4	930.4	870	173.3			BM = Tunnel Bell-Mouth Conditions (Set-Point Conditions)
3.5	100	116.0	11.8	902.1	850	101.4			P_C = Chamber Pressure
3.5	120	137.1	5.0	381.3	351	42.9			
3.5	130	147.6	3.3	252.9	232	28.4			

TABLE II. DATASET/RUN NUMBER COLLATION SUMMARY

PART 1: REFERENCE BASE PRESSURE RUNS

Run	CADDE Reading No.	Config.	Mach	Altitude (K ft)	α	ψ	Chamber Pressure SSME	Chamber Pressure SRB	Nozzle Gimbal Angles #1 SSME P	#1 SSME Y	#2 SSME P	#2 SSME Y	#3 SSME P	#3 SSME Y	Left SRB P	Left SRB Y	Right SRB P	Right SRB Y	Remarks
1	1,2,3	OTS	2.5	70	-5	0	N/A	N/A	0	0	0	0	0	0	0	0	0	0	Tunnel Air Saturated
	4,5,6																		
	7,8,9		↓	↓															
	10,11,12		2.2	60															
	13,14,15		2.9	80	↓														
↓	16,17,18		3.5	120	+5	↓													
2	19,20,21			130	0	+11													
2	22,23,24			120		+11													
3	25,26,27			130		-11													
3	28,29,30			120	↓	-11													↓
4	31,33,34		↓	↓	+5	0													Repeat Run 1
	35,36,37		2.9	80	-5														
	38,39,40		2.5	70															
↓	41,42,43		2.2	60	↓	↓													↓
5	44,45,46		2.9	80	0	+5													
	47,48,49		3.5	100															
	50,51,52			120	↓														
	53,54,55			↓	+5														
	56,57,58			130	0														
↓	59,60,61				+5	↓													
6	62,63,64				0	-5													
	65,66,67			↓	+5														
	68,69,70			120	0														
	71,72,73			120	+5														
↓	74,75,76	↓	↓	100	0	↓	↓	↓	↓	↓	↓	↓	↓	↓	↓	↓	↓	↓	

TABLE II. DATASET/RUN NUMBER COLLATION SUMMARY

PART 1: Concluded

Run	CADDE Reading No.	Config.	Mach	Altitude (K ft)	α	ψ	Chamber Pressure SSME	Chamber Pressure SRB	Nozzle Gimbal Angles #1 SSME P	#1 SSME Y	#2 SSME P	#2 SSME Y	#3 SSME P	#3 SSME Y	Left SRB P	Left SRB Y	Right SRB P	Right SRB Y	Remarks
6	77,78,79	OTS	2.9	80	0	-5	N/A	N/A	0	0	0	0	0	0	0	0	0	0	
7	80,81,84	OT	3.5	130	↓	-7	↓	↓	↓	↓	↓	↓	↓	↓	↓	↓	↓	↓	
7	85,86,87	↓	↓	120	↓	-7	↓	↓	↓	↓	↓	↓	↓	↓	↓	↓	↓	↓	
8	91,92,93	↓	↓	130	↓	+7	↓	↓	↓	↓	↓	↓	↓	↓	↓	↓	↓	↓	
8	94,96,97	↓	↓	120	↓	+7	↓	↓	↓	↓	↓	↓	↓	↓	↓	↓	↓	↓	

TABLE II. DATASET/RUN NUMBER COLLATION SUMMARY

PART 2: HEAT TRANSFER & BASE PRESSURE RUNS

Dataset Identifier	Run	Config.	Mach	Altitude (K ft)	α	ψ	Chamber Pressure SSME	Chamber Pressure SRB	Nozzle Gimbal Angles #1 SSME P	#1 SSME Y	#2 SSME P	#2 SSME Y	#3 SSME P	#3 SSME Y	Left SRB P	Left SRB Y	Right SRB P	Right SRB Y	GTP
001	9	OTS	2.2	60	-5	0	1500	290	0	0	0	0	0	0	0	0	0	0	No
002	10		2.5	70															
003	11		2.9	80															
004	12		3.5	120	+5														
005	13		2.9	80	0	-5													
006	14		3.5	100															
007	15			120															
008	16			130															
009	17		2.9	80		+5													
010	18		3.5	100															
011	19			120															
012	20			130															
013	21			120		+11													
014	22			130		+11													
015	23			120		-11													
016	24			130		-11													
017	25			120	+5	-5		230/290	0	-2	+1	-2.8	-1	-2.8	0	-2	0	-2	
018	26			130	+5	-5		230/290	0	-2	+1	-2.8	-1	-2.8	0	-2	0	-2	
019	27			120		+5		290/230	0	+2	-1	+2.8	+1	+2.8	0	+2	0	+2	
020	28			130		+5		290/230	0	+2	-1	+2.8	+1	+2.8	0	+2	0	+2	
021	29	OT	3.5	120	0	+7	1500	—	0	0	0	0	0	0	—	—	—	—	No
022	30			130		+7													
023	31			120		-7													
024	32			130		-7													

TABLE II. DATASET/RUN NUMBER COLLATION SUMMARY

PART 2: Concluded

Dataset Identifier	Run	Config.	Mach	Altitude (K ft)	α	ψ	Chamber Pressure SSME	Chamber Pressure SRB	Nozzle Gimbal Angles #1 SSME P	#1 SSME Y	#2 SSME P	#2 SSME Y	#3 SSME P	#3 SSME Y	Left SRB P	Left SRB Y	Right SRB P	Right SRB Y	GTP
025	33	OT	3.5	120	0	-7	1500	—	0	0	0	0	0	0	—	—	—	—	Yes
026	34			130		-7													
027	35			120		+7													
028	36			130		+7													
029	37	OTS	3.5	120	+5	+5	1500	290/230	0	+2	-1	+2.8	+1	+2.8	0	+2	0	+2	Yes
030	38			130															
031	39			120															
032	40			120		-5		230/290	0	-2	+1	-2.8	-1	-2.8	0	-2	0	-2	
033	41			130		-5		230/290	0	-2	+1	-2.8	-1	-2.8	0	-2	0	-2	

TABLE III. MODEL DIMENSIONAL DATA

MODEL COMPONENT: BODY - B_{64}

GENERAL DESCRIPTION: The body is to the Baseline Definition Space Shuttle Vehicle Configuration 5, MCR 200, Rev. 7 dated 10-17 "74

MODEL SCALE: .0225

DRAWING NUMBER: VC70-000002, #MDV-70 Baseline IML

DIMENSIONS:	FULL-SCALE	MODEL SCALE
Length: OML X_0 = 235-1538.3 In.	1293.3	29.099
Ref. Length: OML X_0 = 238-1528.3 In.	1290.3	29.032
*Length (IML X_0 = 239.5) In.	1288.8	28.998
OML Max. Width. In. X_0 = 1516.801	262.718	5.911
IML Max. Width. In. X_0 = 1516.301	260.718	5.866
OML Max. Depth. In. X_0 = 1463.316	248.575	5.593
IML Max. Depth. In. X = 1463.316	246.575	5.548
OML Fineness Ratio	5.203	5.203
IML Fineness Ratio	5.227	5.227
Area Ft^2		
Max. Cross-Sectional @ X_0 = 1463.316	340.82	0.173
Planform		
Wetted		
Base		

DSM 387-2 Exp. Date 8/2/73

TABLE III. MODEL DIMENSIONAL DATA (Continued)

MODEL COMPONENT: CANOPY C_{16} Orbiter 102

GENERAL DESCRIPTION: Orbiter 102 Canopy per MCR 1750

R1 Baseline

Scale: 0.0225

DRAWING NUMBER: VC70-000002A, MD-V70

DIMENSIONS:	FULL-SCALE	MODEL SCALE
Length, in, X_0 = 433.0793 to X_0 = 670	236.9207	5.331
Max. Width, In. @ X_0 = 594	194.4394	4.375
Max. Depth, In. @ X_0 = 492	58.8007	1.323
Fineness Ratio		
Area - FT^2		
Max. Cross-Sectional @ X_0 = 520	45.6558	0.0231
Planform		
Wetted		
Base		

TABLE III. MODEL DIMENSIONAL DATA (Continued)

MODEL COMPONENT : ELEVON - E_{63}

GENERAL DESCRIPTION : Elevon for Configuration 5, hingeline at X_0 = 1387, Elevon split line, Y_0 = 312.5 6.0" gaps beveled edges, and centerbodies "OML" used on W_{129} Ref. MCR 200, Rev. 7, dated 10-17-74.

MODEL SCALE: 0.0225

DRAWING NUMBER : VC70-000002A

DIMENSIONS :	FULL SCALE	MODEL SCALE
Area used for C_{He} computation	210.0	0.106
Area - FT^2	206.57	0.105
Span (equivalent), In.	346.44	7.795
Inb'd equivalent chord, In.	116.50	2.621
Outb'd equivalent chord, In.	55.219	1.242
Ratio movable surface chord/ total surface chord		
At Inb'd equiv. chord	0.2137	0.2137
At Outb'd equiv. chord	0.3999	0.3999
Sweep Back Angles, degrees		
Leading Edge	0.00	0.00
Trailing Edge	- 10.056	- 10.056
Hingeline	0.000	0.000
Area Moment (Area X MAC) - FT^3	1540.74	0.0175
Mean Aerodynamic chord, In.	89.50	2.014

TABLE III. **MODEL DIMENSIONAL DATA** (Continued)

MODEL COMPONENT: BODY FLAP (OUTER MOLD LINES): F_{14}

GENERAL DESCRIPTION: Orbiter body flap vehicle 5 Configuration, MCR 200, Rev. 7. "OML" to be used with B_{64} Hingeline X_O 1532.0 Y_O = -1280.

MODEL SCALE: 0.0225

DRAWING NUMBER: VC70-000002, MDV-70

DIMENSIONS:	**FULL SCALE**	**MODEL SCALE**
Area (Total) Ft^2	134.125	0.068
Span (equivalent), In.	238.00	5.355
Inb'd equivalent chord, In.	81.00	1.823
Outb'd equivalent chord, In.	81.00	1.823
Ratio movable surface chord/ total surface chord		
At Inb'd equiv. chord		
At Outb'd equiv. chord		
Sweep Back Angles, degrees		
Leading Edge	0.0	0.0
Trailing Edge	0.0	0.0
Hingeline	0.0	0.0
Area Moment (Product of $\bar{c}$ & Area) Ft^3	905.344	0.0103
Mean Aerodynamic Chord In.	81.0	1.823

TABLE III. MODEL DIMENSIONAL DATA (Continued)

MODEL COMPONENT: OMS PODS (OML) - M_{18}

GENERAL DESCRIPTION: Vehicle 5 configuration MCR 200, Rev. 7, Orbiter OMS pod - short pod.

MODEL SCALE: 0.0225

DRAWING NUMBER: VC70-000002, VL70-008410, MDV-70

DIMENSIONS:	FULL-SCALE	MODEL SCALE
Length, In. (X_O1311 to 1511)	200.00	4.500
Max. Width, In. (X_P304, X_O1511)	135.75	3.054
Max. Depth, In. (X_P304, X_O1511	74.50	1.676
Fineness Ratio	1.937	1.937
Area - Ft^2		
Max. Cross-Sectional @ X_p 304	58.169	0.029
Planform		
Wetted		
Base		

TABLE III. MODEL DIMENSIONAL DATA (Continued)

MODEL COMPONENT: OMS NOZZLES - N_{92}

GENERAL DESCRIPTION: The two orbiter maneuvering system nozzles are laval-bell shaped and are located at the aft end of the OMS pod. OMS nozzles in stowed position are outboard 9° and down 7° from null position.

MODEL SCALE: 0.0225

DRAWING NUMBER: VD70-000002, SS-A01240

DIMENSIONS:	FULL SCALE	MODEL SCALE
MACH NO.		
Length - In.		
Gimbal Point to Exit Plane	56.00	1.260
Throat to Exit Plane		
Diameter - In.		
Exit	50.00	1.125
Throat	27.778	0.625
Inlet		
Area - ft^2		
Exit	13.634	0.0069
Throat	4.205	0.0021
Gimbal Point (Station) - In.		
Left Nozzle		
X_0	1518.00	34.155
Y_0	- 88.00	- 1.980
Z_0	492.00	11.070
Nozzles		
X_0	1518.00	34.155
Y_0	+ 88.0	+ 1.980
Z_0	492.0	11.070
Null Position - Deg.		
Left Nozzle		
Pitch	15°49' Up	15°49' Up
Yaw	6°30' Outb'd	6°30' Outb'd
Right Nozzle		
Pitch	15°49' Up	15°49' Up
Yaw	6°30' Outb'd	6°30' Outb'd

TABLE III. MODEL DIMENSIONAL DATA (Continued)

MODEL COMPONENT: MPS NOZZLES - N_{94}

GENERAL DESCRIPTION: The main propulsion nozzles are laval-bell shaped and are located on the aft planes of the orbiter. The dimensions are external and not to be scaled for plume tests.

MODEL SCALE: 0.0225

DRAWING NUMBER: VC70-000002, VL70-008144, RS09189, SS-A01216

DIMENSIONS:

	FULL SCALE	MODEL SCALE
MACH NO.		
Length - In.		
Gimbal Point to Exit Plane	156.69	3.526
Throat to Exit Plane		
Diameter - In.		
Exit	93.75	2.109
Throat		
Inlet		
Area - ft^2		
Exit	1445.00	0.732
Throat		
Gimbal Point (Station) - In.		
Upper Nozzle		
X_O	1445.00	32.513
Y_O	0.00	0.0
Z_O	443.00	9.968
Lower Nozzles		
X_O	1468.170	33.034
Y_O	+ 53.00	± 1.193
Z_O	34.264	0.771
Null Position - Deg.		
Upper Nozzle		
Pitch	16.0° Up	16.0° Up
Yaw	0.0°	0.0°
Lower Nozzle		
Pitch	10.0° Up	10.0° Up
Yaw	3.5° Outb'd	3.5° Outb'd

TABLE III. MODEL DIMENSIONAL DATA (Continued)

MODEL COMPONENT: VERTICAL - V_{23}

GENERAL DESCRIPTION: The vertical tail is double wedge shaped and mounted dorsally on the aft fuselage. These data correspond to Vehicle 5 configuration, MCR 200, Rev. 7.

MODEL SCALE: 0.0225

DRAWING NUMBER: VC70-000002, master dimensions.

DIMENSIONS:

	FULL SCALE	MODEL SCALE
TOTAL DATA		
Area (Theo) - Ft^2		
Planform	413.253	0.209
Span (Theo) - In.	315.72	7.104
Aspect Ratio	1.675	1.675
Rate of Taper	0.507	0.507
Taper Ratio	0.404	0.404
Sweep-Back Angles, Degrees.		
Leading Edge	45.00	45.00
Trailing Edge	26.25	26.25
0.25 Element Line	41.13	41.13
Chords:		
Root (Theo) WP	268.50	6.041
Tip (Theo) WP	108.47	2.441
MAC	199.81	4.496
Fus. Sta. of .25 MAC	1463.50	32.929
W.P. of .25 MAC	635.52	14.299
B.L. of .25 MAC	0.0	0.0
Airfoil Section		
Leading Wedge Angle - Deg.	10.0	10.0
Trailing Wedge Angle - Deg.	14.92	14.92
Leading Edge Radius	2.00	0.045
Void Area	13.17	0.007
Blanketed Area	0.00	0.00

MODEL COMPONENT: WING-W129

GENERAL DESCRIPTION: The wing is the primary lifting device and is mounted horizontally and is symmetric about the plane $Y_0 = 0$. A cuff fairs the fuselage to the wing's leading edge @ T_0 940 to 1084.

MODEL SCALE: 0.0225

TEST NO. DWG. NO.

DIMENSIONS:	FULL-SCALE	MODEL SCALE
TOTAL DATA		
Area (Theo.) Ft^2		
Planform	2690.00	1.362
Span (Theo In.	936.68	21.075
Aspect Ratio	2.265	2.265
Rate of Taper	1.177	1.177
Taper Ratio	0.200	0.200
Dihedral Angle, degrees	3.500	3.500
Incidence Angle, degrees	0.500	0.500
Aerodynamic Twist, degrees		
Sweep Back Angles, degrees		
Leading Edge	45	45
Trailing Edge	10.056	10.056
0.25 Element Line	35.209	35.209
Chords:		
Root (Theo) B.P.0.0.	689.243	15.508
Tip, (Theo) B.P.	137.849	3.102
MAC	474.812	10.683
Fus. Sta. of .25 MAC	1136.834	25.579
W.P. of .25 MAC	290.857	6.544
B.L. of .25 MAC	182.132	4.098
EXPOSED DATA		
Area (Theo) Ft^2	1751.50	0.887
Span, (Theo) In. BP108	720.68	16.215
Aspect Ratio	2.060	2.060
Taper Ratio	0.245	0.245
Chords		
Root BP108	562.090	12.64
Tip 1.00 $\frac{b}{2}$	137.849	3.102
MAC	392.826	8.839
Fus. Sta. of .25 MAC	1186.50	26.696
W.P. of .25 MAC	293.683	6.608
B.L. of .25 MAC	251.769	5.665
Airfoil Section (Rockwell Mod NASA) XXXX-64		
Root $\frac{b}{2}$ =	0.1136	0.1136
Tip $\frac{b}{2}$ =	0.120	0.120
Data for (1) of (2) Sides		
Leading Edge Cuff Planform Area Ft^2	145.4	0.074
Leading Edge Intersects Fus M. L. @ Sta	500.0	11.25
Leading Edge Intersects Wing @ Sta	1084.0	24.39

TABLE III. MODEL DIMENSIONAL DATA (Continued)

MODEL COMPONENT: BOOSTER SOLID ROCKET MOTOR - S_{22}

GENERAL DESCRIPTION: The BSRM is an external propulsion system which is jettisoned and recoverable after burnout. The BSRM's can be refurbished and reused after recovery.

MODEL SCALE: 0.0225

DRAWING NUMBER: VC77-000002C VC70-000002A, VC72-000002C

DIMENSIONS:	**FULL-SCALE**	**MODEL SCALE**
Length, In.	1789.60	40.266
Max. Width, Tank Dia. In.	146.00	3.285
Max. Depth, Aft Shroud Dia., In.	208.20	4.685
Fineness Ratio	8.596	8.596
Area - Ft^2		
Max. Cross-Sectional	236.423	0.120
Planform		
Wetted		
Base		
WP of BSRM centerline (Z_T)	400.0	9.000
FS of BSRM nose (X_T)	743.0	16.718
BP of BSRM centerline (Y_T)	250.5	5.636

TABLE III. MODEL DIMENSIONAL DATA (Continued)

MODEL COMPONENT: SOLID ROCKET BOOSTER NOZZLES - N_{106}

GENERAL DESCRIPTION: SRB nozzle to new lines to use with S_{22}

MODEL SCALE: 0.0225

DRAWING NUMBER: VC77-000002D

DIMENSIONS:

	FULL SCALE	MODEL SCALE
MACH NO.		
Length - In.		
Gimbal Point to Exit Plane		
Throat to Exit Plane		
Diameter, D_{ex} - In. (I.D.)	145.64	3.277
Diameter, D_{ex} - In. (O.D.)	147.64	3.322
Diameter, DT - In.	-	-
Diameter, D_{in} - In.	-	-
Area - ft²	115.688	0.059
Exit		
Throat		
Gimbal Point (Station) - In.		
Left Nozzle		
X_B - cold	1863.458	41.928
X_B - hot	1875.358	42.196
Y_O	-250.50	-5.636
Z_T	400.0	0.000
Right Nozzles		
X_B	1863.458	41.928
X_B	1875.358	42.196
Y_O	250.50	5.636
Z_T	400.0	9.000
Null Position - Deg.		
Left **Nozzle**		
Pitch	0	0
Yaw	0	0
Right **Nozzle**		
Pitch	0	0
Yaw	0	0

TABLE III. MODEL DIMENSIONAL DATA (Concluded)

MODEL COMPONENT: EXTERNAL TANK - T_{33}

GENERAL DESCRIPTION: External tank with spike nose. Dimensions are calculated to the outer mold line (OML).

MODEL SCALE: 0.0225

DRAWING NUMBER: VC78-000002B Spike nose Dwg. No.: 82600203049

DIMENSIONS:	**FULL-SCALE**	**MODEL SCALE**
Length	1852.486	41.681
Max. *Dia. (OML), In.	333.00	7.493
Max. Depth		
Fineness Ratio	5.563	5.563
Area		
Max. Cross-Sectional	604.807	0.306
Planform		
Wetted		
Base		

DSM 387-2 Exp. Date 8/2/73

TABLE IV. INSTRUMENTATION NUMBERING SYSTEM

Component Or Instrumentation	Number Series	Actual Numbers: Comp. or Instr.	Actual Numbers: Numbers
Orbiter	1 - 200	Total Thin-Film Gauges	1 - 119
		Radiation Gauges	120 - 134
		PCB Transducer Locations	135 - 161
External Tank	201 - 300	Total Thin-Film Gauges	201 - 229,237
		Radiation Gauges	230 - 233
		PCB Transducer Locations	234 - 236
SRB's	301 - 400	Total Thin-Film Gauges	301 - 320, 326 - 329
		Radiation Gauges	321 - 322
		PCB Transducers Locations	323 - 325
Reference Static Pressures	501 - 600	Orbiter	501 - 513
		External Tank	514 - 516
Thermocouples	601 - 699	See Table V for breakdown	
Model Operating Pressures	700 - 750	SSME Pc	700
		Left SRB Pc	701
		Right SRB Pc	702
		O_2 Venturi	703
		H_2 Venturi	704
		O_2 Injector	705
		H_2 Injector	706
Gas Temperature Probes	751 - 799	Orbiter	752 - 754
		External Tank	756 - 758
		SRB (Left Hand)	759
Hatband Nozzle	166 - 180	Total Thin-Film Gauges (Flat and contoured)	166 - 180

TABLE V. THERMOCOUPLE LOCATIONS

NUMBER	LOCATION	TYPE
601	Orbiter base heat shield (attached)	Chromel-Alumel
602	Orbiter base heat shield	↓
603	Orbiter base heat shield	
604	ET base cavity	
605	ET base cavity	
606	Left OMS pod	
607	Right OMS pod	
608	Valcor valve cavity	
609	Valcor valve cavity	
610	Hydrogen charge tube	Iron Constantan (Type J)
611	Oxygen charge tube	Iron Constantan (Type J)
612	Left SRB shroud	Chromel-Alumel
613	Right SRB shroud	↓
616	Venturi housing	
622	Gas Temperature Probe (GTP) 752 (Orbiter)	Iron Constantan (Type J)
623	GTP 753 ↓	↓
624	GTP 754	
626	GTP 756 (External Tank)	
627	GTP 757 ↓	
628	GTP 758	
629	GTP 759 (Left SRB Skirt Curtain)	

TABLE VI. INSTRUMENTATION PATTERNS

PATTERN	DESCRIPTION	RUNS USED
1	First-Stage Configuration (OTS) (W/O Gas Temperature Probes)	9 - 28
2	First-Stage Configuration (OTS) (W/GTP)	37 - 41
3	Second-Stage Configuration (OT) (W/O GTP)	29 - 32
4	Second-Stage Configuration (OT) (W/GTP) (Orbiter GTP Only)	33 - 36

TABLE VII. INSTRUMENTATION SIGNAL CONDITIONING

INSTRUMENTATION	EXCITATION		SERIES	CADDE	AMPLIFIER		TIME
	VOLTAGE	CURRENT	RESISTOR	SYSTEM	TYPE	GAIN	CONSTANT
PCB Pressure Transducers [1]	22V	12mA			Preston	1	10 sec.
Thin-Film Gauges	10V	10mA	1K	10V System ($10V = 10^4$ counts)	Preston (Grounded gauges only)	1	2 sec.
Gas Temperature Probes	10V	1mA	10K	50mV System ($50mV = 10^4$ counts)	Preston	Variable [2]	2 sec.
Thermocouples	150° Reference Junction			50mV System			

(1) PCB transducer excitation was supplied by a 110V multi-channel power unit. Kistler transducers were supplied by the facility; signal conditioning is unknown.

(2) Most common GTP Preston amplifier gains were: Orbiter and ET - Short wire = 200
Long wire = 50
SRB - Short wire = 500
Long wire = 100

TABLE VIII. TRANSDUCER/THERMOCOUPLE CORRELATION

TRANSDUCER LOCATION	ORIFICE LOCATION ON MODEL	TRANSDUCER LOCATION IN MODEL	THERMOCOUPLES FOR DETERMINING TRANSDUCER TEMPERATURE
135	Orbiter Fuselage (left)	Venturi Housing	616
136	Orbiter Fuselage (left)	Behind Orbiter Base	Average 601, 602, 603
137	Upper Body Flap	↓	↓
138	Lower Body Flap	↓	↓
139	Body Flap Trailing Edge	↓	↓
140	Left OMS Pod Base	Left OMS Pod	606
141	↓	↓	↓
142	↓	↓	↓
143	Right OMS Pod Base	Right OMS Pod	607
145	Orbiter Base Heat Shield	Behind Orbiter Base	Average 601, 602, 603
146	↓	↓	↓
147	↓	↓	↓
148	↓	↓	↓
149	↓	↓	↓
150	↓	↓	↓
151	↓	↓	↓
152	↓	↓	↓
153	↓	↓	↓

TABLE VIII. TRANSDUCER/THERMOCOUPLE CORRELATION (Concluded)

TRANSDUCER LOCATION	ORIFICE LOCATION ON MODEL	TRANSDUCER LOCATION IN MODEL	THERMOCOUPLES FOR DETERMINING TRANSDUCER TEMPERATURE
154	Orbiter Base Heat Shield	Behind Orbiter Base	Average 601, 602, 603
155	↓	↓	↓
156	↓	↓	↓
157	↓	↓	↓
158	↓	↓	↓
160	#2 SSME Nozzle	↓	↓
161	#3 SSME Nozzle	↓	↓
234	External Tank Base	Behind ET Base	Average 604, 605
235	↓	↓	↓
236	↓	↓	↓
324	Left SRB Shroud	Under Left SRB Shroud	612
325	Right SRB Shroud	Under Right SRB Shroud	613

TABLE IX. REFERENCE PRESSURE ASSIGNMENTS

TRANSDUCER LOCATION NO.	TRANSDUCER ORIFICE LOCATION ON MODEL	REFERENCE PRESSURE NO.
135	Orbiter Fuselage (Left Side)	501
136	↓	502
137	Upper Body Flap	508
138	Lower Body Flap	503
139	Body Flap Trailing Edge	504
140	Left OMS Pod	505
141	↓	505
142	↓	506
143	Right OMS Pod Side	507
145	Orbiter Base Heat Shield	508
146	↓	509
147	↓	510
148	↓	509
149	↓	511
150	↓	511
151	↓	511
152	↓	512
153	↓	512
154	↓	508
155	↓	509

TABLE IX. REFERENCE PRESSURE ASSIGNMENTS (Concluded)

TRANSDUCER LOCATION NO.	TRANSDUCER ORIFICE LOCATION ON MODEL	REFERENCE PRESSURE NO.
156	Orbiter Base Heat Shield	508
157	↓	509
158	↓	509
160	#2 SSME Nozzle	513
161	#3 SSME Nozzle	513
234	External Tank Base	514
235	↓	515
236	↓	516
324	Left SRB Nozzle	None Required
325	Right SRB Nozzle	None Required

NOTES: 1. Gimbal angle deflection is away from null.
2. Positive pitch is nozzle trailing edge down.
3. Positive yaw is nozzle trailing edge left.
4. (P) is the absolute magnitude of the angle.
5. (Y) is measured counterclockwise from the positive yaw axis.

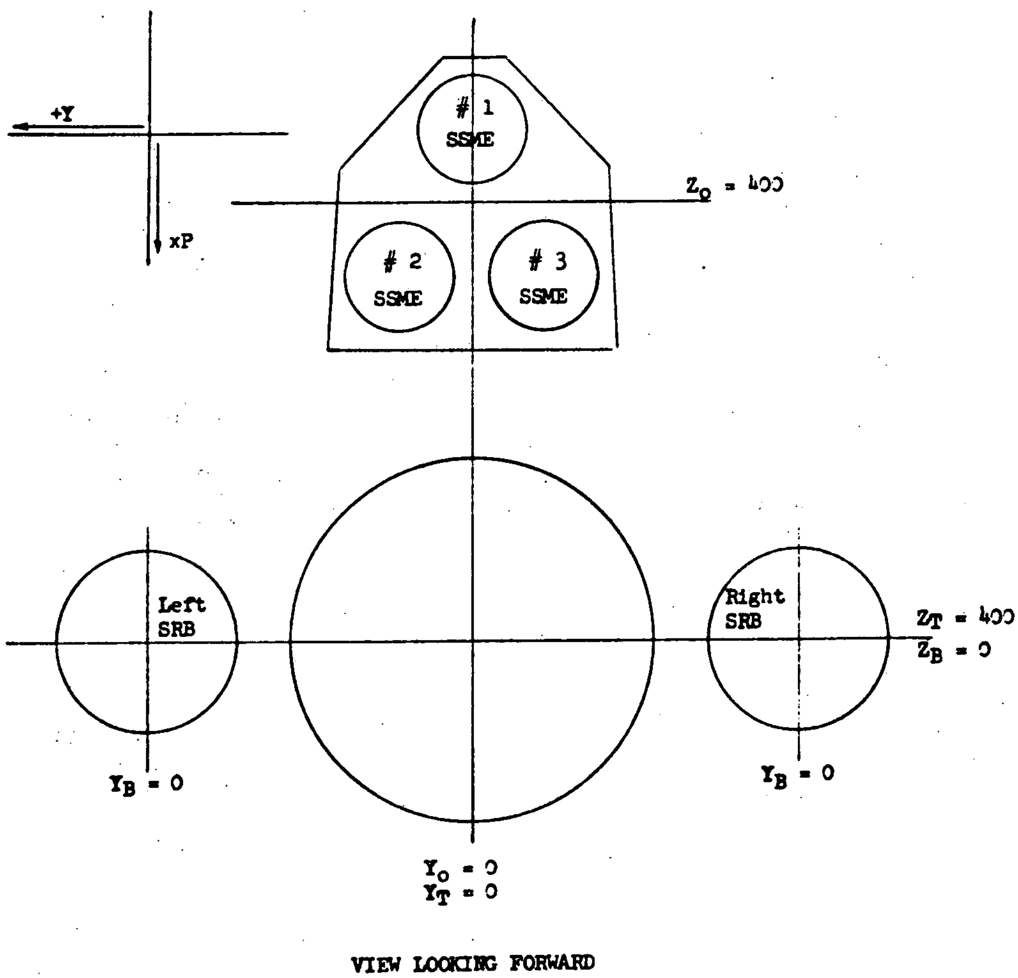

Figure 1. Gimbal angle definition.

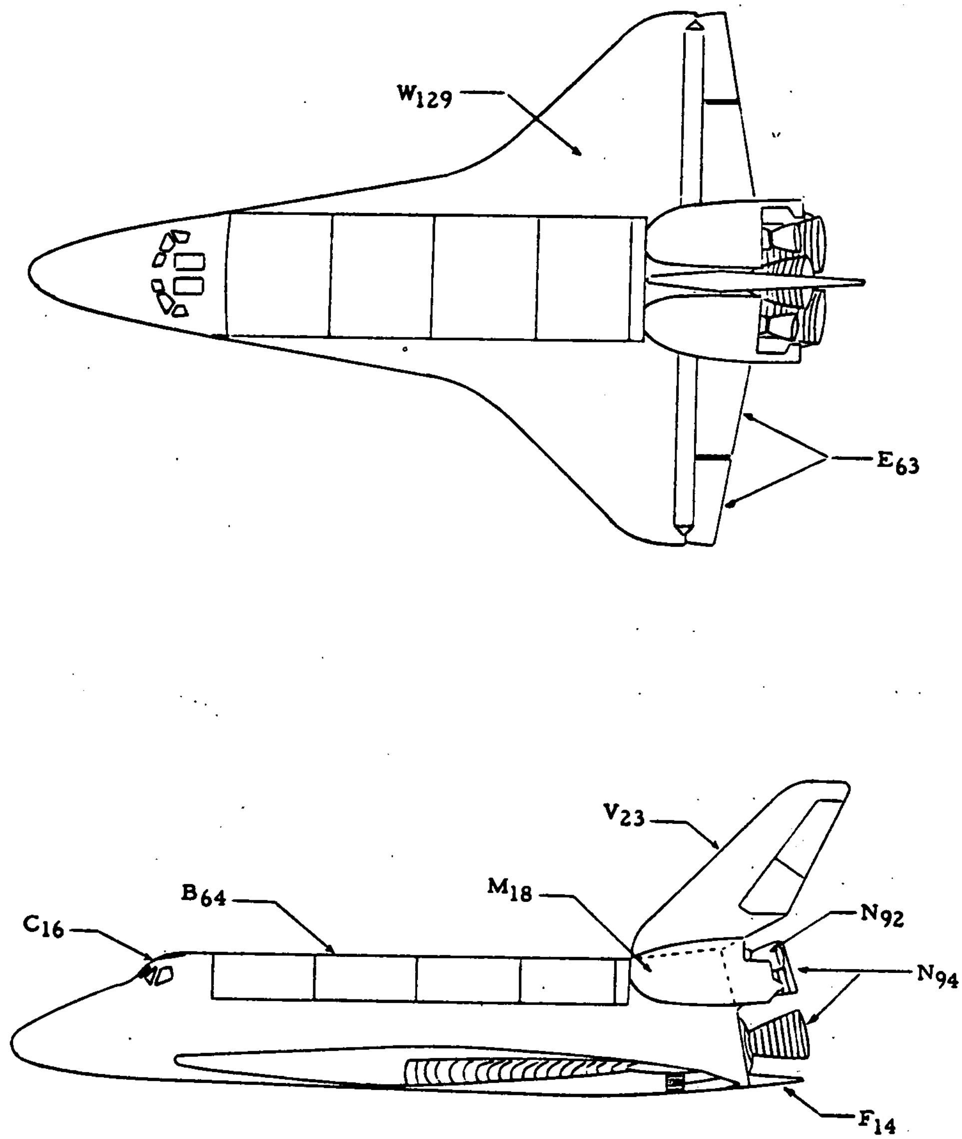

Figure 2. Orbiter vehicle.

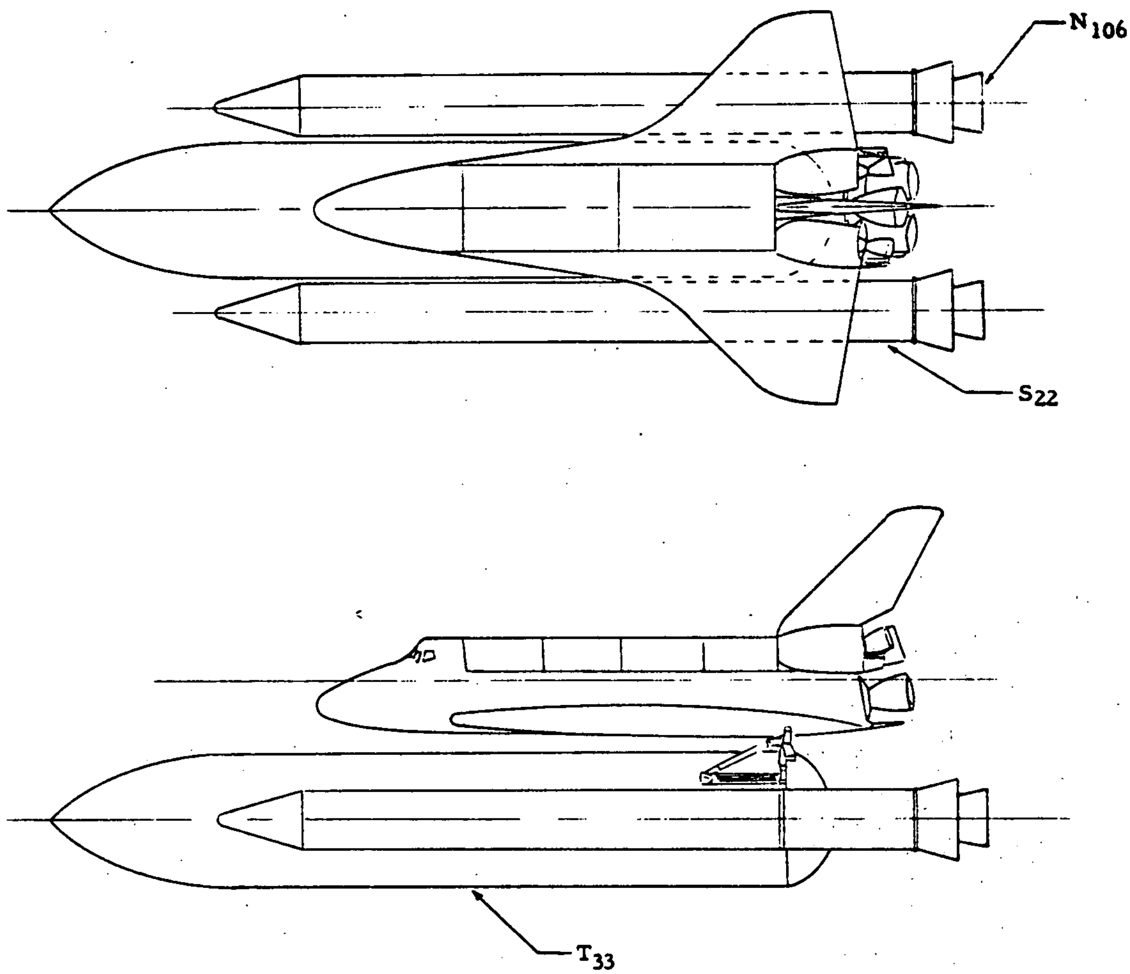

Figure 3. Integrated vehicle.

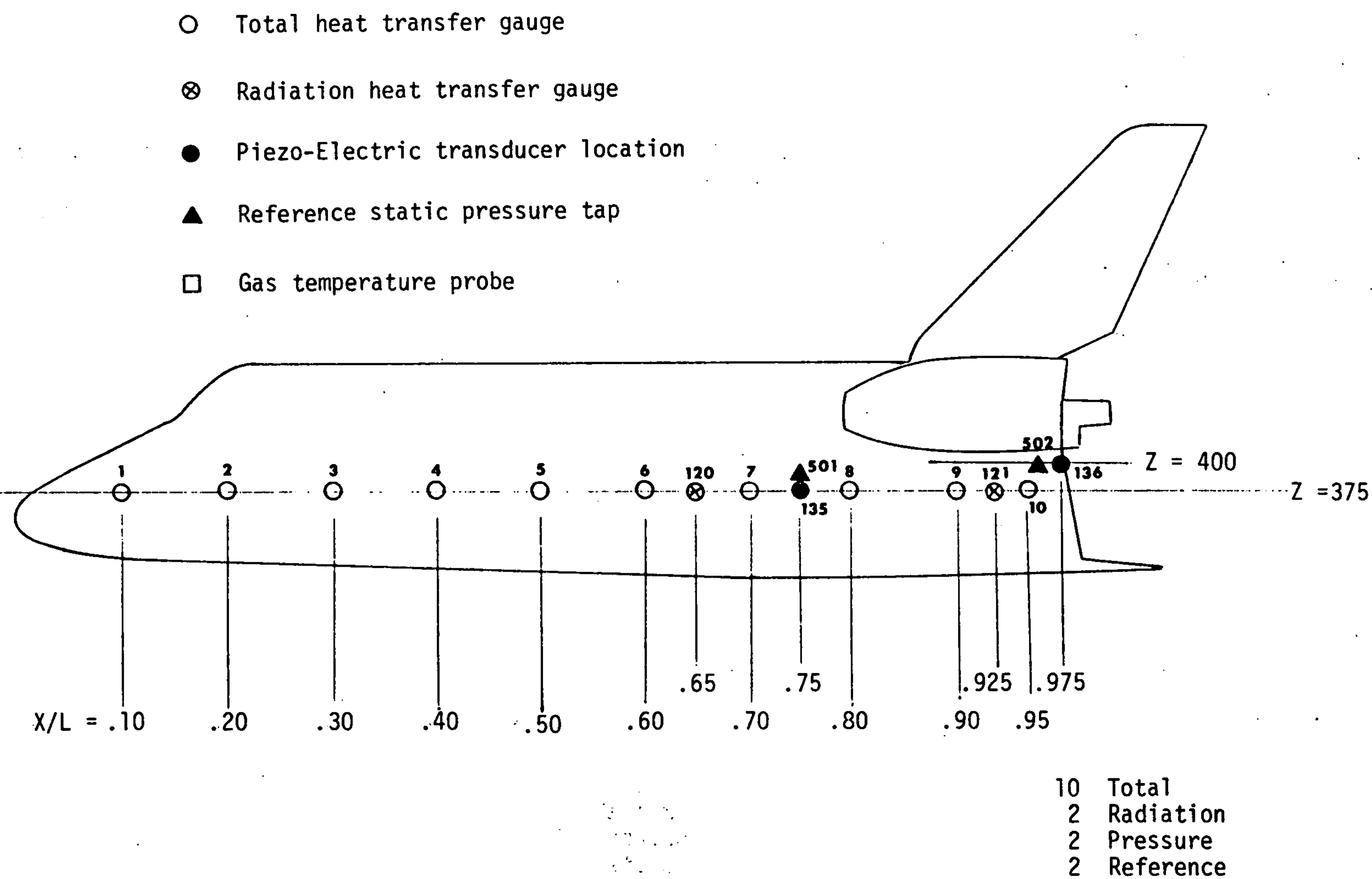

a. Orbiter Side
Figure 4. Instrumentation

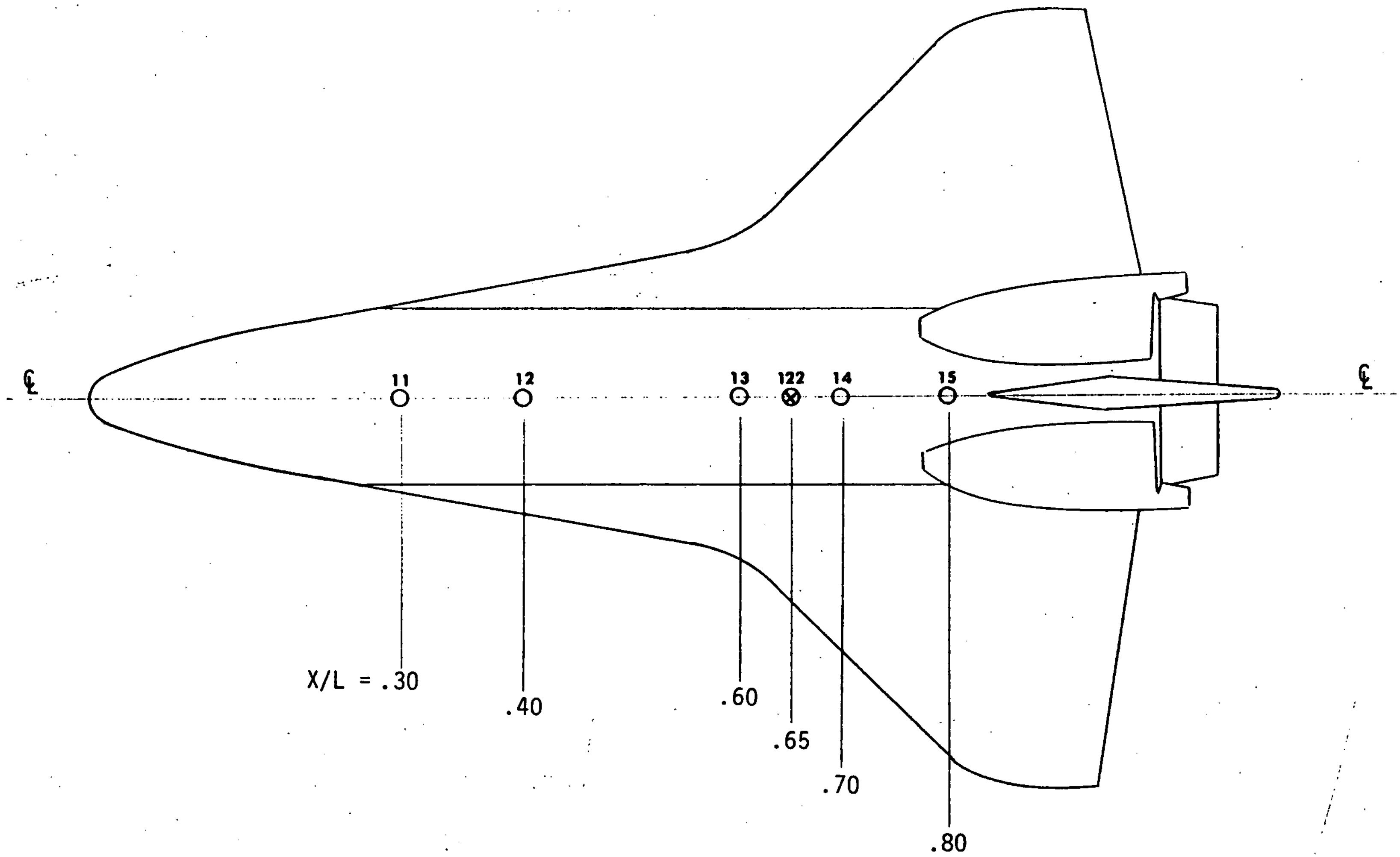

5 Total
1 Radiation

b. Orbiter Top
Figure 4. Continued.

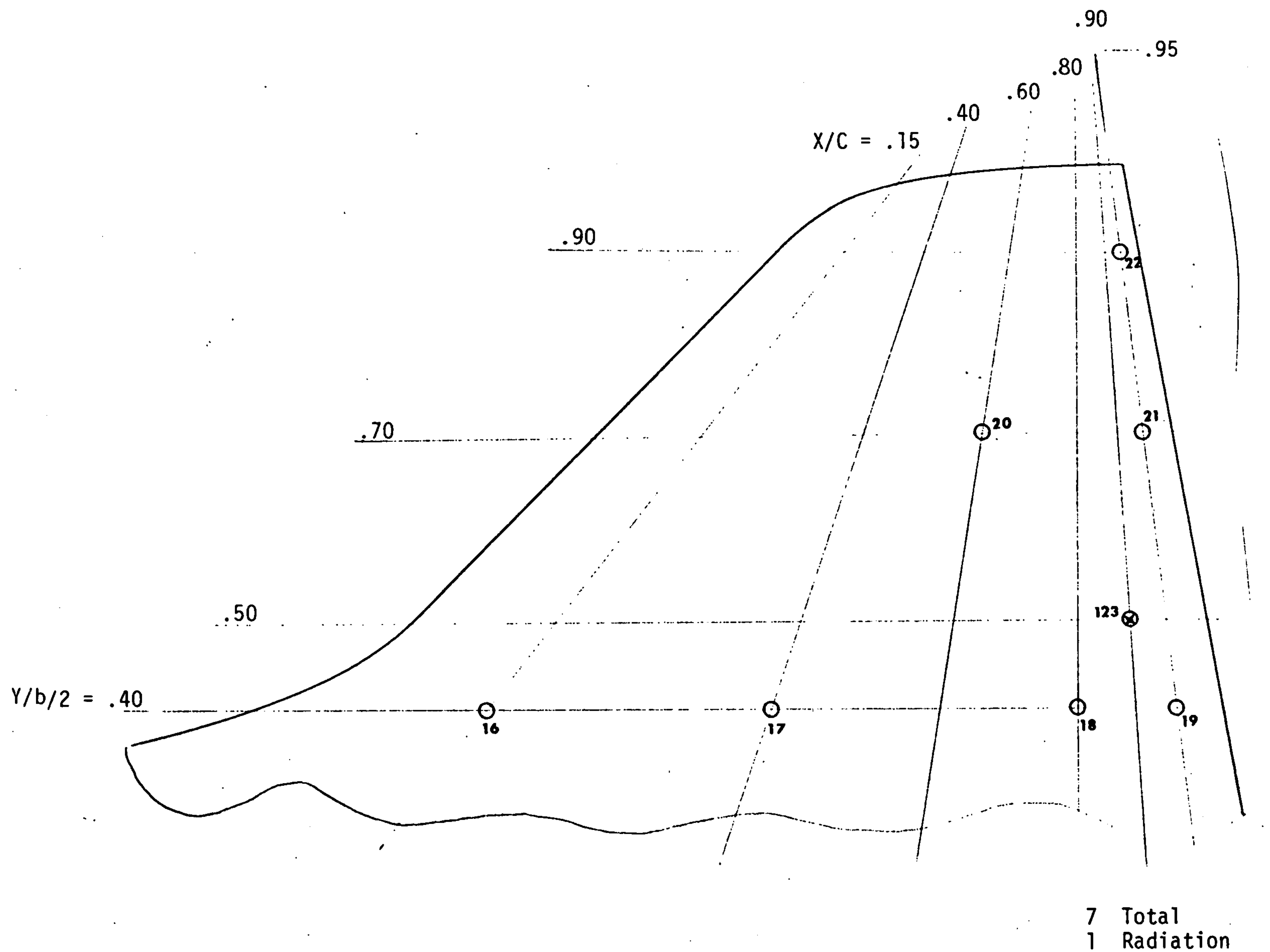

c. Wing Lower Surface
Figure 4. Continued.

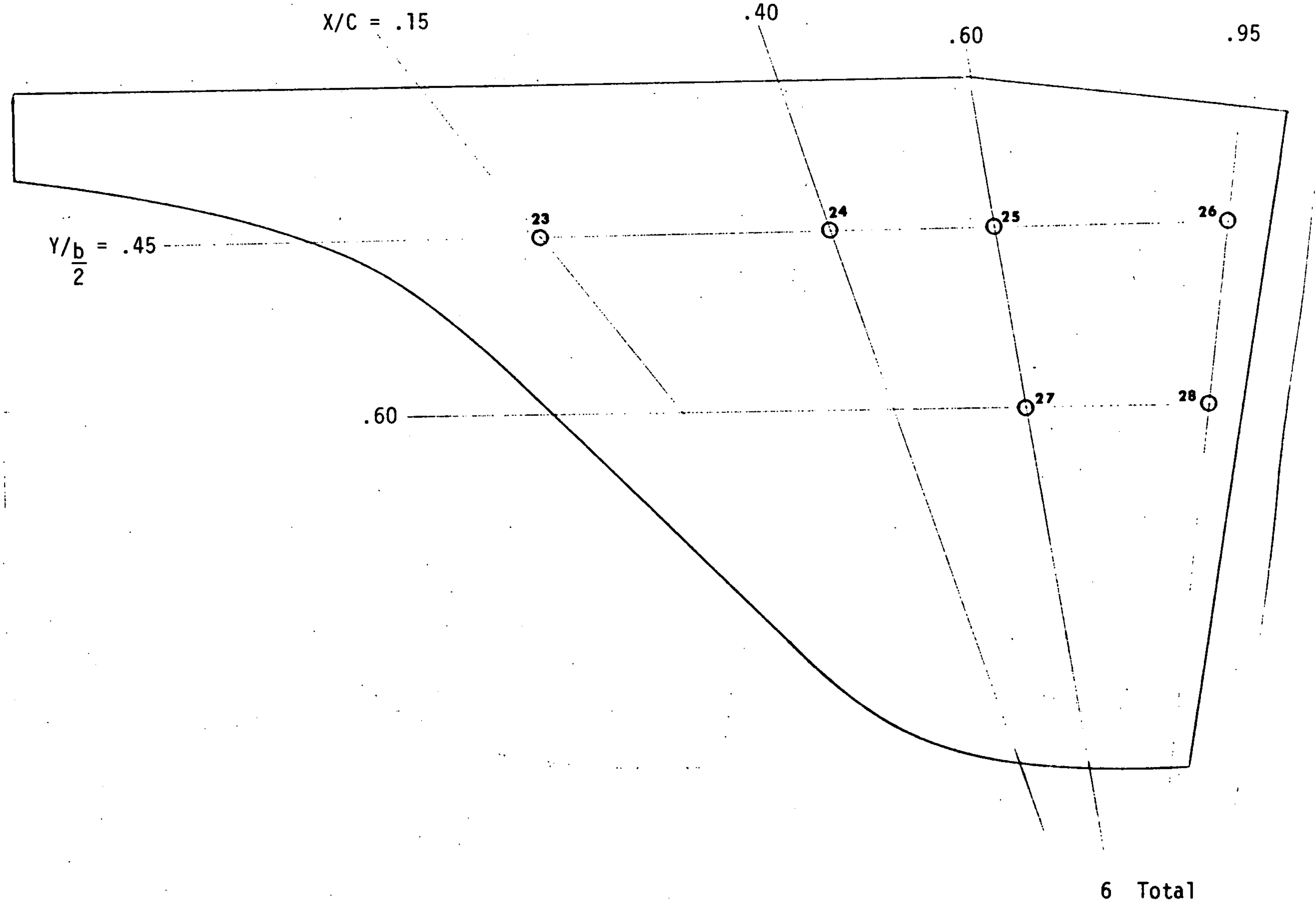

d. Wing Upper Surface
Figure 4. Continued.

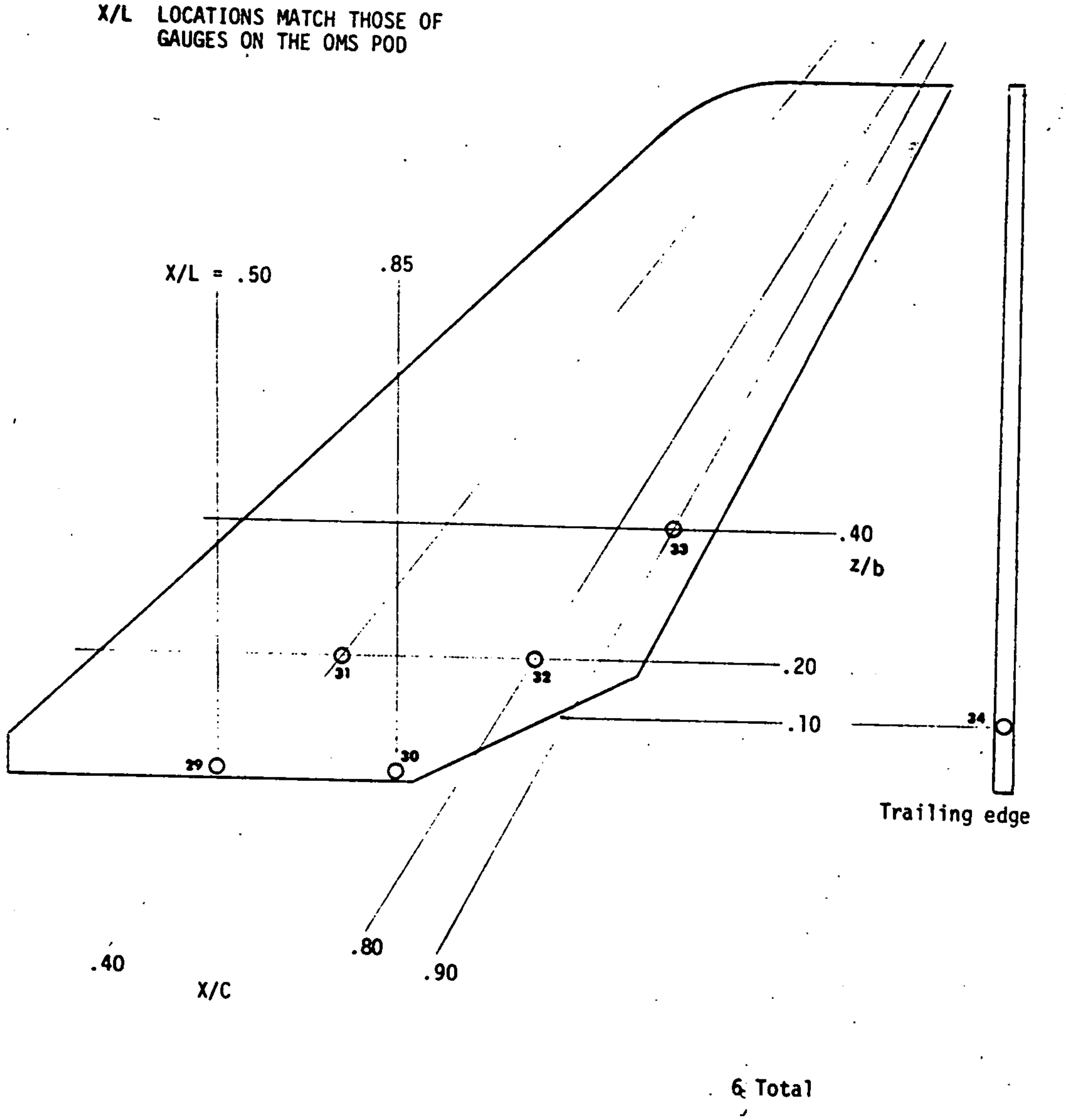

e. Vertical Tail
Figure 4. Continued.

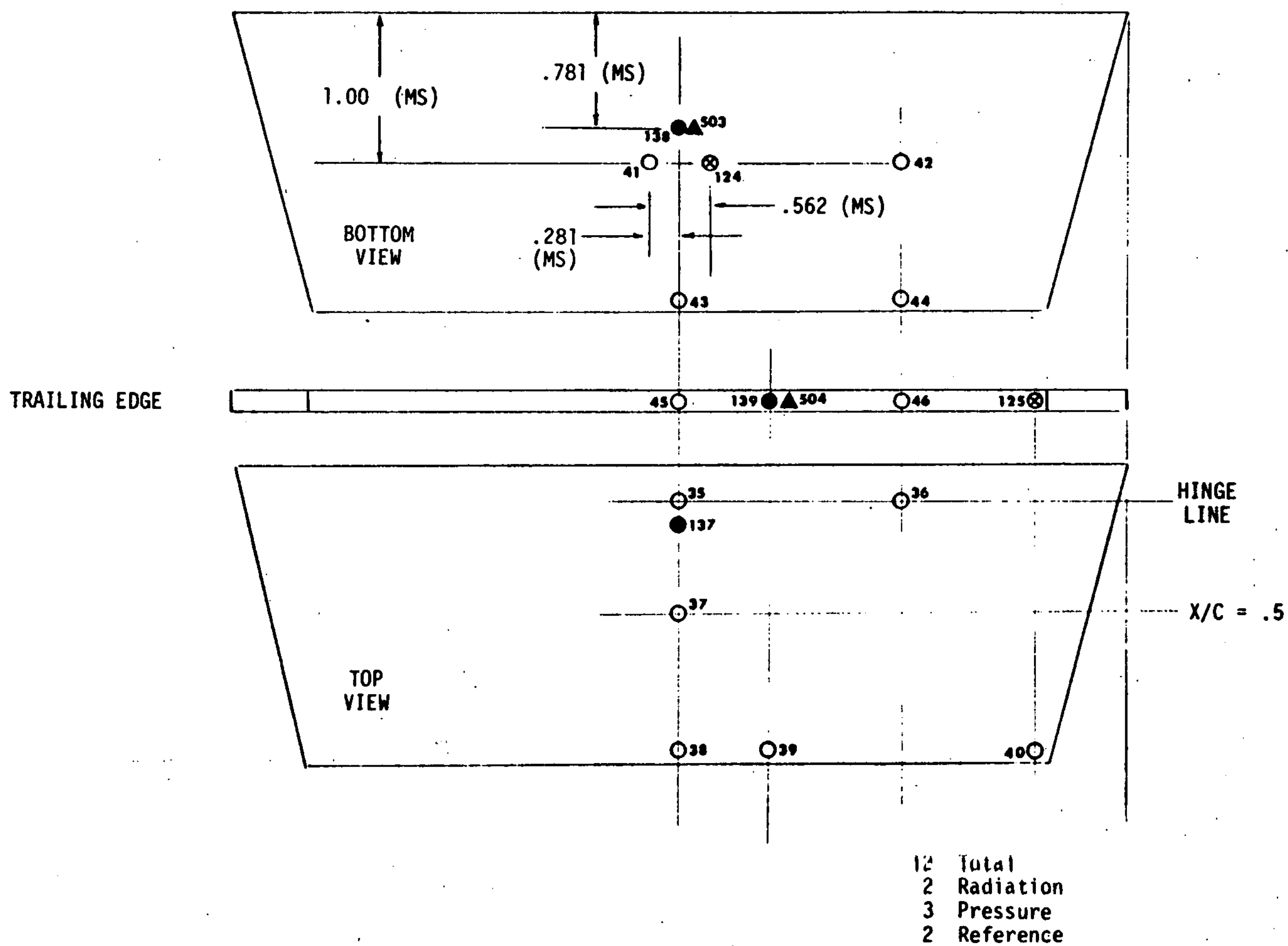

f. Body Flap
Figure 4. Continued.

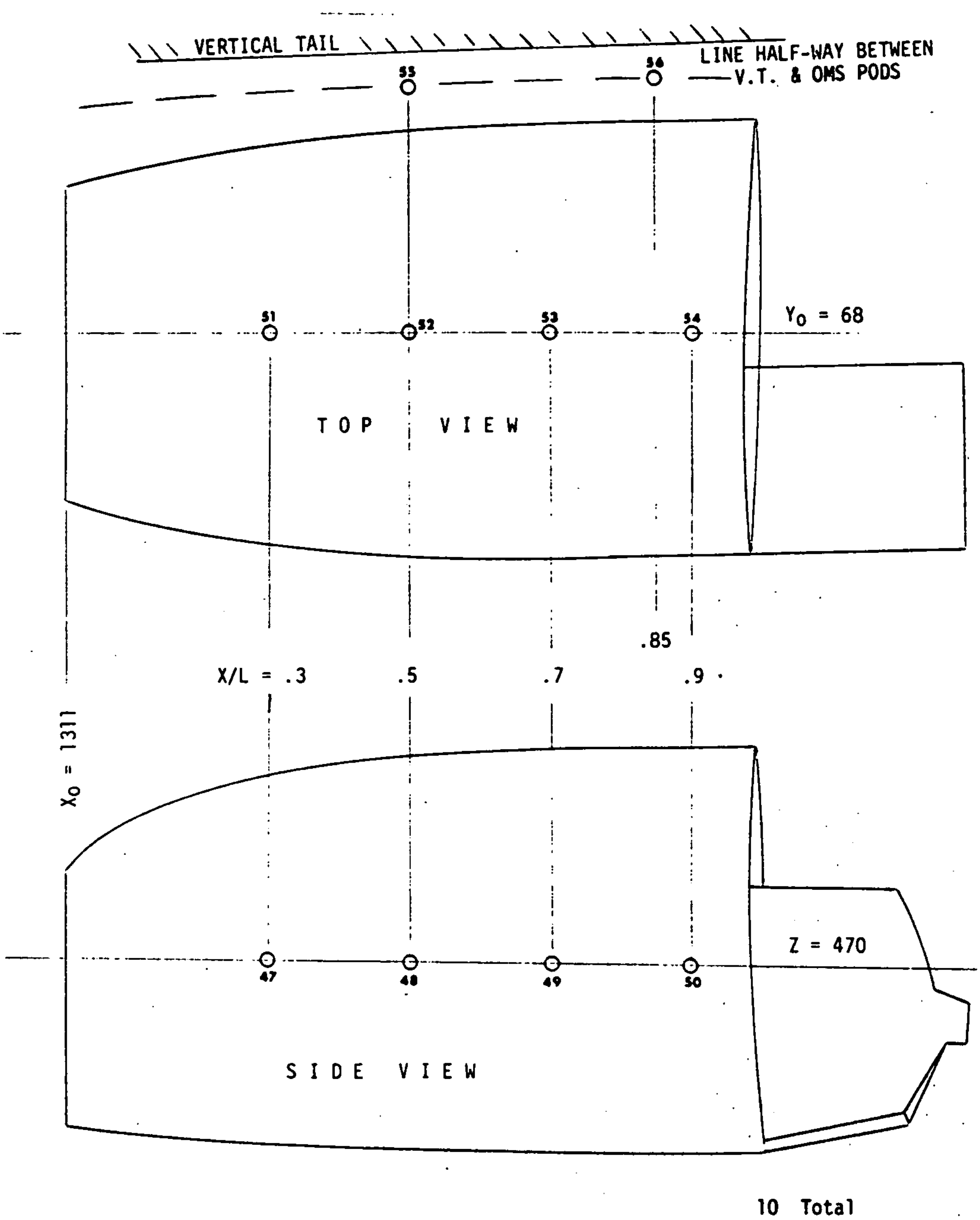

g. Left OMS Pod
Figure 4. Continued.

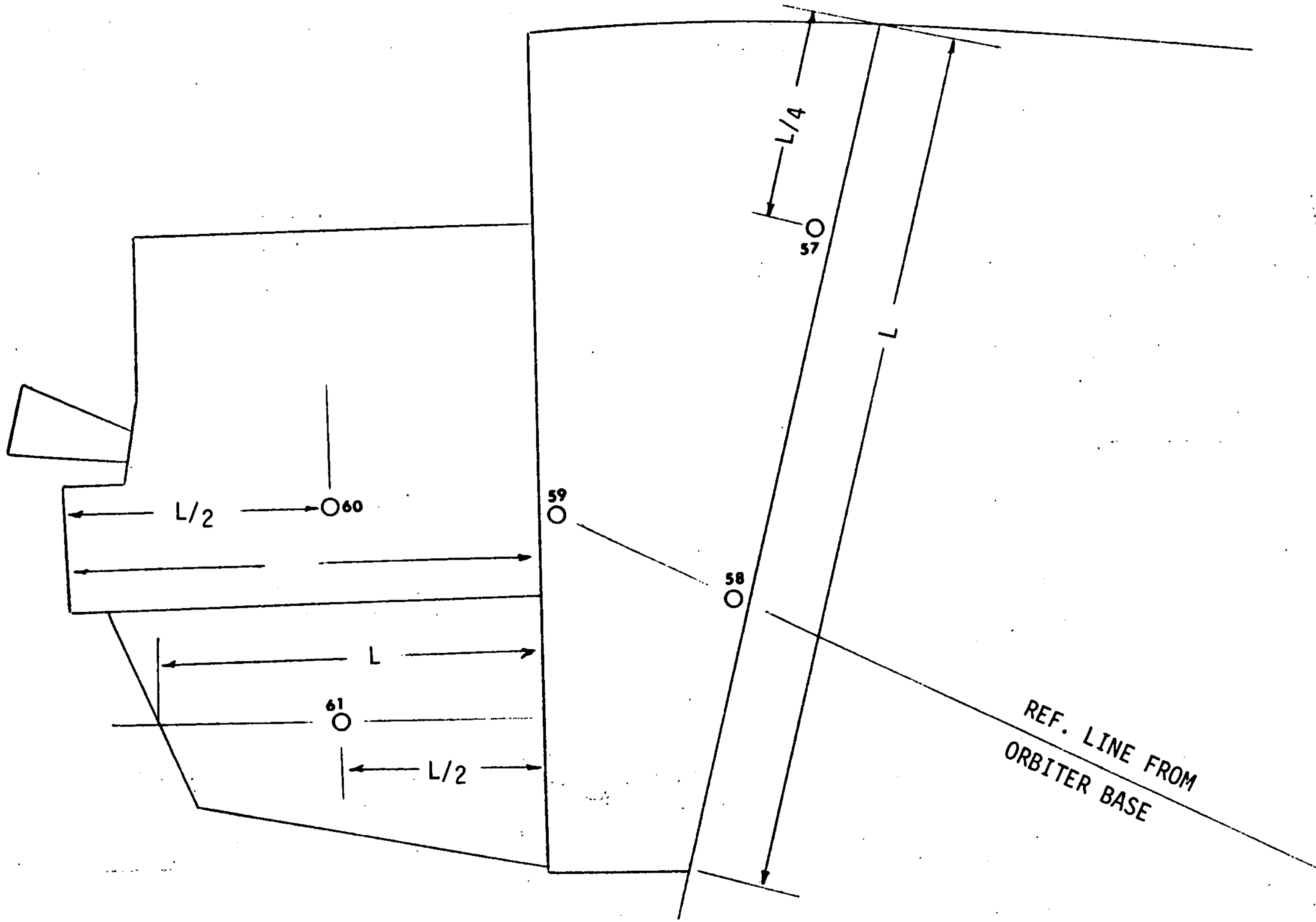

5 Total

h. Left OMS/RCS - Inside Surfaces
Figure 4. Continued.

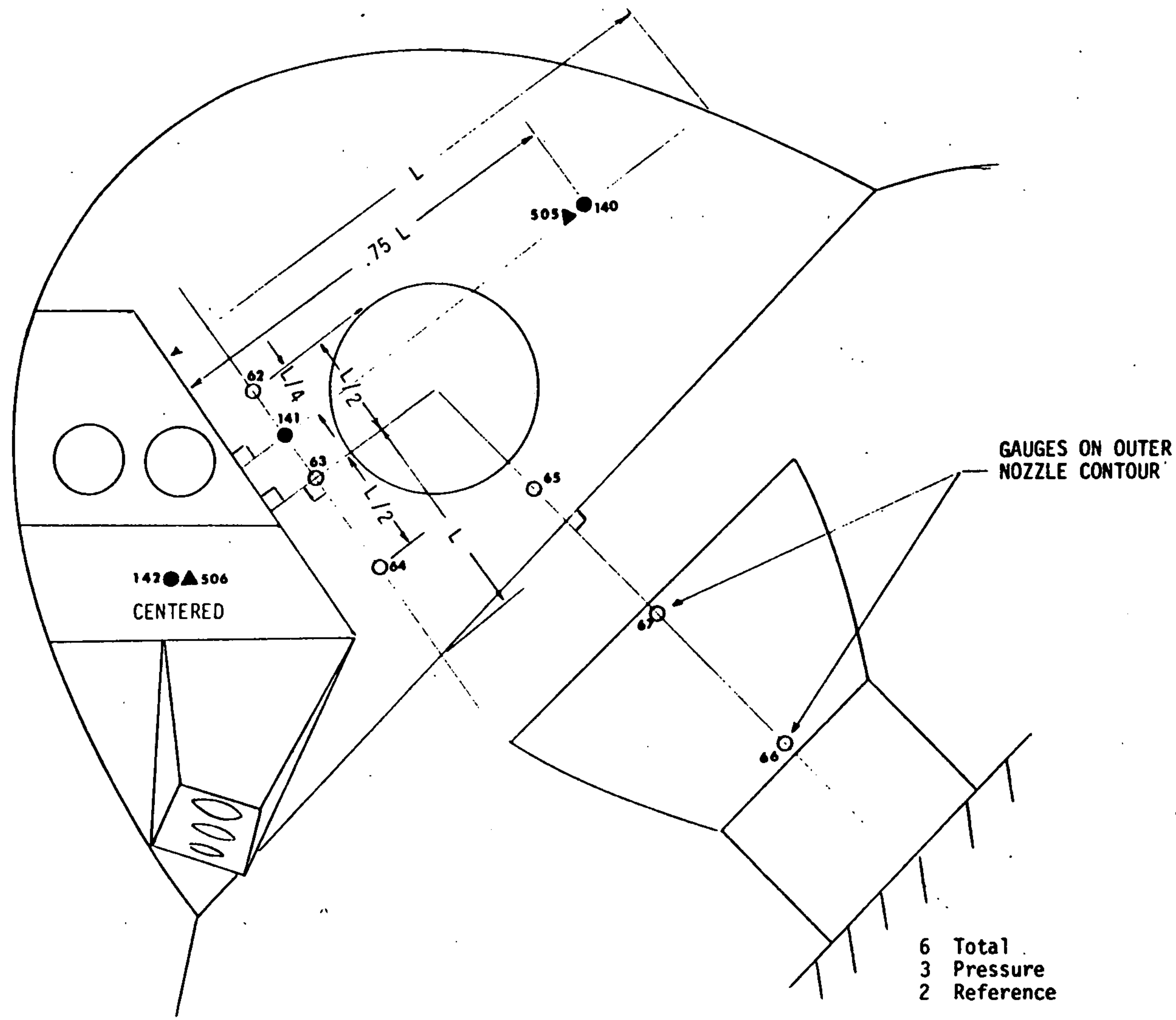

i. Left OMS/RCS - Aft Surfaces
Figure 4. Continued.

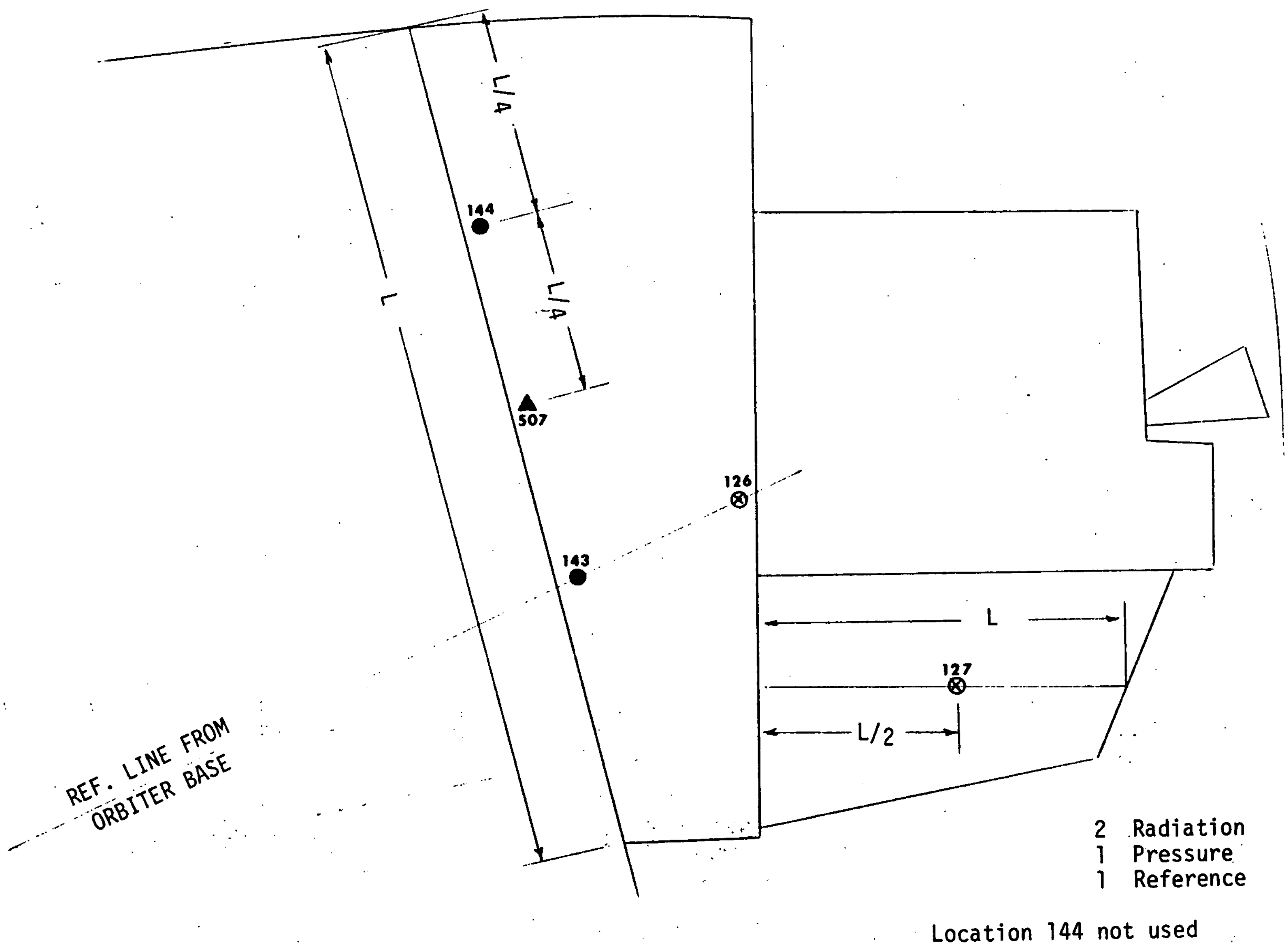

j. Right OMS/RCS - Inside Surfaces
Figure 4. Continued.

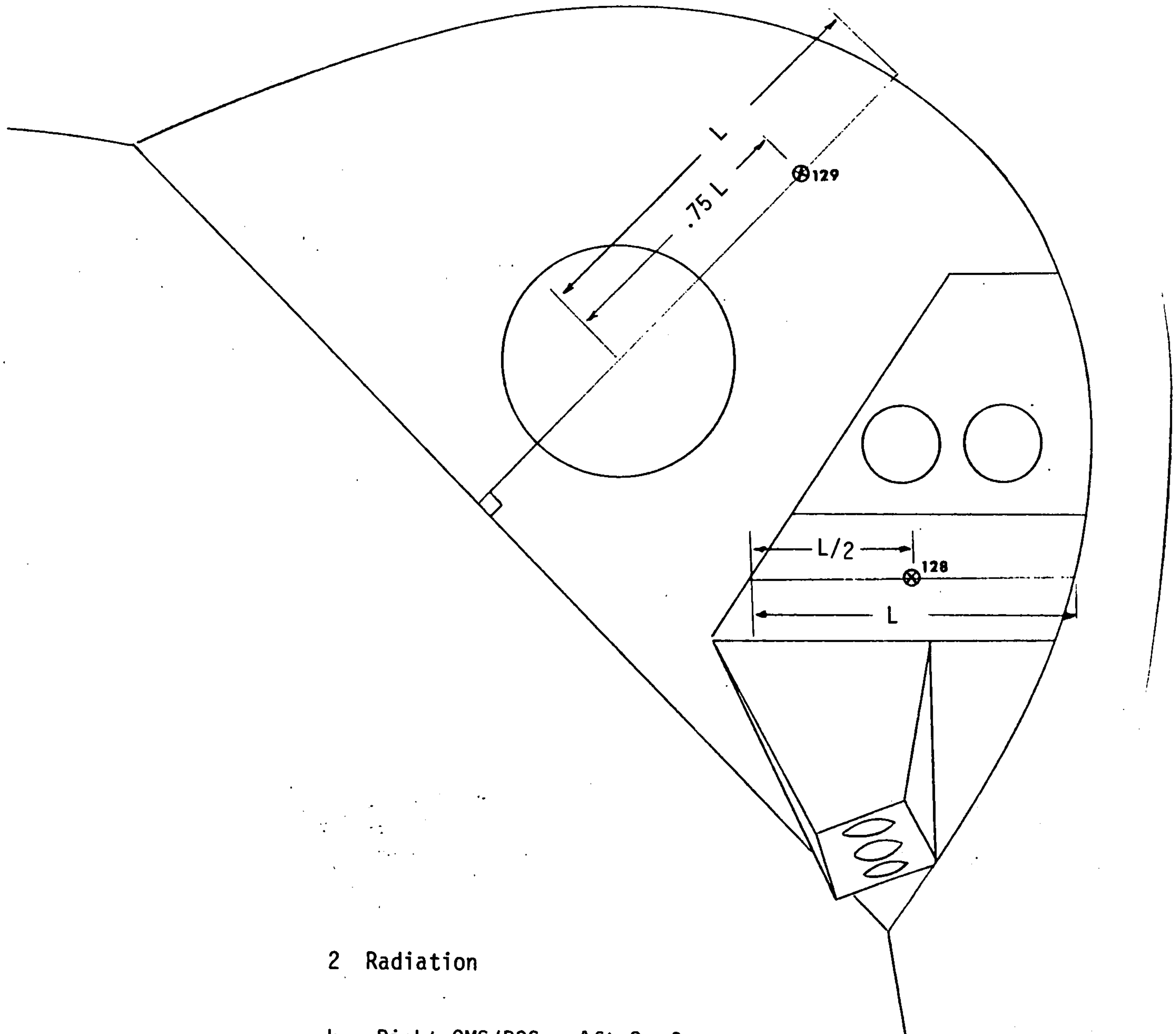

2 Radiation

k. Right OMS/RCS - Aft Surfaces
Figure 4. Continued.

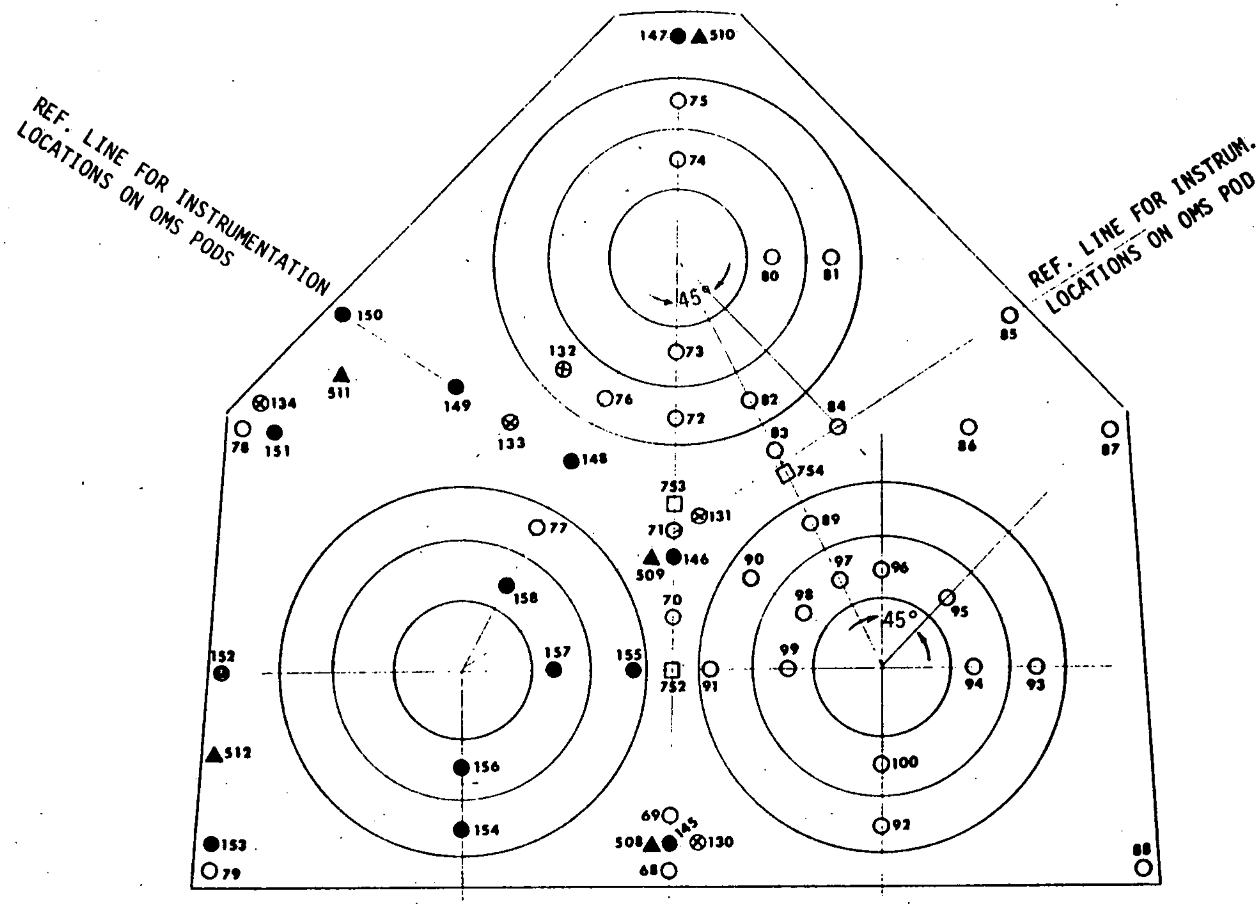

33 Total
5 Radiation
14 Pressure
5 Reference
3 GTP

1. Orbiter Base Heat Shield
Figure 4. Continued.

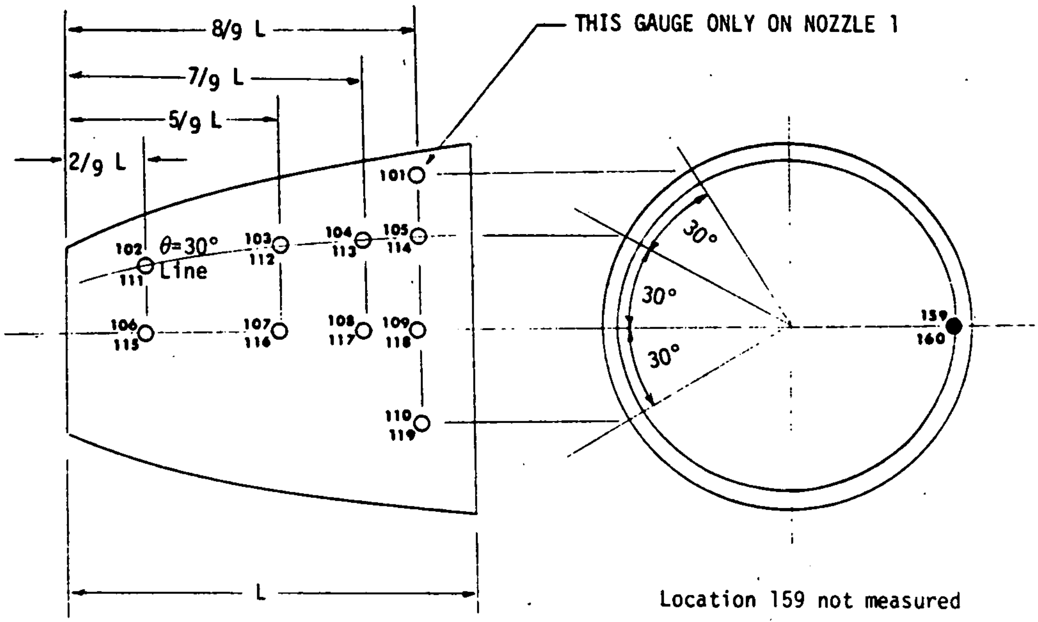

NOZZLES 1 & 2 — 19 Total, 1 Pressure

No.	Nozzle	Type
159	1	Pressure
101-110	1	Total
160	2	Pressure
111-119	2	Total
161	3	Pressure
513	3	Ref. Pressure

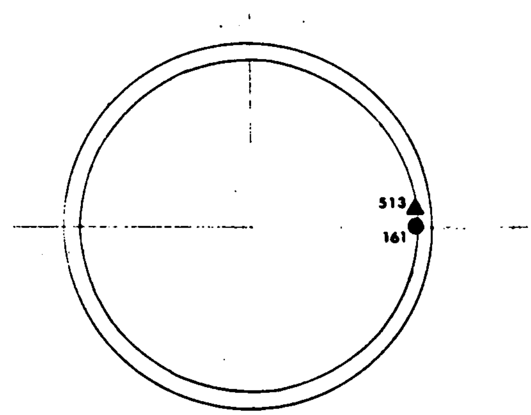

NOZZLE 3 — 1 Pressure, 1 Reference

m. SSME Firing Nozzles
Figure 4. Continued.

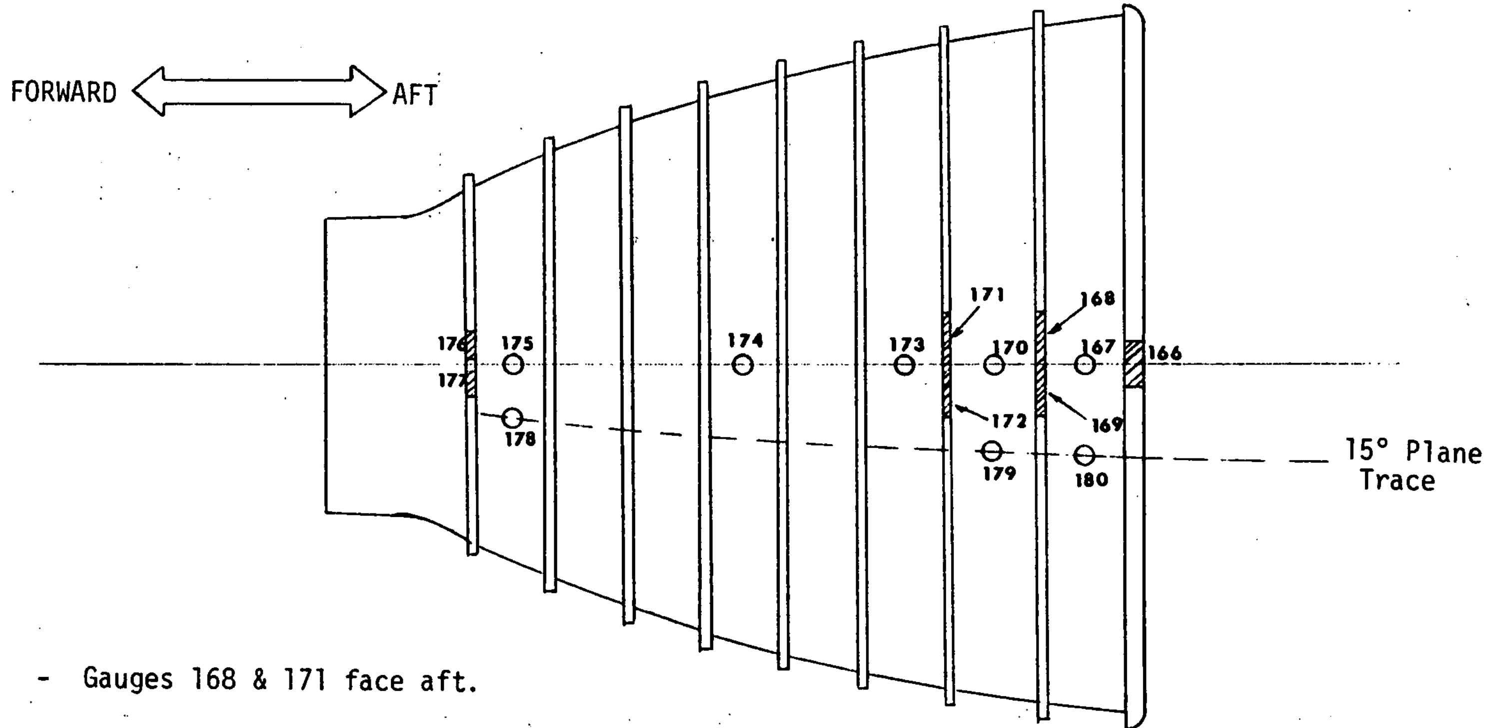

- Gauges 168 & 171 face aft.
- Gauge 176 faces forward.
- All other gauges are perpendicular to the nozzle surface.

15 Total

n. Hatband Nozzle
Figure 4. Continued.

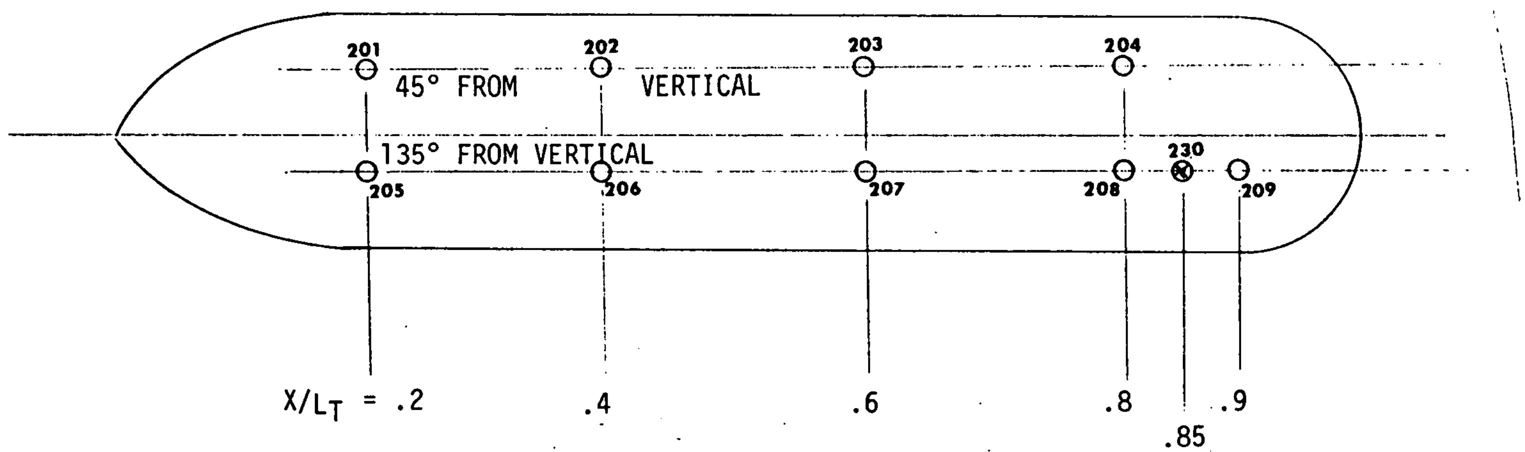

9 Total
1 Radiation

o. External Tank Sidewall
Figure 4. Continued.

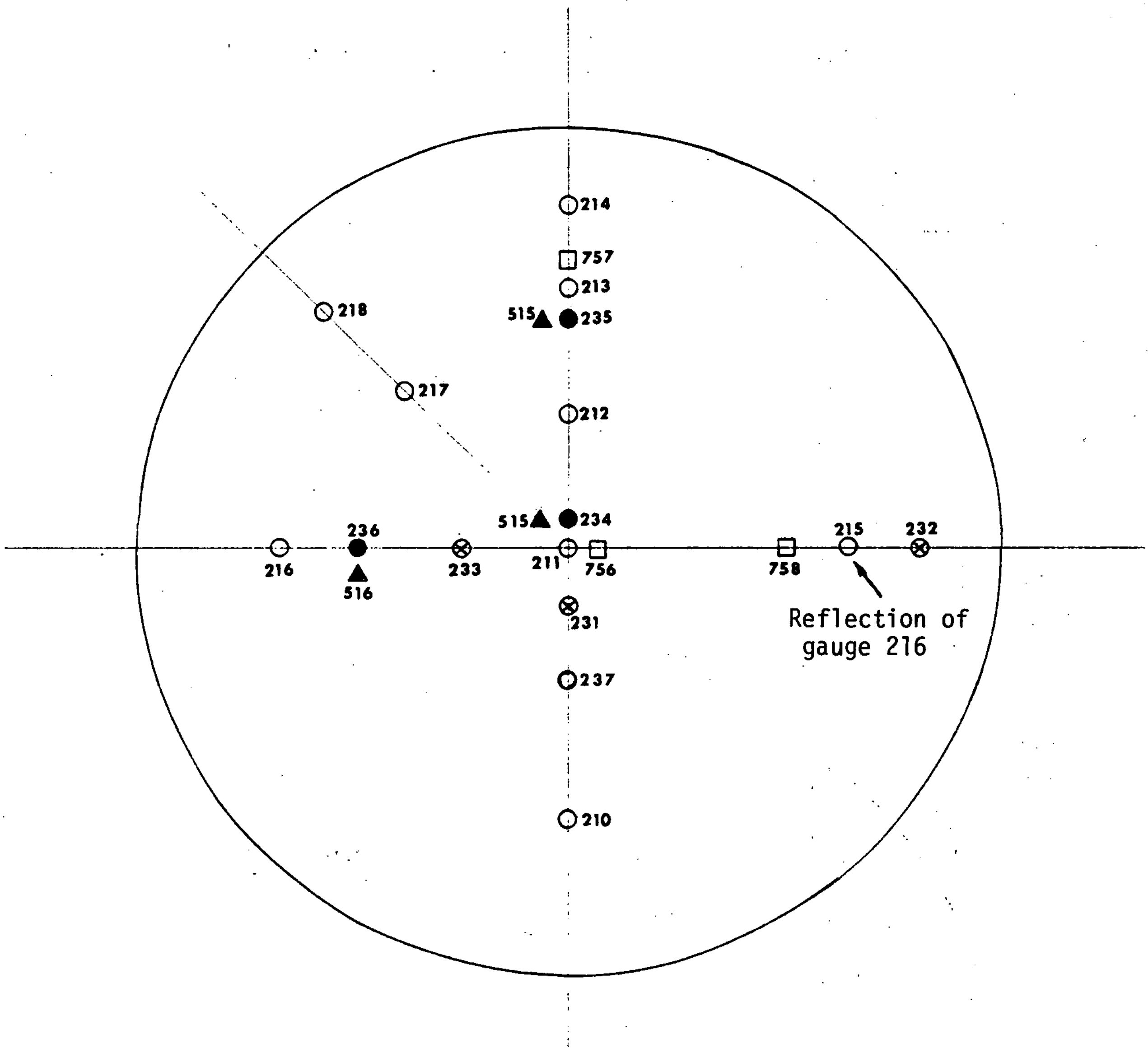

10 Total
3 Radiation
3 Pressure
3 Reference
3 GTP

p. External Tank Aft Dome
Figure 4. Continued.

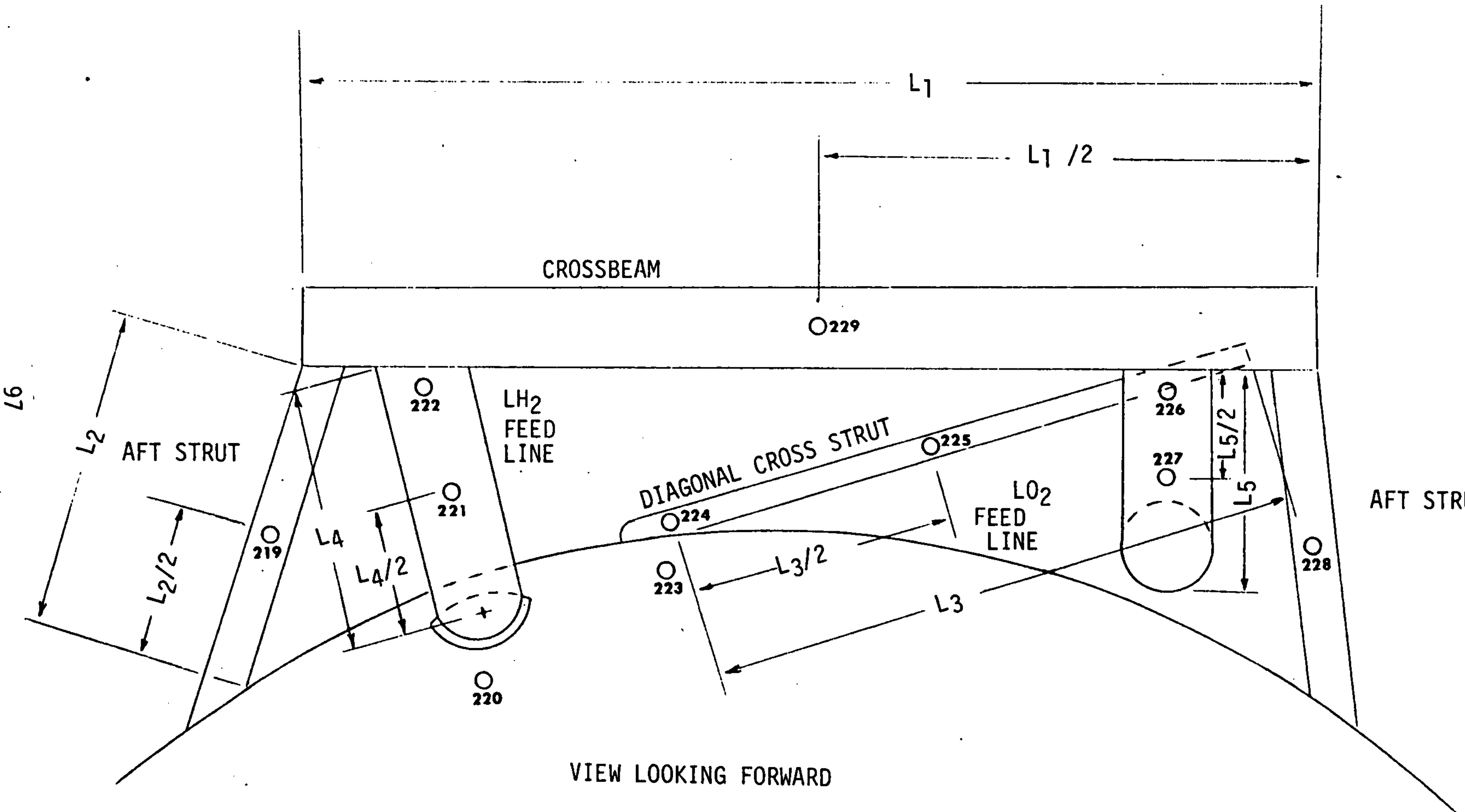

11 Total

q. External Tank Hardware
Figure 4. Continued.

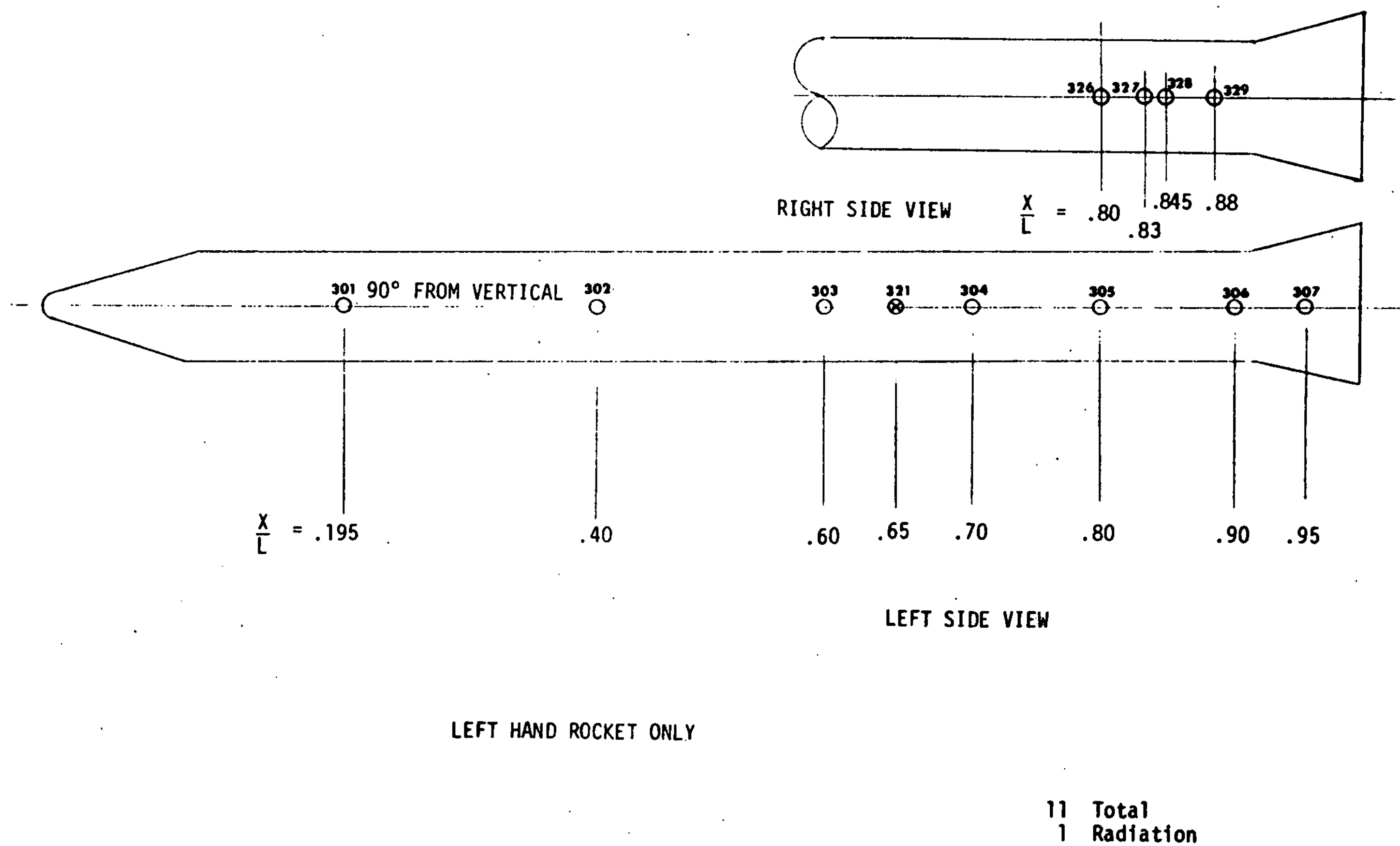

r. Left SRB Sidewall
Figure 4. Continued.

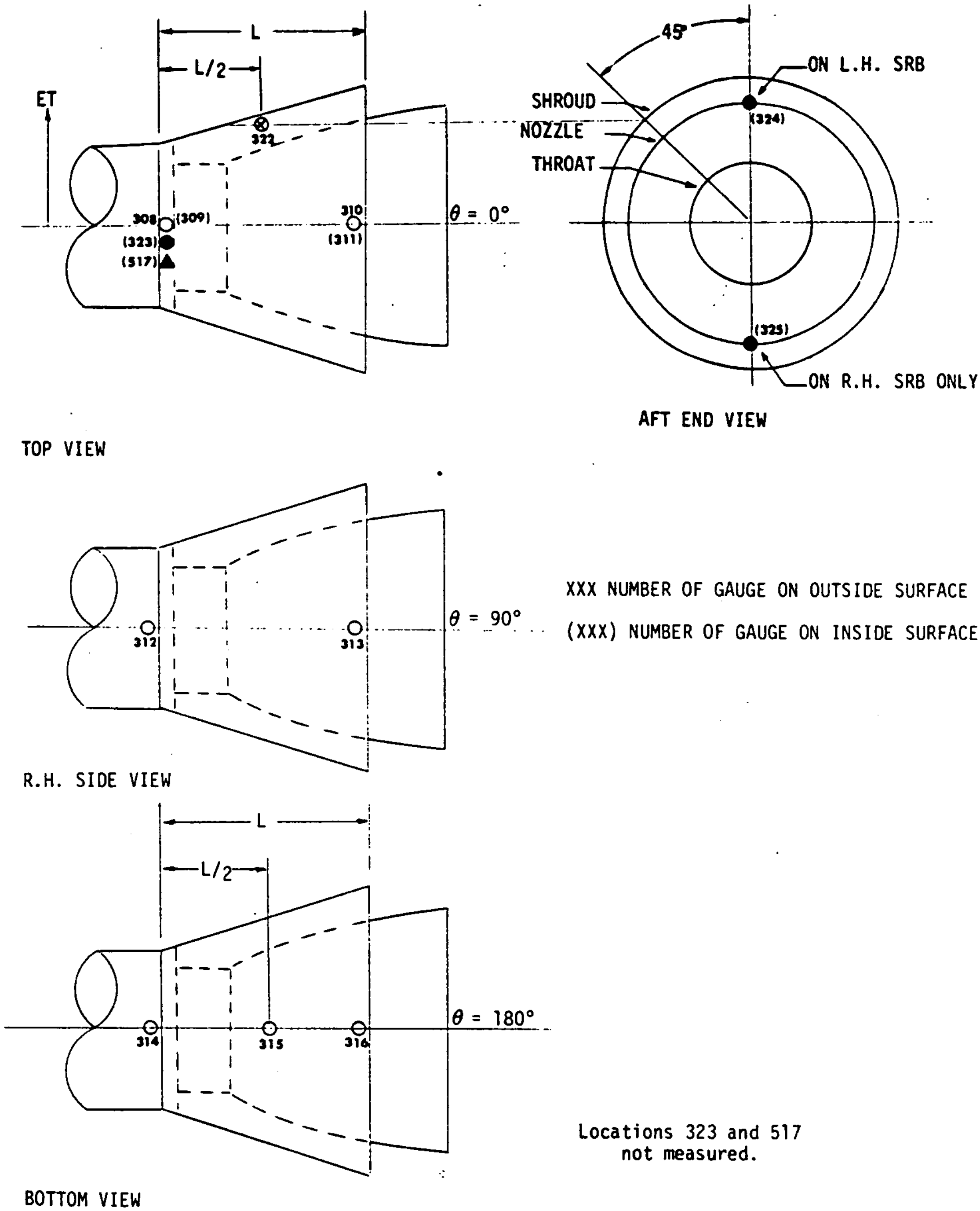

Locations 323 and 517
not measured.

9 Total
1 Radiation
2 Pressure

s. Left SRB Nozzle and Shroud
Figure 4. Continued.

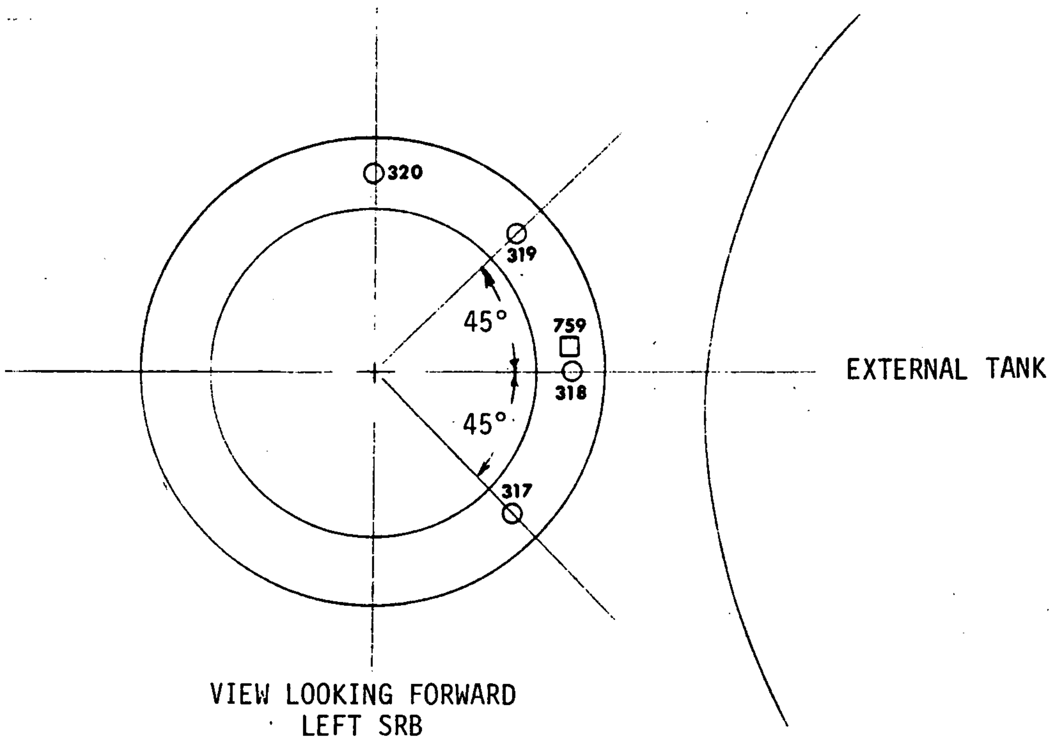

4 Total
1 GTP

t. Left SRB Skirt Curtain
Figure 4. Concluded.

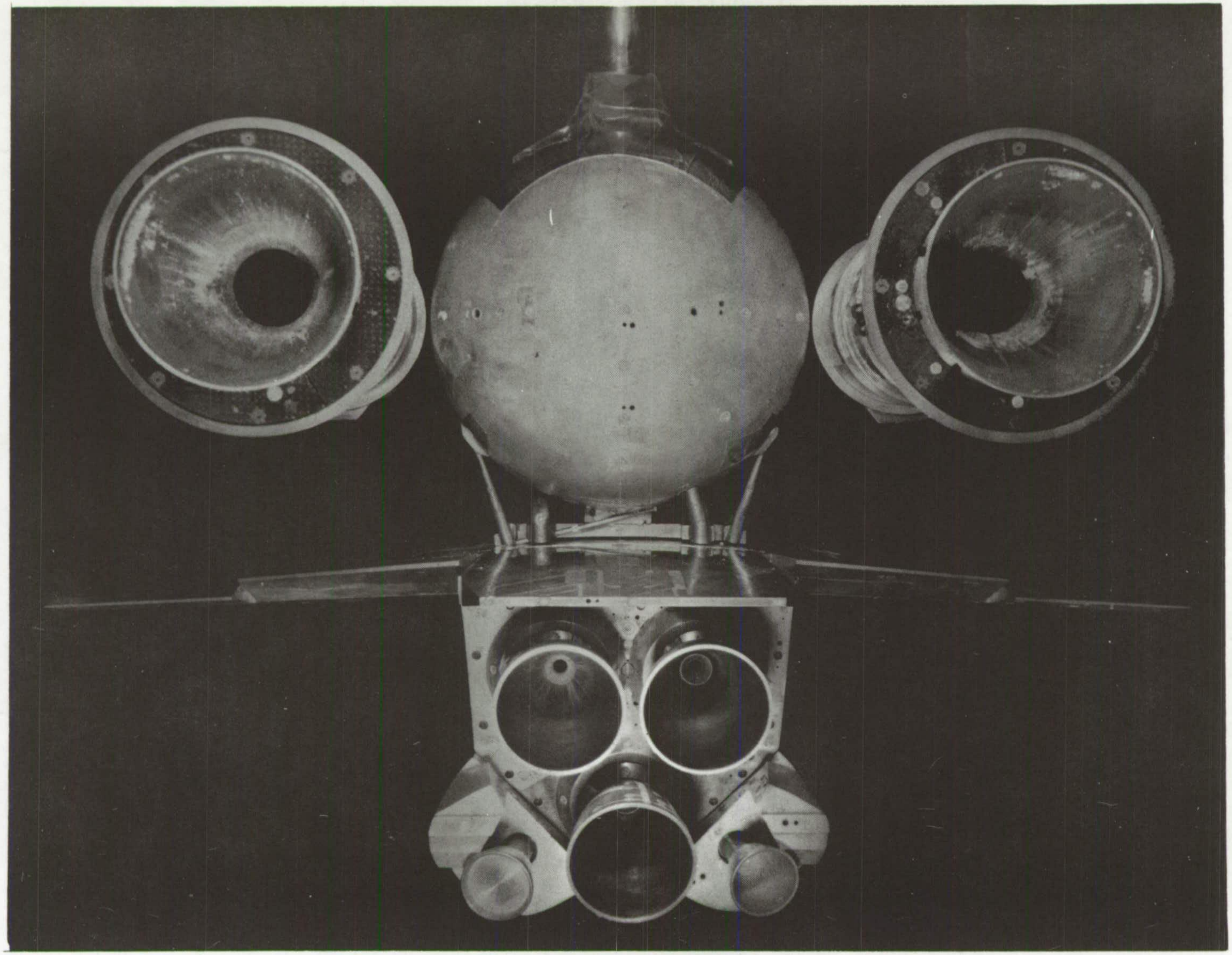

a. Model 19-OTS
Figure 5. Total and radiation heat transfer gauges.

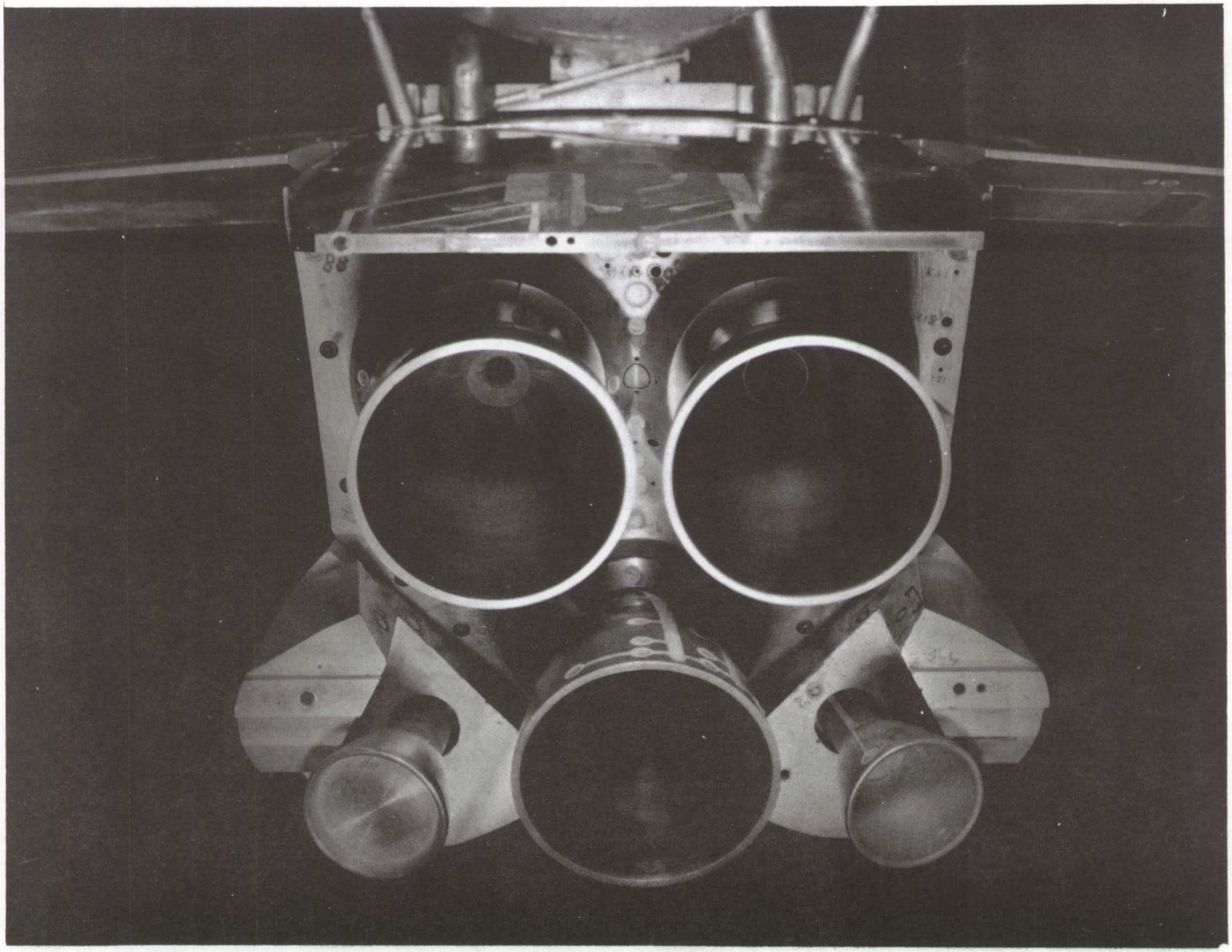

b. Orbiter

Figure 5. Continued.

c. Orbiter Base Heat Shield
Figure 5. Continued.

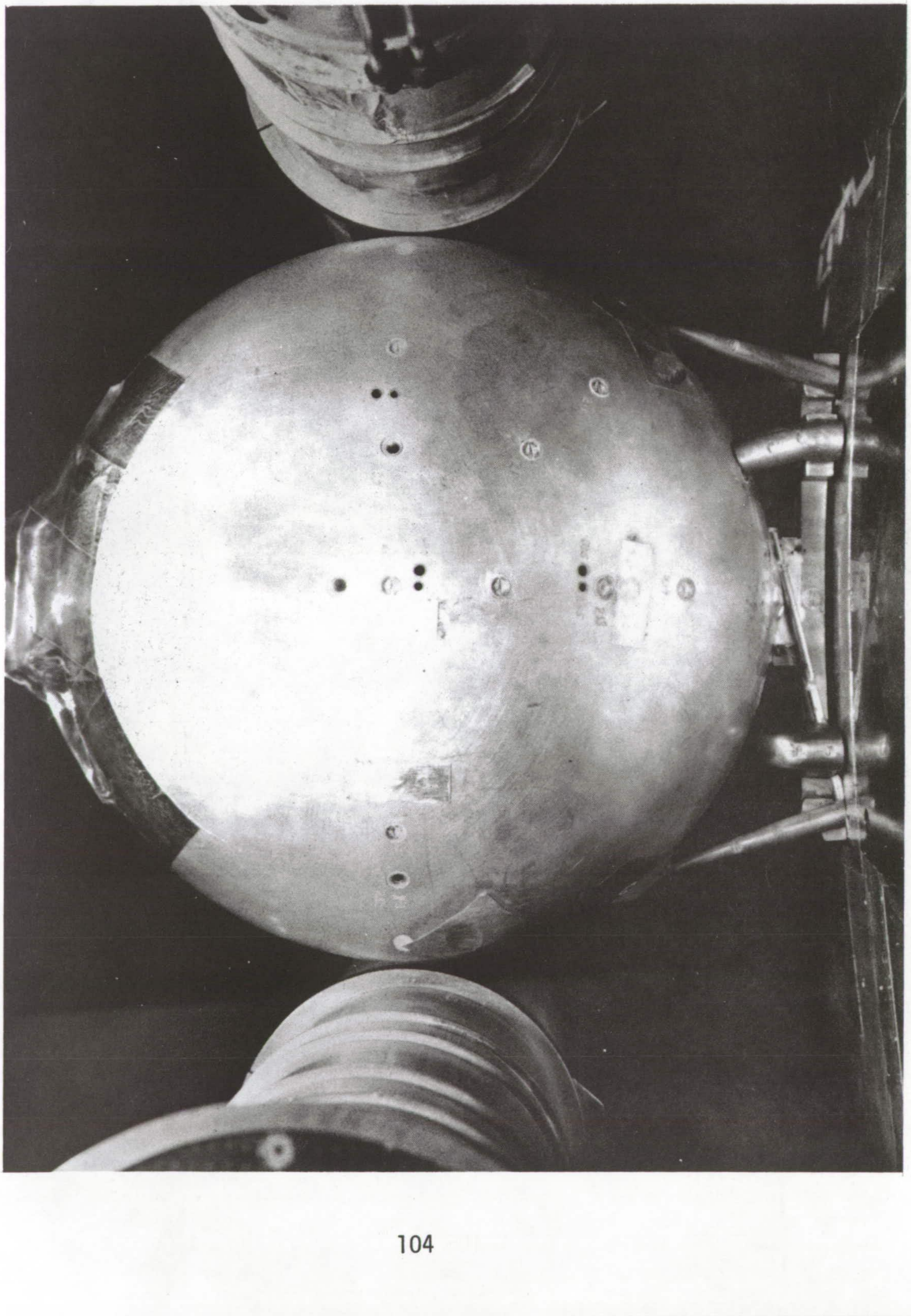

d. External Tank
Figure 5. Continued.

Figure 5. Concluded.
e. SRB

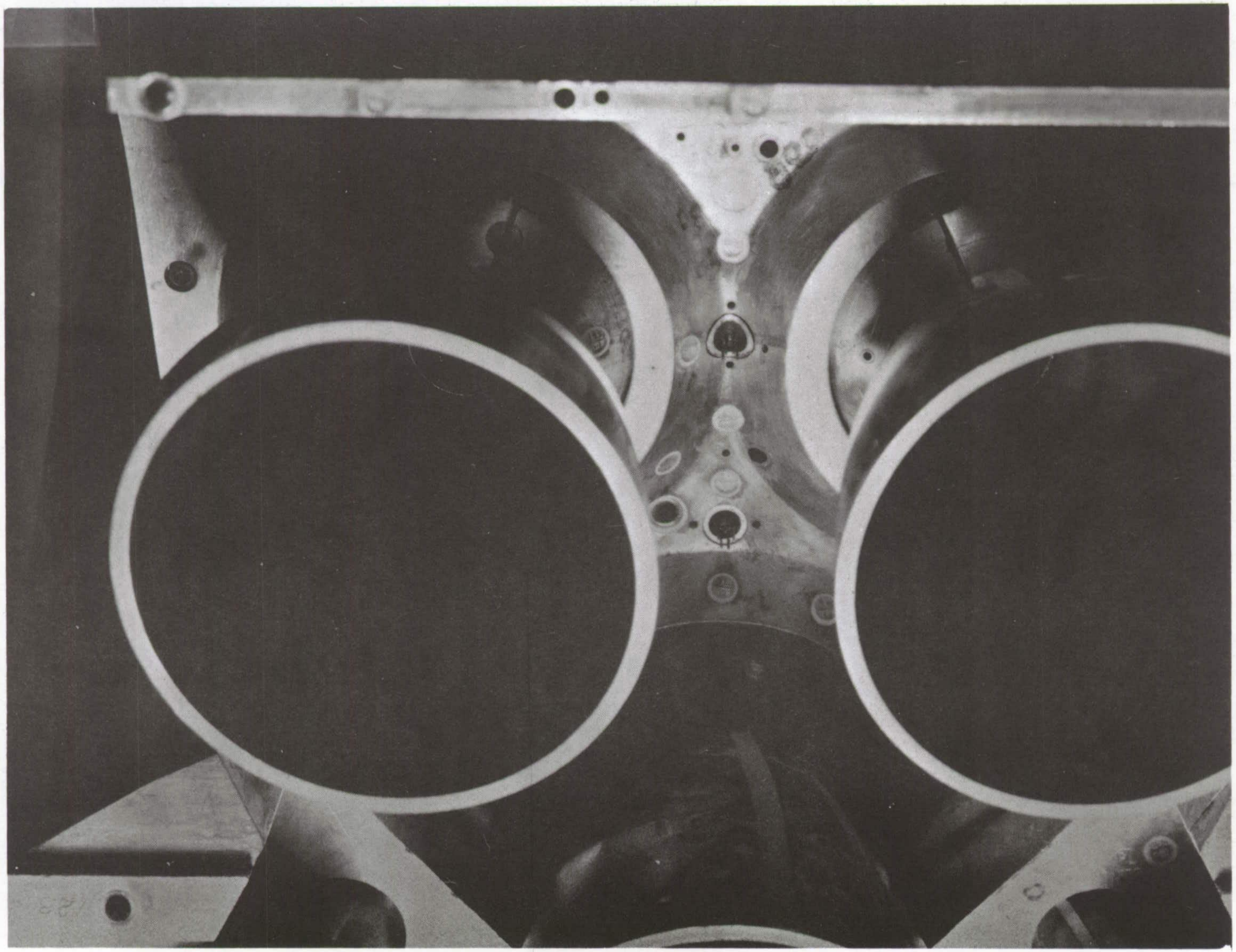

a. Orbiter
Figure 6. Gas temperature probes.

b. Orbiter
Figure 6. Continued.

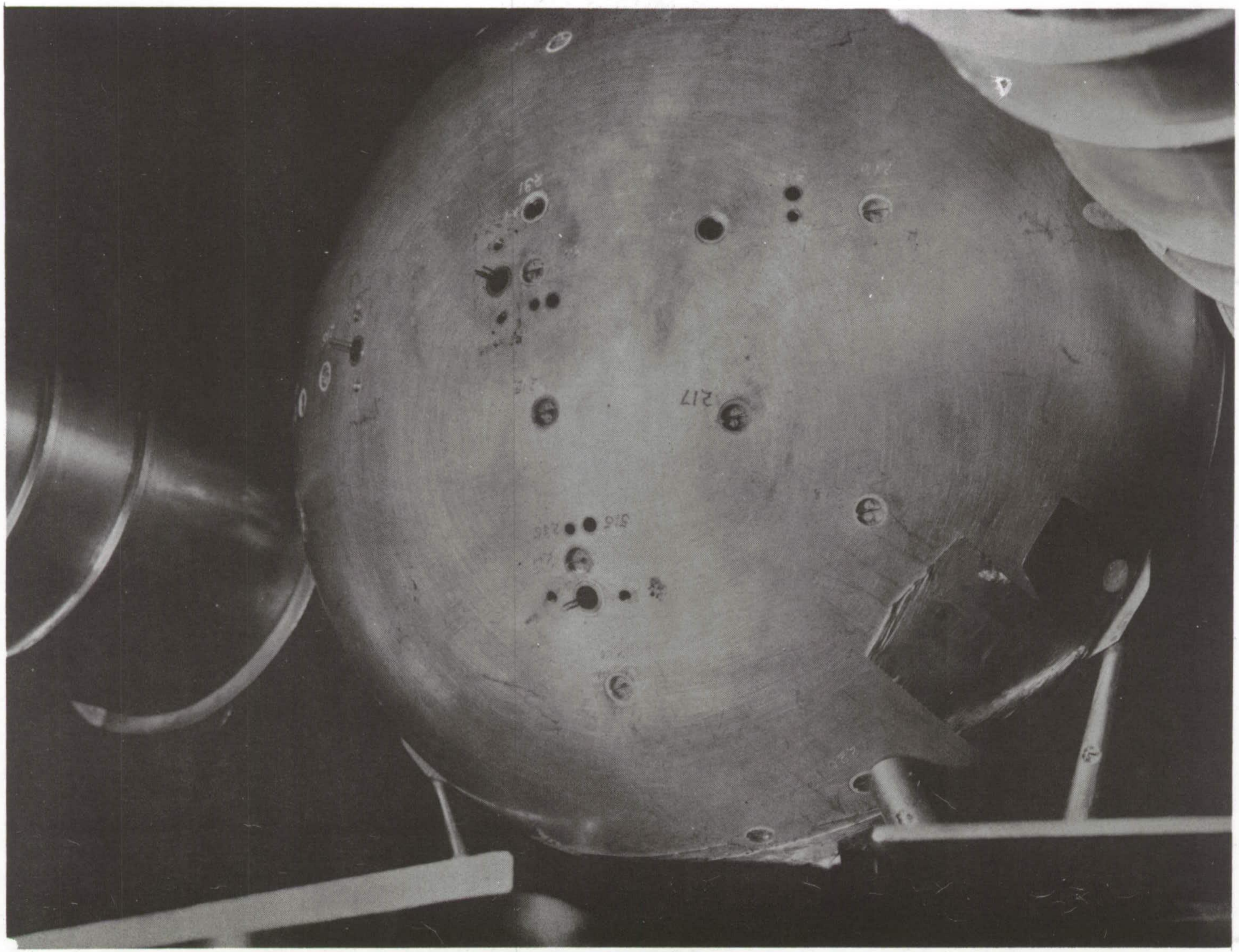

c. External Tank
Figure 6. Continued.

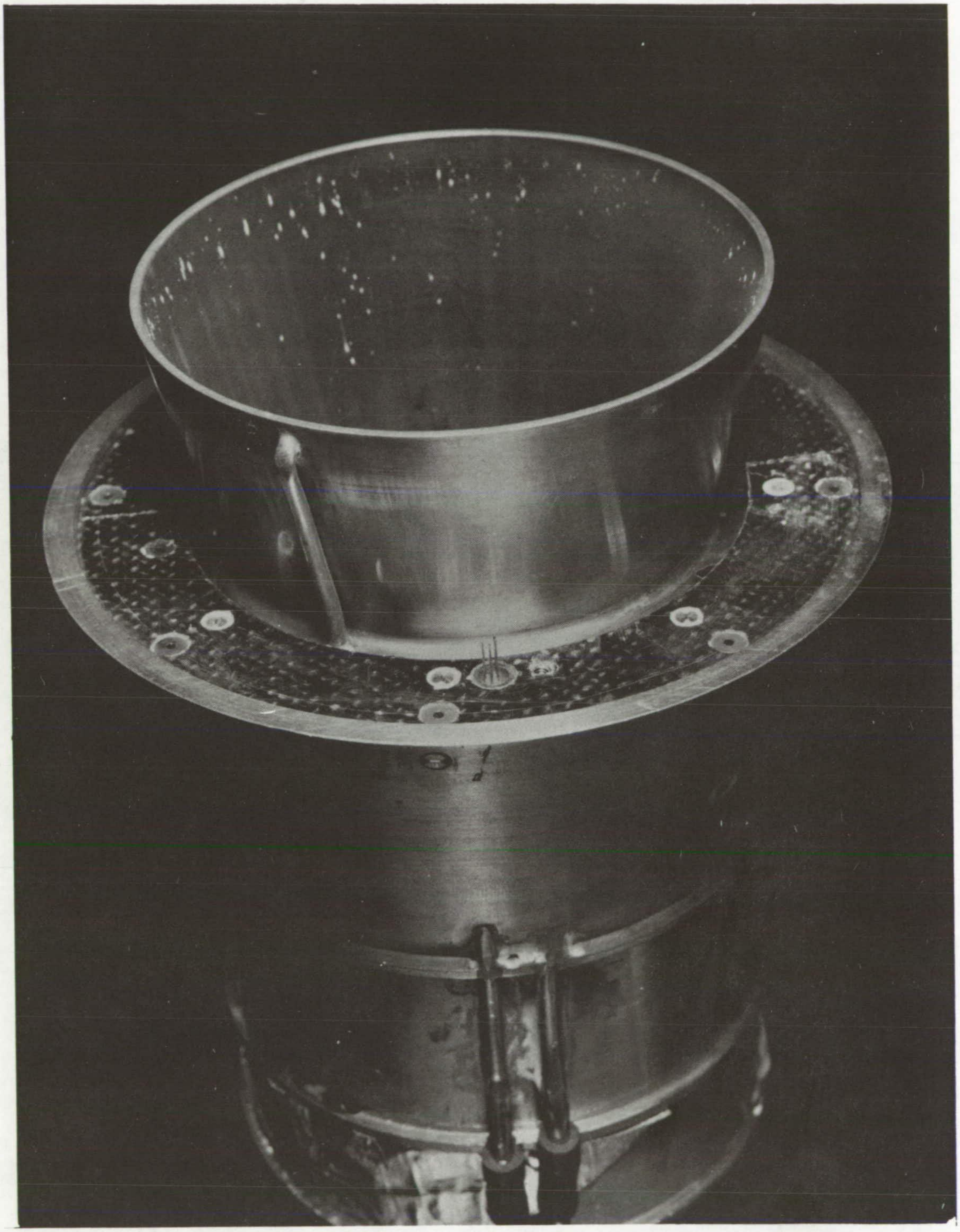

d. SRB
Figure 6. Concluded.

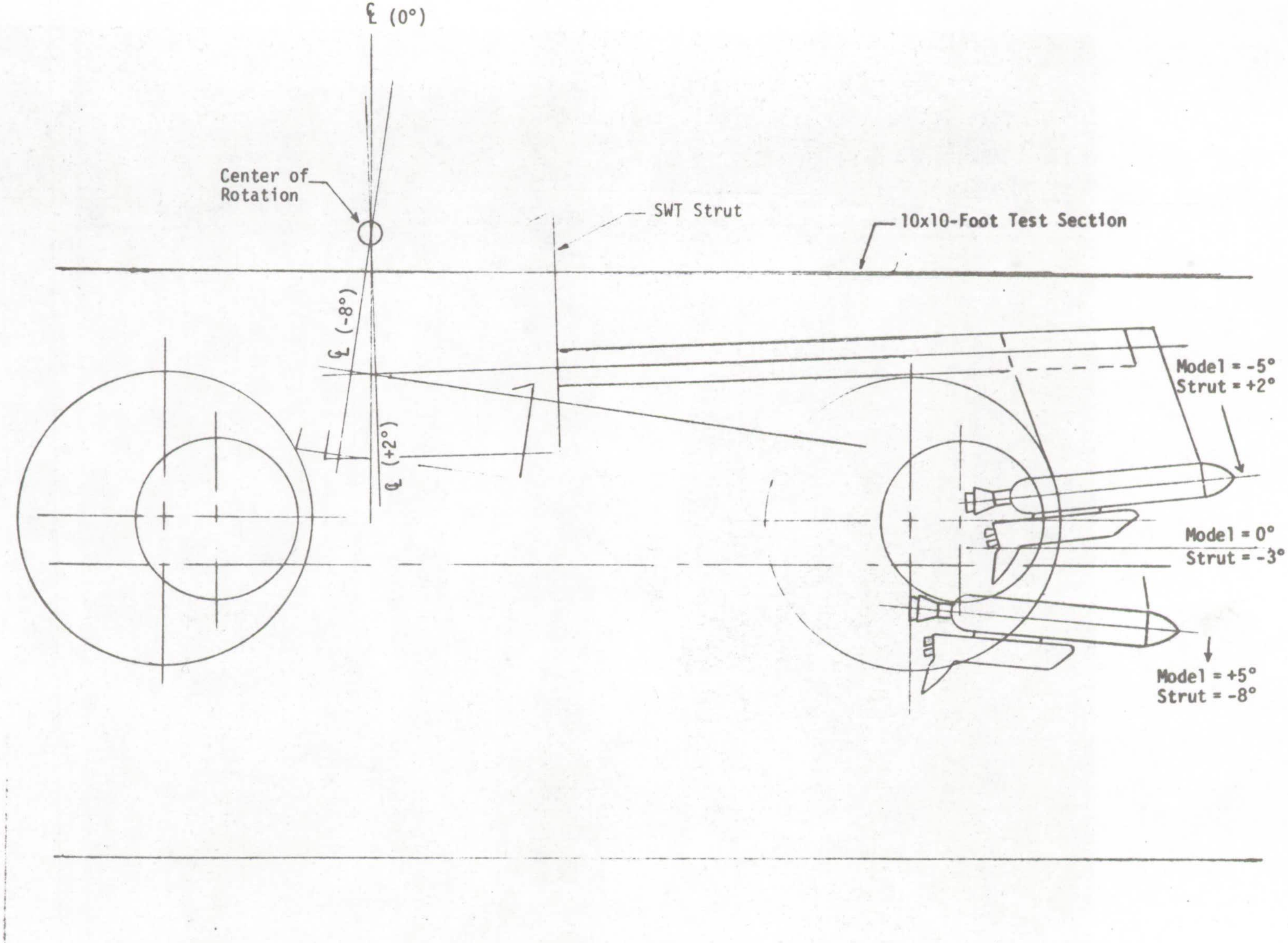

Figure 7. Model installation in the 10 x 10-foot supersonic wind tunnel.

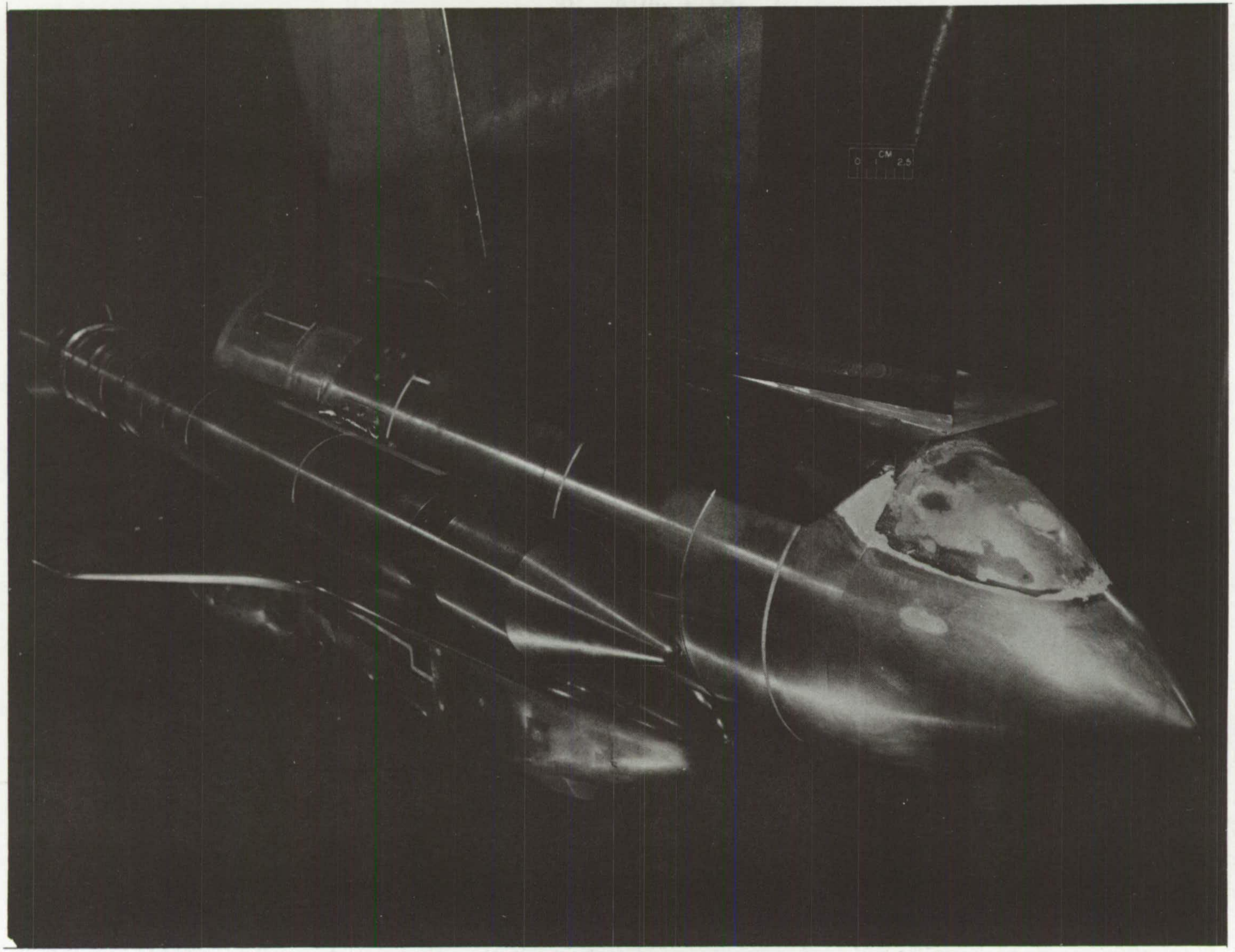

a. Side View
Figure 8. Model Yaw Strut.

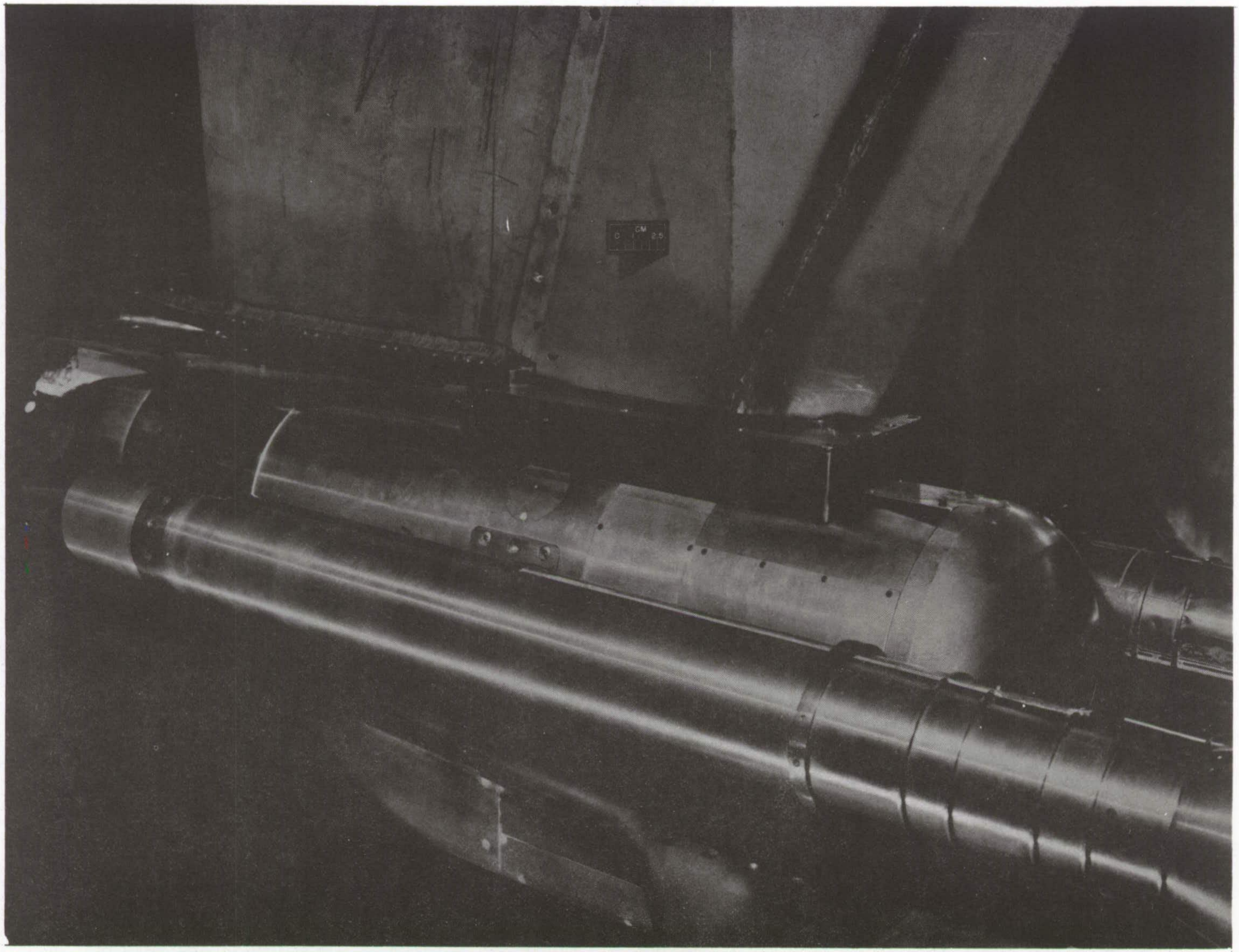

b. Side View
Figure 8. Continued.

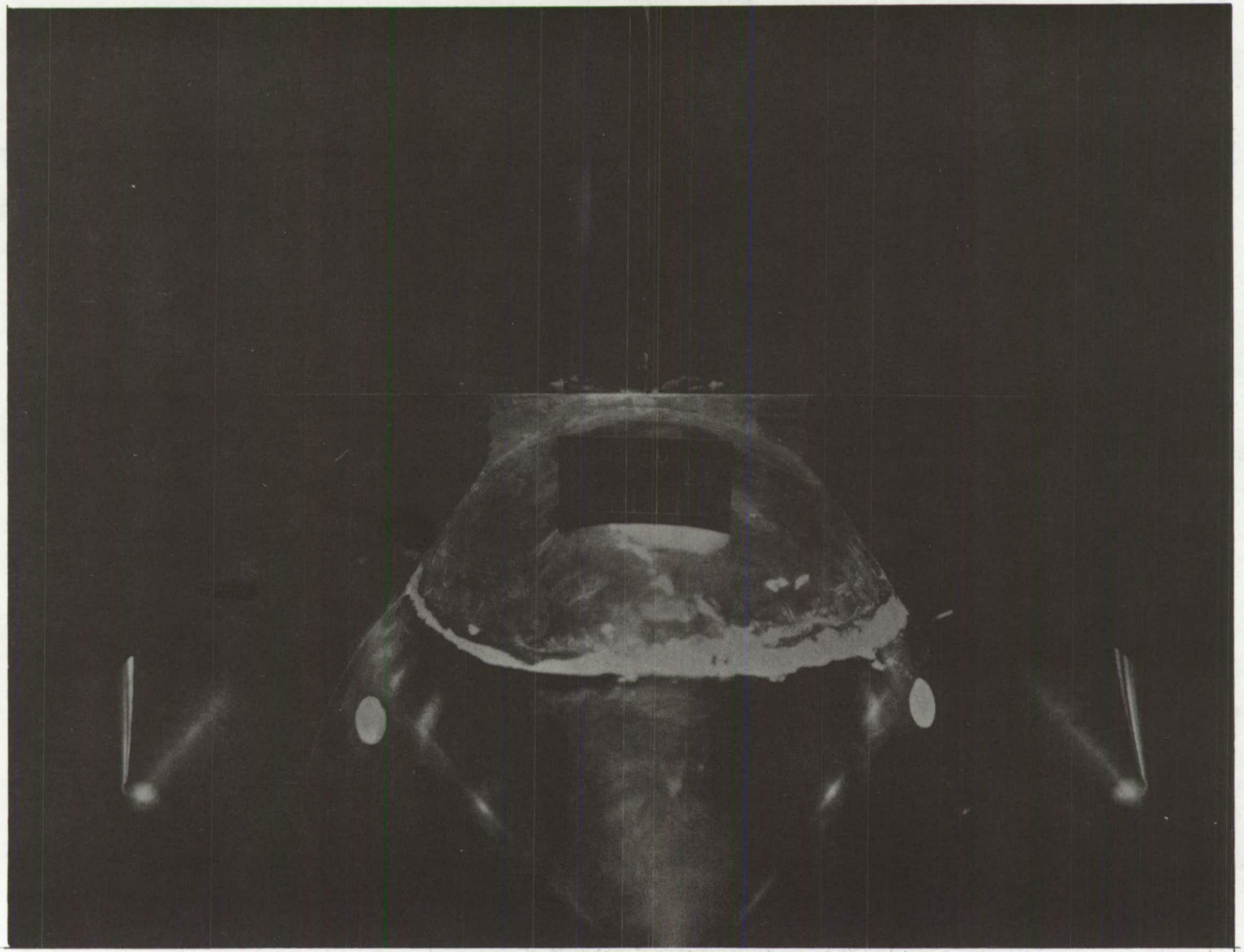

c. Front View
Figure 8. Continued.

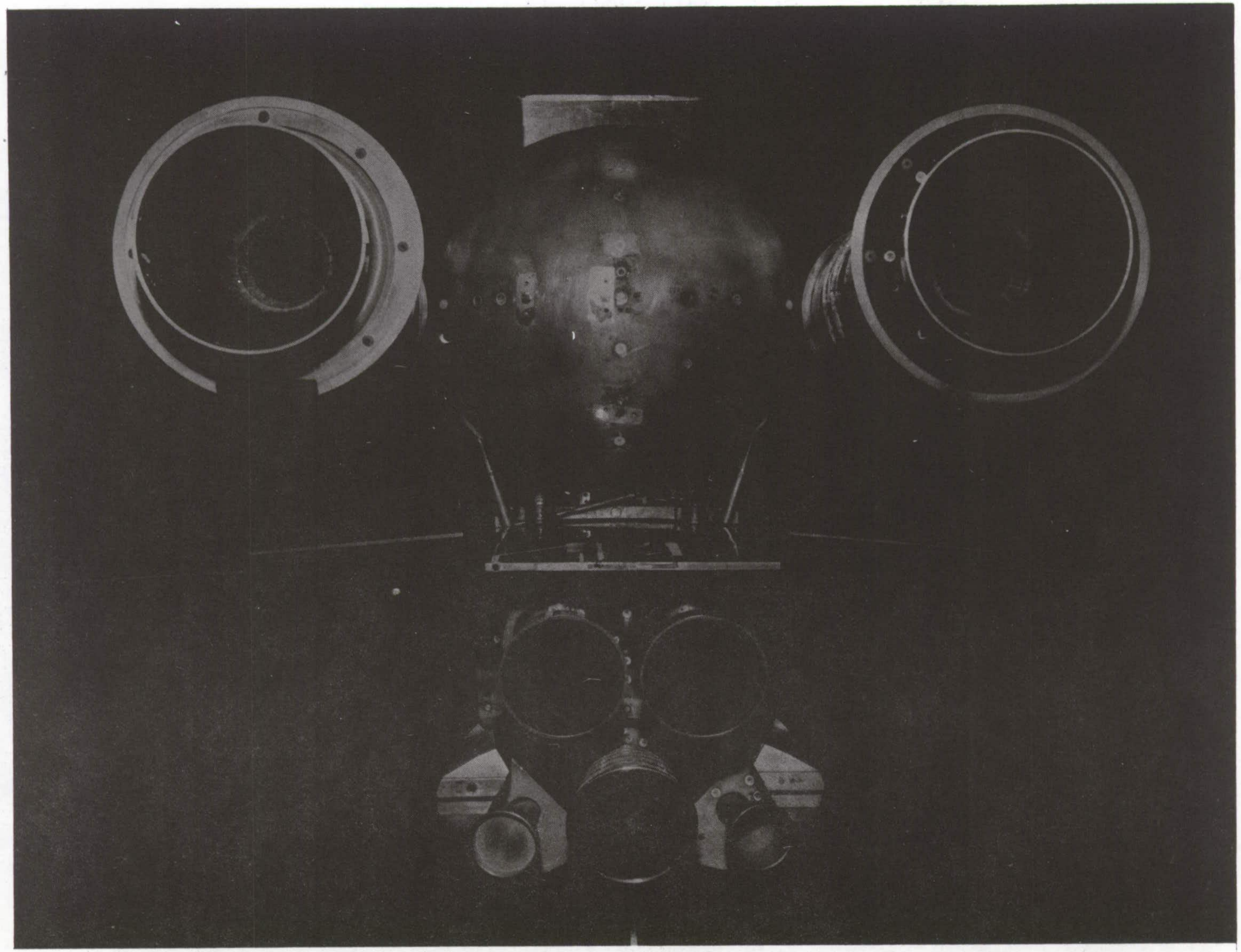

d. Rear View
Figure 8. Concluded.

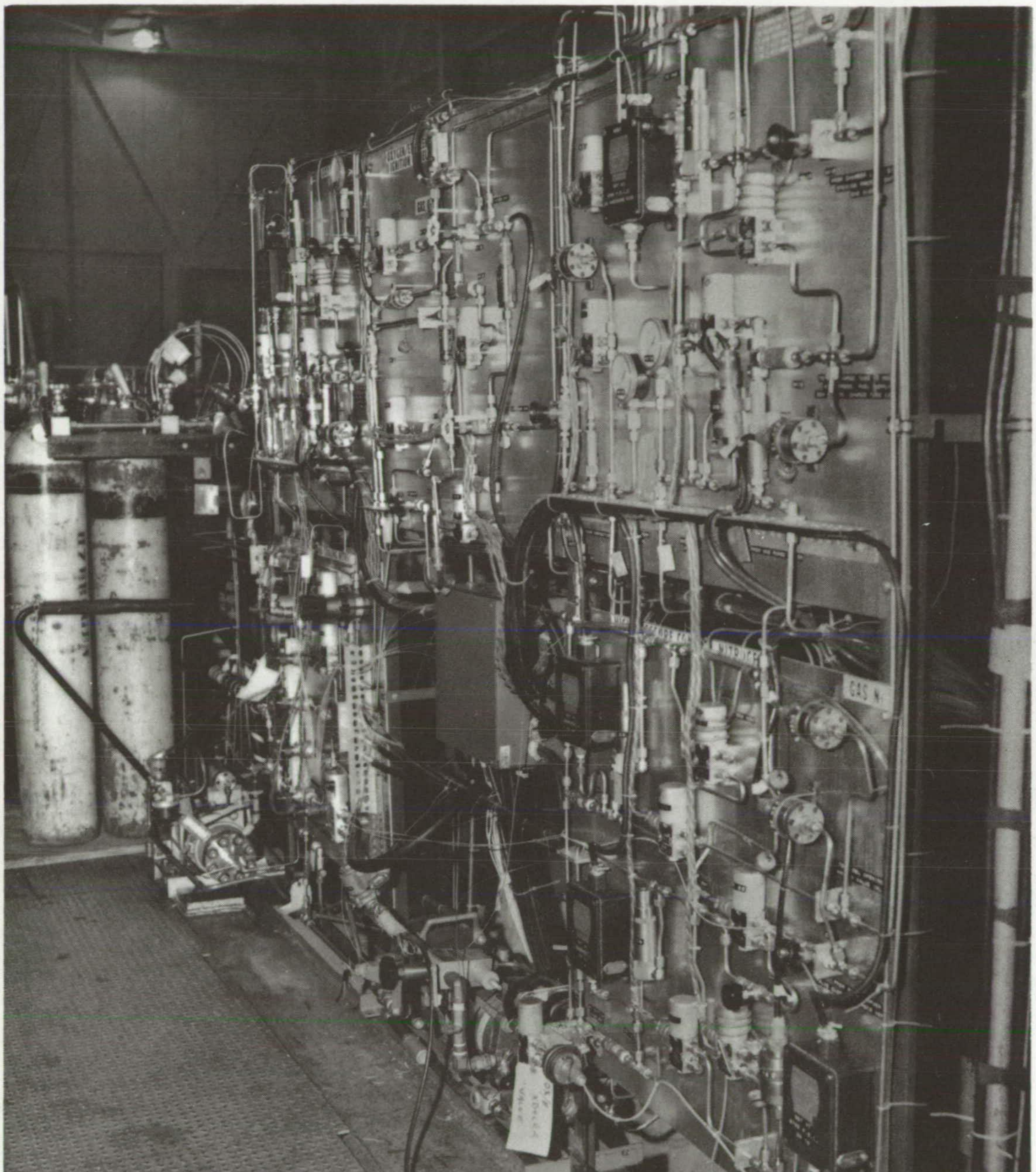

Figure 9. Gas System Panels.

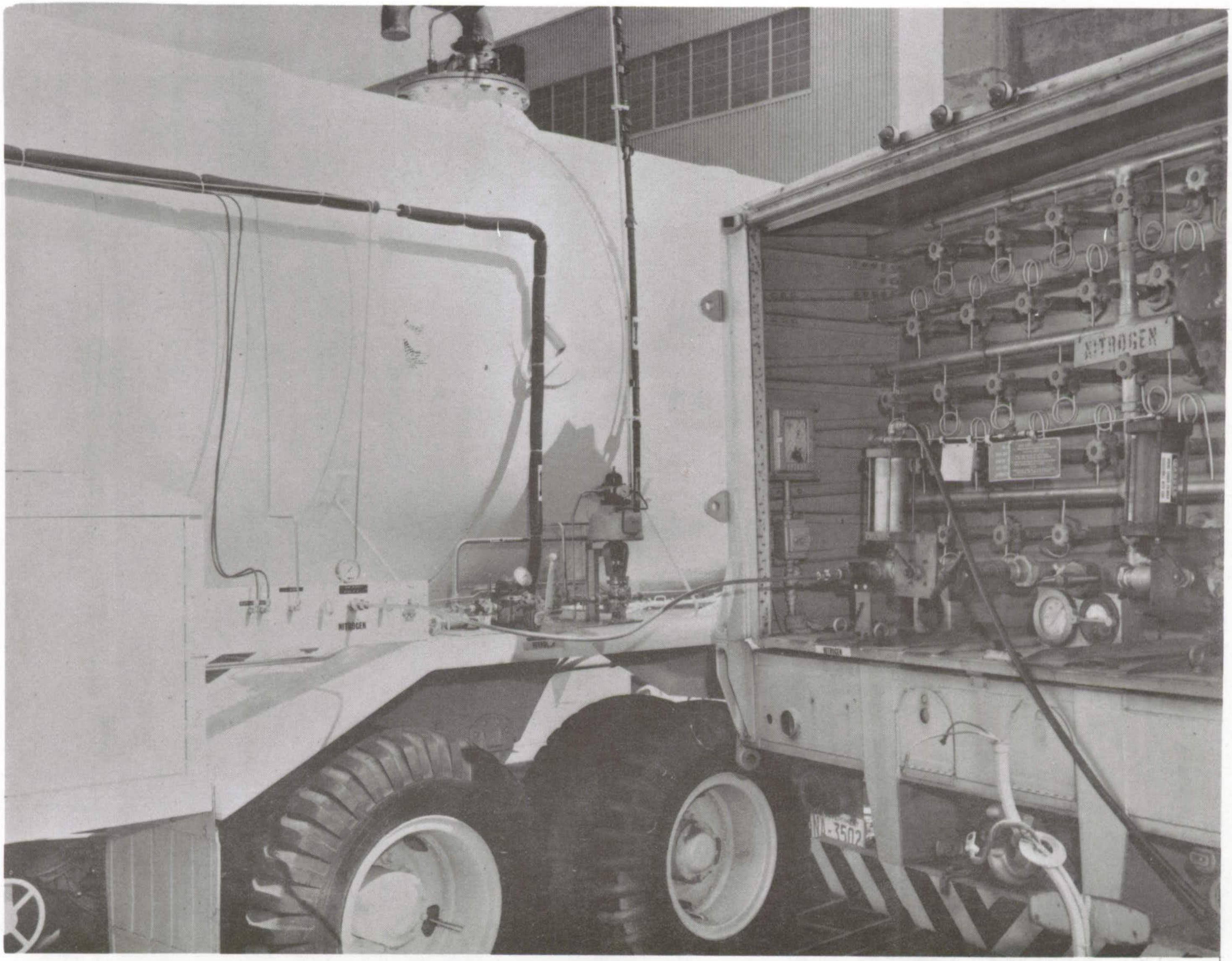

Figure 10. Cooling Nitrogen Supply Trailers.

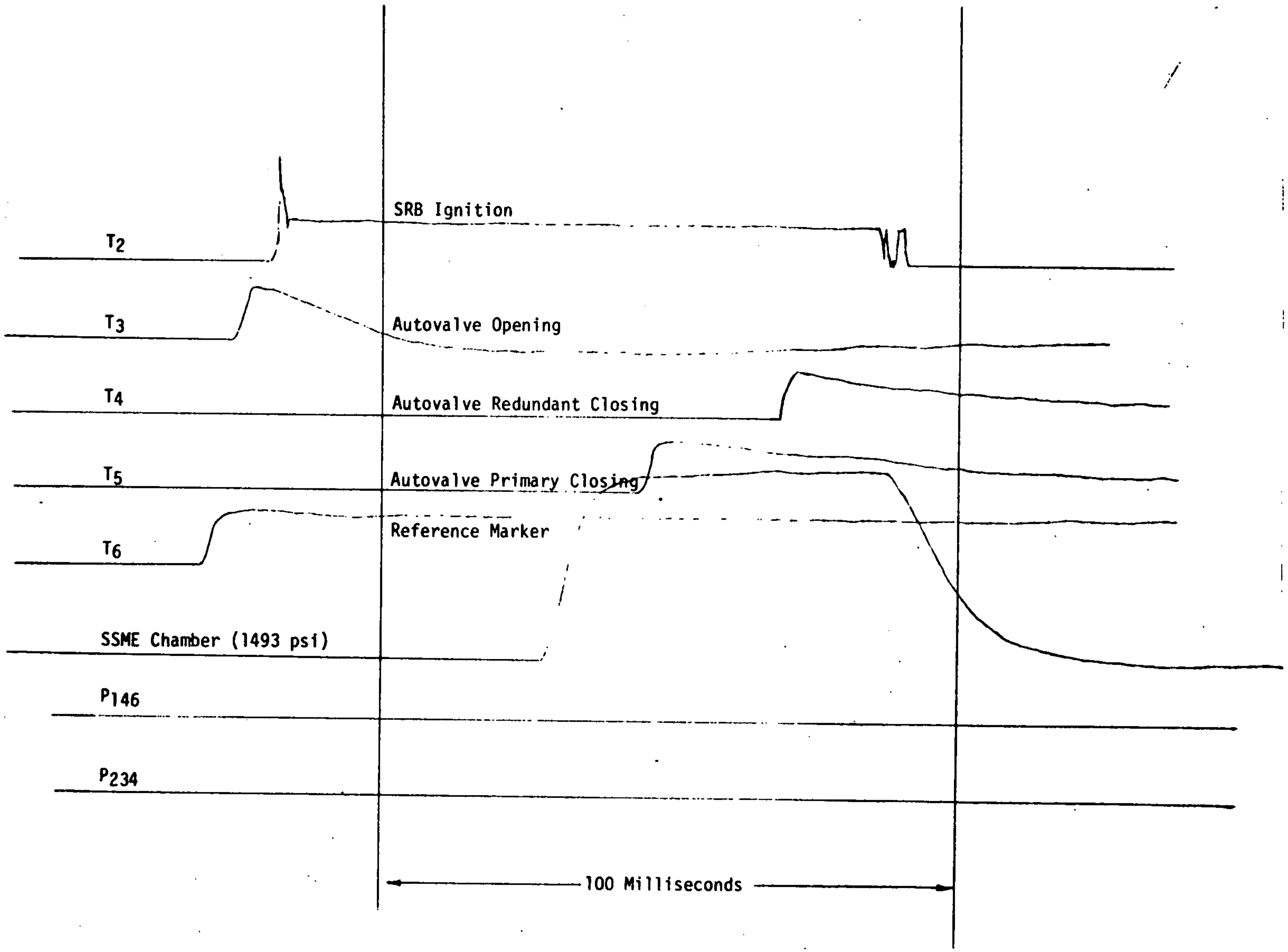

Figure 11. Orbiter and SRB Timing Functions.

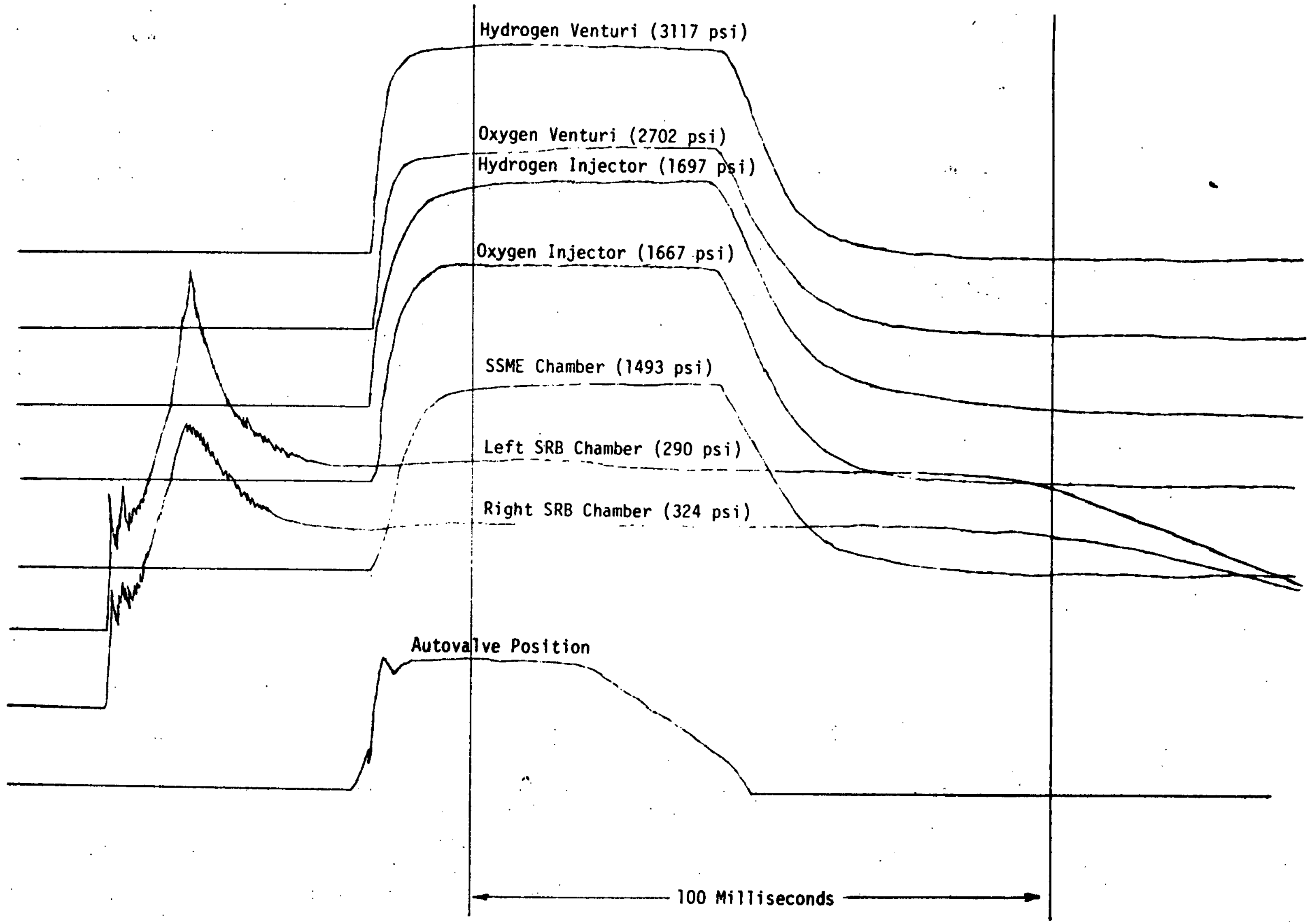

Figure 12. Orbiter and SRB Operation Pressures.

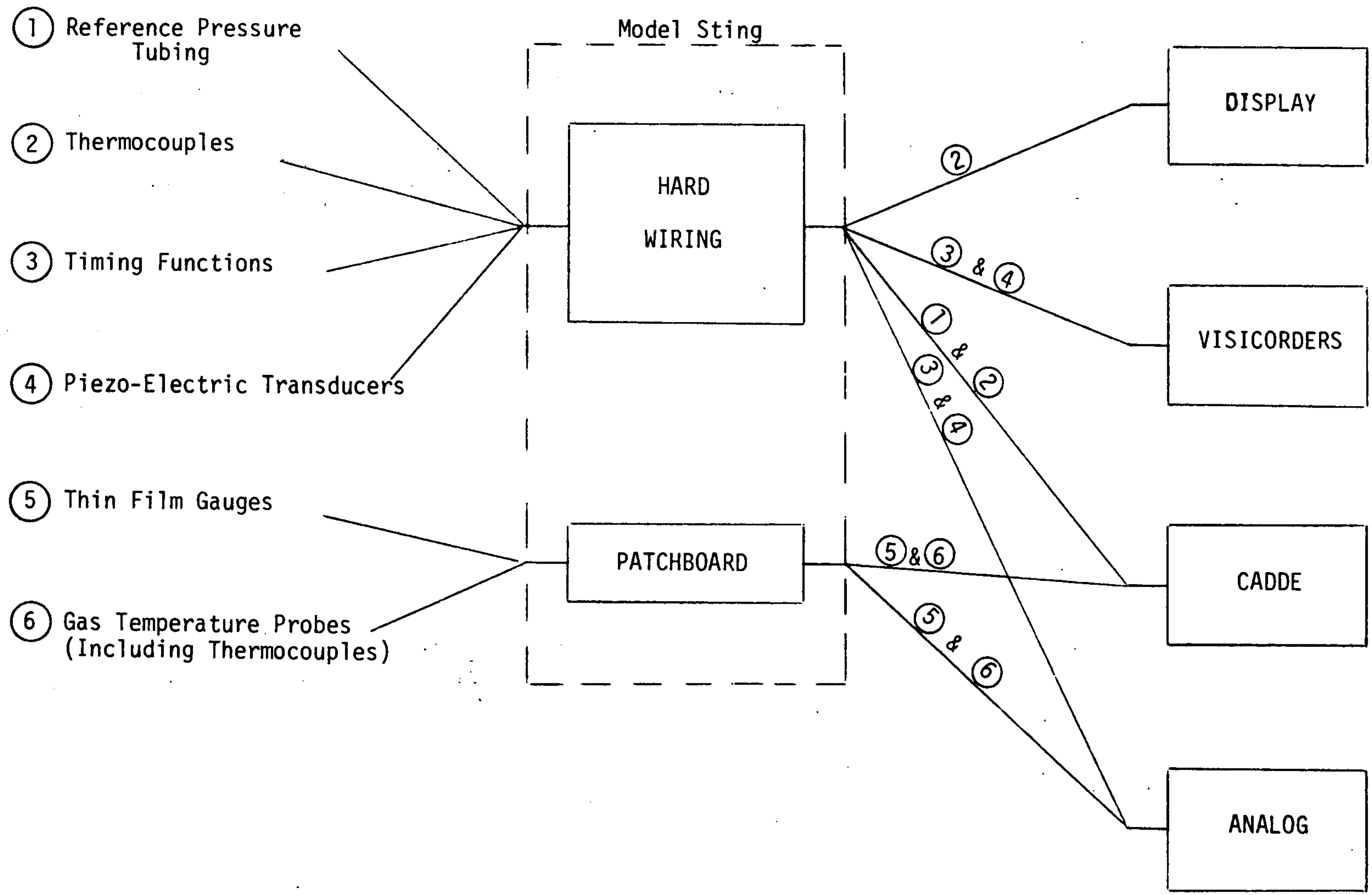

Figure 13. Model Instrumentation Data Acquisition Block Diagram.

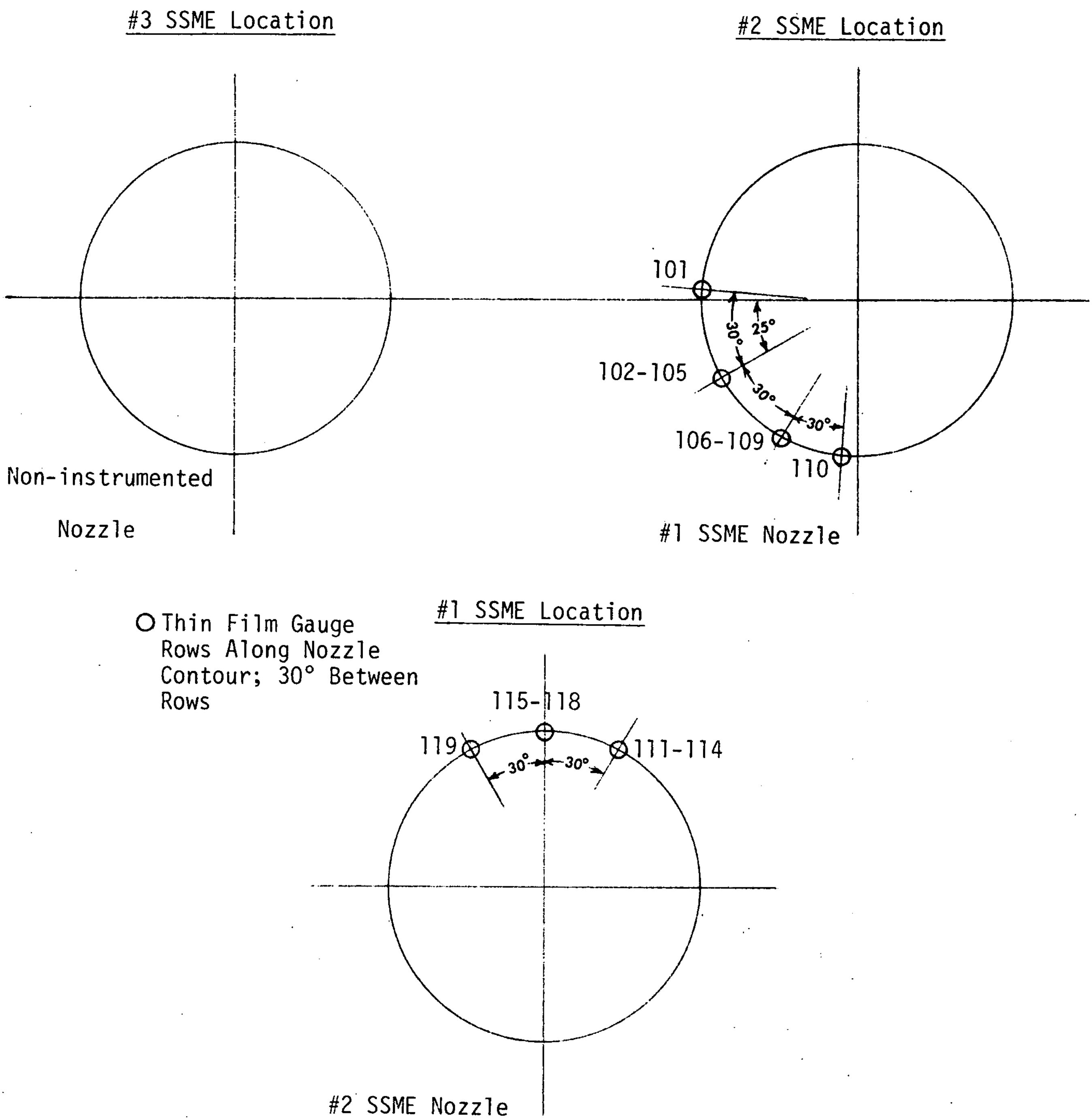

a. Runs 9-32 (w/o GTP)
Figure 14. SSME Nozzle Position and Orientation

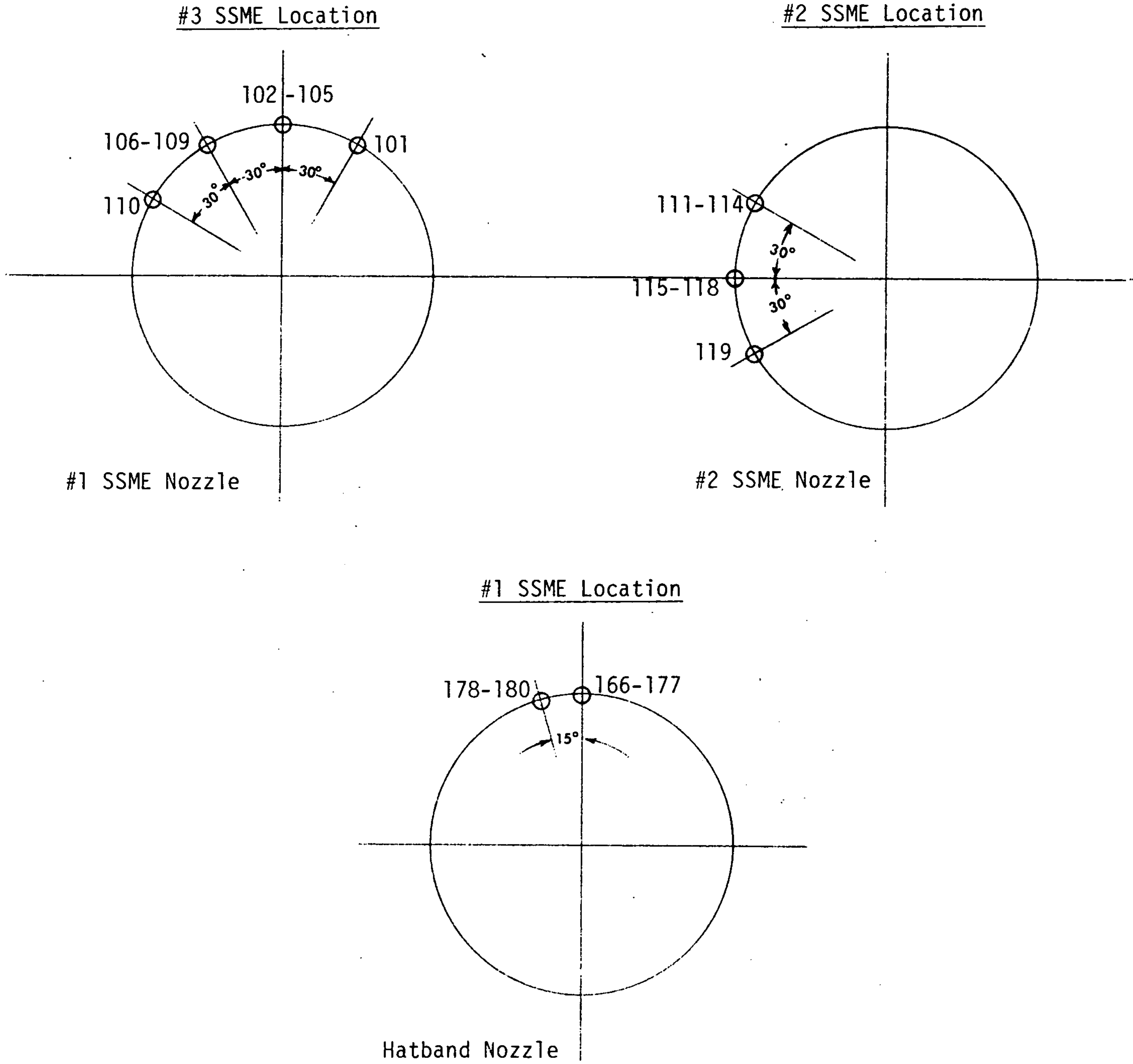

b. Runs 33-41 (w/GTP)
Figure 14. Concluded.

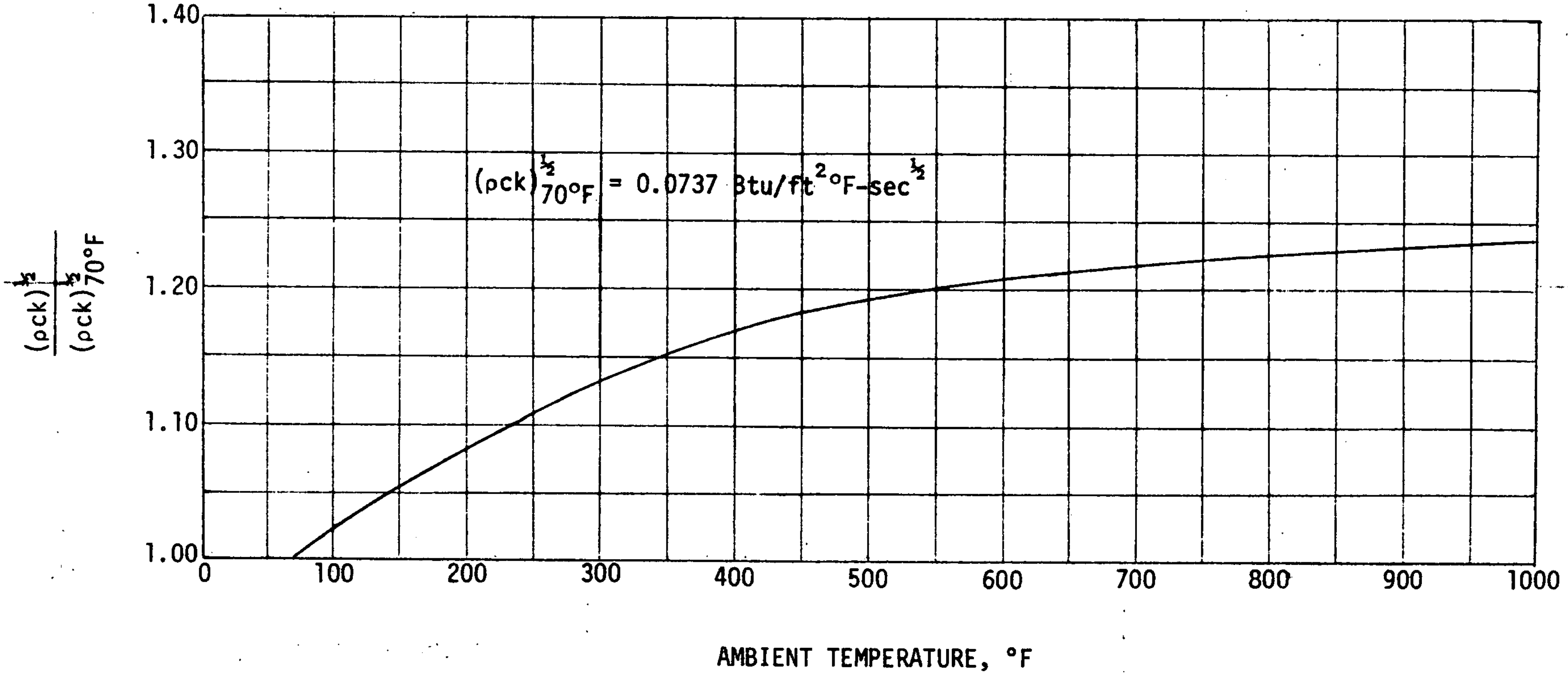

Figure 15. Variation of Thin-Film Gauge Substrate (#7740 Pyrex) Properties with Temperature.

APPENDIX A

SOURCE DATA REFERENCES

SOURCE DATA REFERENCES

DATA	ROCKWELL INTERNATIONAL SHUTTLE AERO SCIENCES DEPARTMENT	
Tabulated	Wind Tunnel Operations Group (R. S. Crowder, Supervisor)	Aeroheating Group (M. H. Harthun, Supervisor)
Plot		Aeroheating Group (M. H. Harthun, Supervisor)

APPENDIX B

GAS RECOVERY TEMPERATURES

STEADY STATE DATA

ND - NO DATA

DNC - DID NOT CONVERGE

Alt. Kft.	Run #	Pos 752	Pos 753	Pos 754	Pos 756	Pos 757	Pos 758	Pos 759	Comments
120	33	ND	1073	1002					
130	34	1289	1043	1050					2nd Stage Config.
120	35	1277	719	1084					
130	36	1365	711	1044					
120	37	ND	ND	823	578	510	ND	(~340) DNC	
130	38	372	573	795	518	471	558	395	
120	39	(~400) DNC	558	728	529	419	550	ND	
120	40	363	524	701	594	513	611	ND	
130	41	402	561	822	586	542	681	ND	

Figure C-3 Test IH-83 Gas Recovery Temperature (°K) Data

STEADY STATE DATA

ND - NO DATA

DNC - DID NOT CONVERGE

Alt. Kft.	Run #	Pos 752	Pos 753	Pos 754	Pos 756	Pos 757	Pos 758	Pos 759	Comments
120	33	ND	4.24-03	5.85-03					2nd Stage Config. (Runs 33–36)
130	34	3.44-03	5.83-03	2.38-03					
120	35	2.88-03	1.26-02	4.45-03					
130	36	2.46-03	1.19-02	5.82-03					
120	37	ND	ND	5.23-03	1.03-02	4.67-03	ND	DNC	
130	38	1.52-01	1.06-02	5.16-03	7.58-03	4.73-03	6.95-03	2.53-03	
120	39	DNC	1.14-02	6.51-03	1.25-02	2.29-02	7.98-03	ND	
120	40	8.52-03	2.04-02	5.75-03	8.33-03	5.93-03	4.55-03	ND	
130	41	1.37-01	2.19-02	6.01-03	1.19-02	6.38-03	3.99-03	ND	

Figure C-4 Test IH-83 Heat Transfer Coefficient (Cal/cm^2-sec-°K) Data

(EXAMPLE)

TIME HISTORY DATA

JOB NO 1KED33451033 PAGE 9

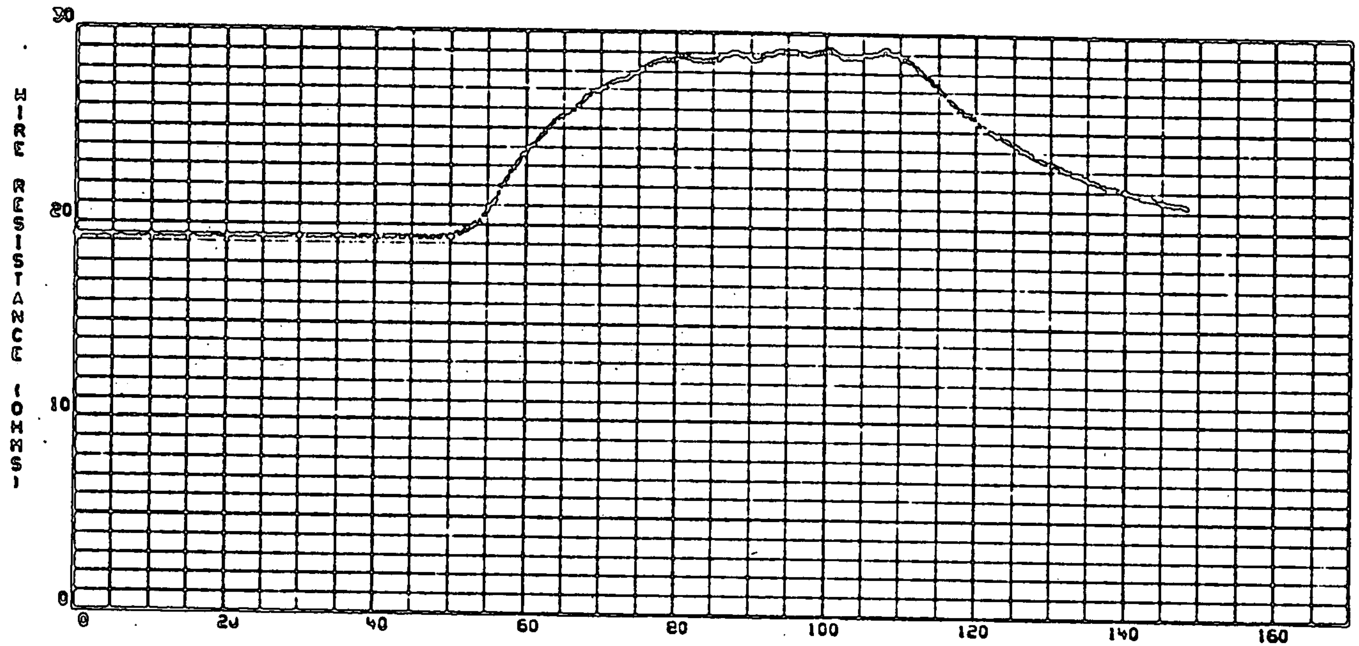

IH-83 RUN 33 POS 754 WIRE RESISTANCE VS TIME (MSEC)

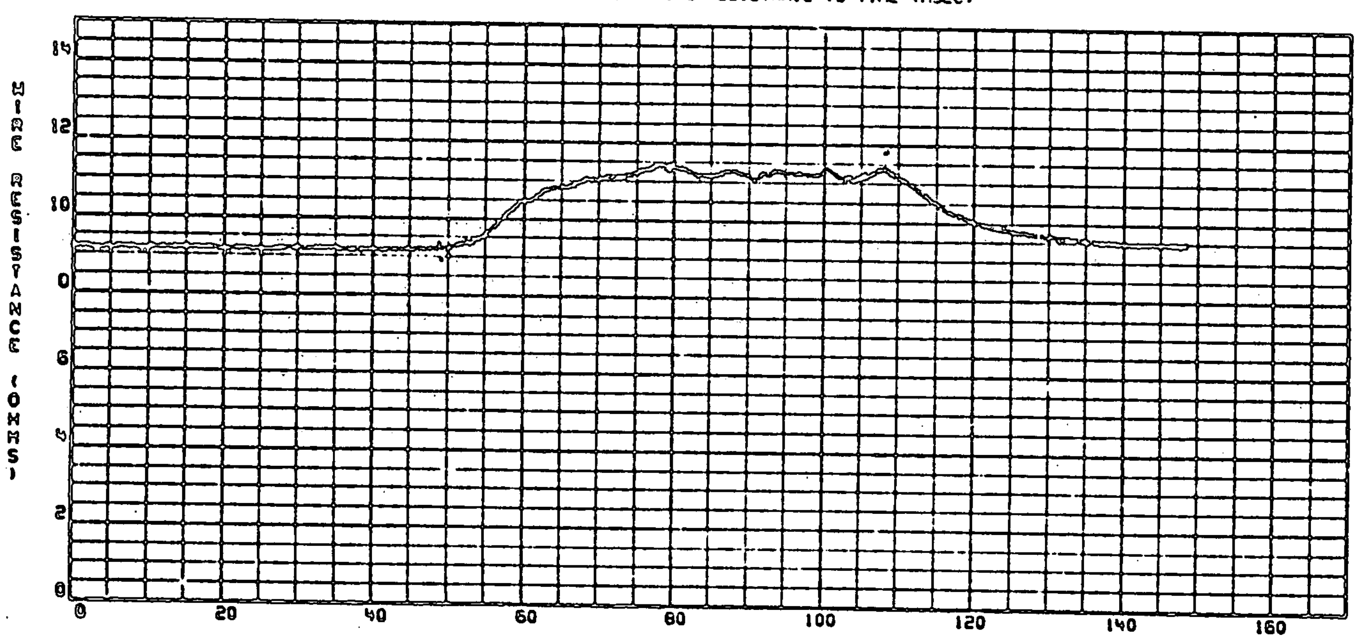

IH-93 RUN 33 POS 754 WIRE RESISTANCE VS TIME (MSEC)

(EXAMPLE)

TIME HISTORY DATA

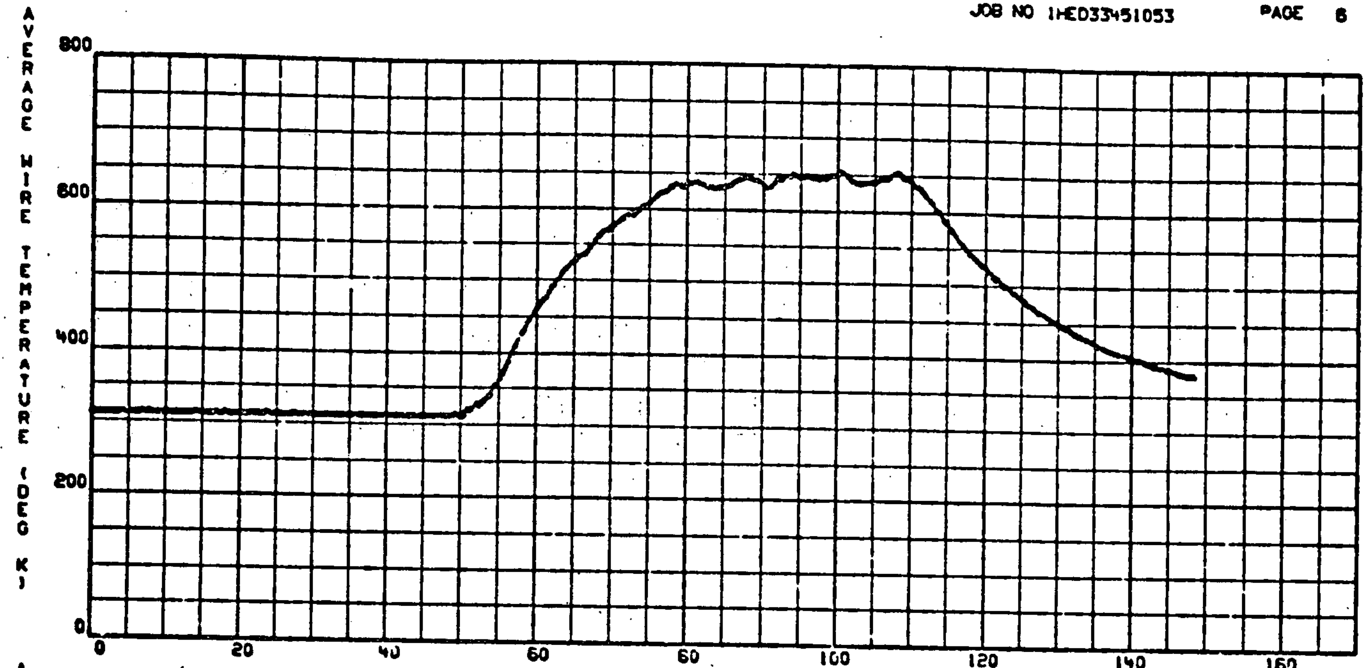

1H-83 RUN 33 POS 754 WIRE TEMPERATURE VS TIME (MSEC)

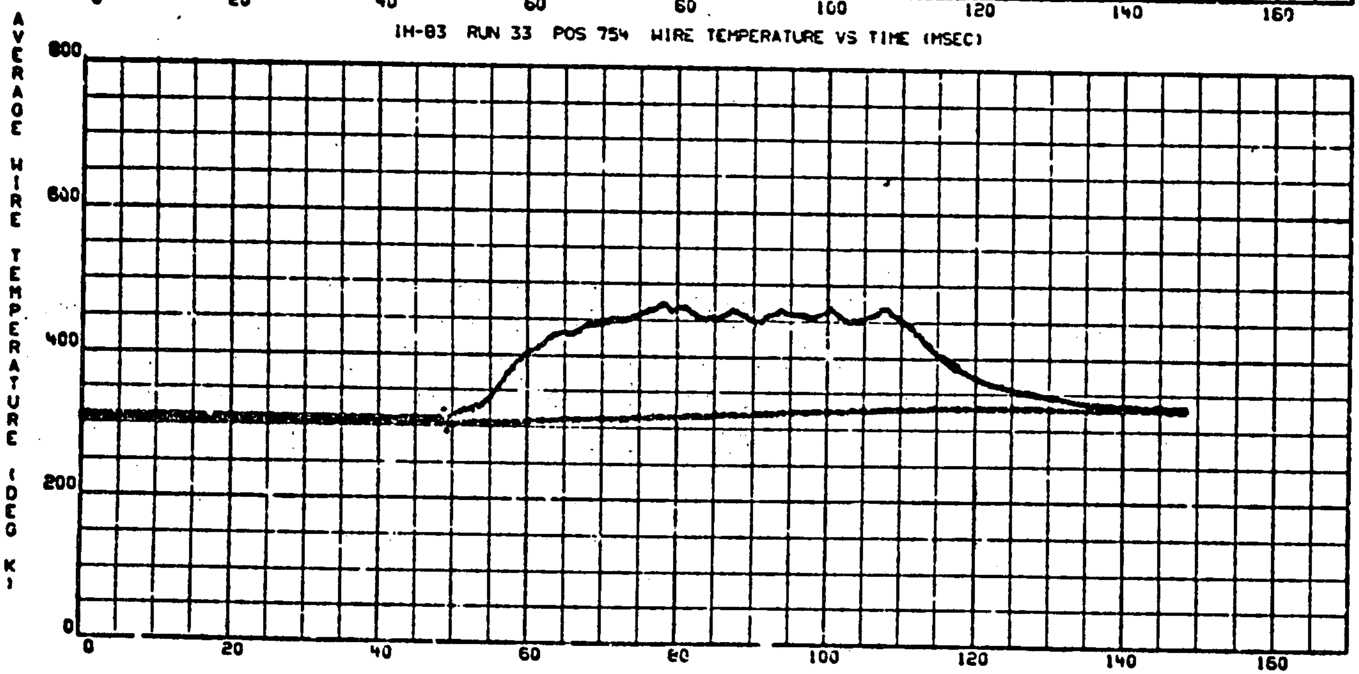

1H-83 RUN 33 POS 754 WIRE TEMPERATURE VS TIME (MSEC)

(EXAMPLE)

TIME HISTORY DATA

JOB NO 1HED33451053 PAGE 7

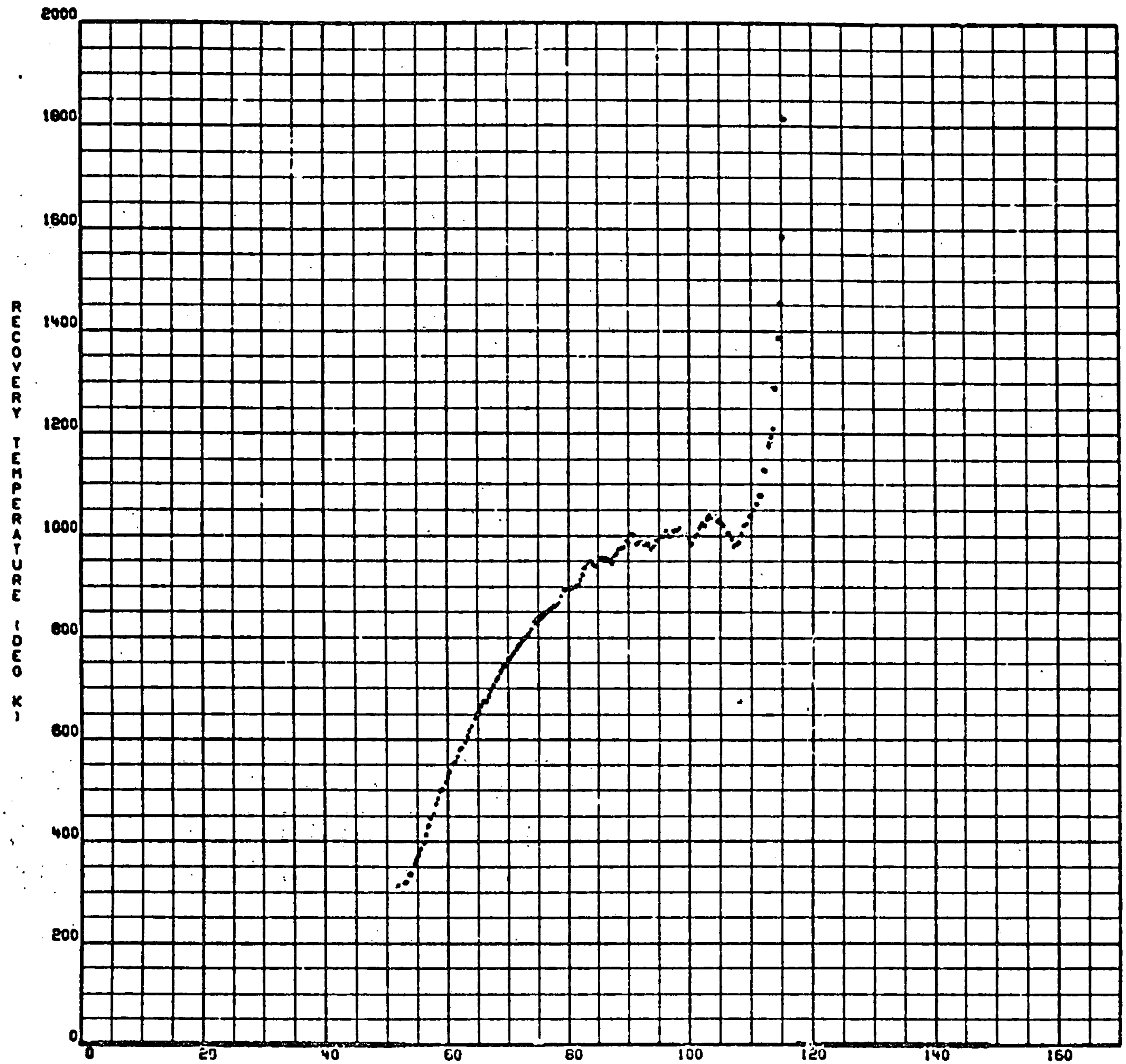

1H-83 RUN 33 POS 754 RECOVERY TEMPERATURE VS TIME (MSEC)

(EXAMPLE)

TIME HISTORY DATA

JOB NO 1HE033451053 PAGE 8

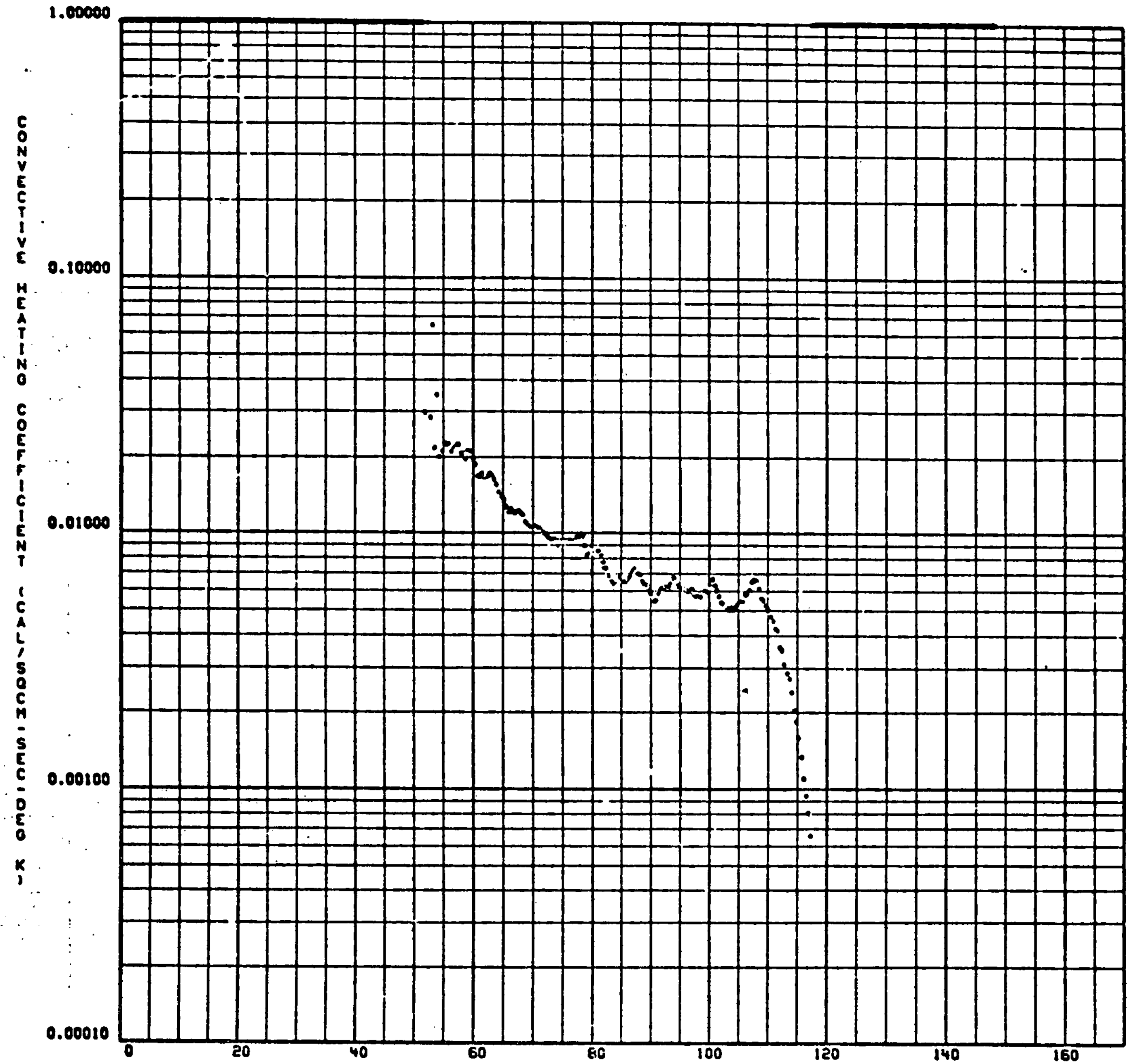

IH-83 RUN 33 POS 754 CONVECTIVE HEATING COEFFICIENT VS TIME (MSEC)

APPENDIX C

REFERENCE PRESSURE DATA

REFERENCE BASE PRESSURES (0° yaw) (psia)

Mach	2.2	2.5	2.9	3.5
Altitude	60K	70K	80K	120K
Config.	OTS	OTS	OTS	OTS
α	-5	-5	-5	+5
ψ	0	0	0	0
501	.4932	.2907	.1753	.0249
502	.5151	.3257	.2476	.0430
503	.2414	.1434	.0728	.0185
504	.2069	.1150	.0615	.0130
505	.1956	.1056	.0549	.0125
506	.2007	.1108	.0584	.0127
507	.2161	.1153	.0571	.0127
508	.2073	.1123	.0590	.0125
509	.2107	.1140	.0604	.0122
510	.2206	.1388	.0886	.0127
511	.2066	.1100	.0576	.0115
512	.2002	.1085	.0576	.0122
513	.2191	.1223	.0633	.0131
514	.1937	.1132	.0562	.0156
515	.1894	.1067	.0554	.0153
516	.1819	.1105	.0525	.0173

REFERENCE BASE PRESSURES (+5° yaw) (psia)

Mach	2.9	3.5	3.5	3.5	3.5	3.5
Altitude	80K	100K	120K	120K	130K	130K
Config.	OTS	OTS	OTS	OTS	OTS	OTS
α	0	0	0	+5	0	+5
ψ	+5	+5	+5	+5	+5	+5
501	.1702	.0801	.0335	.0282	.0232	.0196
502	.2140	.1427	.0675	.0609	.0460	.0421
503	.0717	.0288	.0127	.0157	.00983	.0116
504	.0551	.0202	.00956	.0100	.00886	.00908
505	.0522	.0218	.0101	.0102	.00935	.00892
506	.0544	.0216	.0100	.0108	.00959	.00908
507	.0542	.0192	.00908	.00969	.00886	.00859
508	.0532	.0200	.0106	.0107	.00886	.00892
509	.0529	.0197	.00883	.00936	.00814	.00827
510	.0537	.0254	.0100	.00937	.00886	.00811
511	.0524	.0202	.00884	.00936	.00862	.00811
512	.0516	.0198	.00859	.00904	.00838	.00762
513	.0550	,0208	.00908	.0102	.00838	.00908
514	.0641	.0252	.0103	.0139	.00935	.0107
515	.0554	.0208	.0110	.0129	.00984	.0104
516	.0606	.0247	.0137	.0155	.0128	.0128

REFERENCE BASE PRESSURES (-5° yaw) (psia)

Mach	2.9	3.5	3.5	3.5	3.5	3.5
Altitude	80K	100K	120K	120K	130K	130K
Config.	OTS	OTS	OTS	OTS	OTS	OTS
α	0	0	0	+5	0	+5
ψ	-5	-5	-5	-5	-5	-5
501	.1209	.0512	.0230	.0210	.0171	.0164
502	.1360	.0593	.0315	.0323	.0625	.0430
503	.0792	.0315	.0135	.0169	.00960	.0117
504	.0539	.0204	.0109	.0125	.00742	.00861
505	.0475	.0194	.0107	.0116	.00669	.00812
506	.0531	.0199	.0106	.0123	.00790	.00981
507	.0501	.0194	.0101	.0120	.00718	.00885
508	.0516	.0201	.0109	.0109	.00887	.00981
509	.0538	.0209	.00992	.0113	.00645	.00812
510	.0545	.0223	.0114	.0111	.00548	.00812
511	.0514	.0196	.0102	.0113	.00645	.00812
512	.0505	.0196	.0109	.0111	.00573	.00812
513	.0534	.0201	.0114	.0121	.00693	.00885
514	.0635	.0262	.0119	.0152	.00887	.0110
515	.0638	.0228	.0126	.0154	.00863	.0105
516	.0567	.0245	.0140	.0172	.0108	.0127

REFERENCE BASE PRESSURES (±11° yaw) (psia)

Mach	3.5	3.5	3.5	3.5
Altitude	120K	130K	120K	130K
Config.	OTS	OTS	OTS	OTS
α	0	0	0	0
ψ	+11	+11	-11	-11
501	.0532	.0358	.0251	.0205
502	.0732	.0569	.0189	.0215
503	.0147	.0109	.0136	.0103
504	.0121	.00994	.00972	.00882
505	.0137	.0111	.00940	.00834
506	.0121	.0106	.0103	.00915
507	.0123	.0102	.0101	.00898
508	.0123	.0104	.0105	.00962
509	.0113	.00896	.00922	.00818
510	.0108	.00872	.00777	.00689
511	.0121	.00993	.00922	.00834
512	.0118	.00968	.00874	.00753
513	.0121	.0101	.00906	.00834
514	.0132	.0111	.0131	.00962
515	.0142	.0108	.0131	.0103
516	.0169	.0137	.0152	.0122

REFERENCE BASE PRESSURES (±7° yaw) (psia)

Mach	3.5	3.5	3.5	3.5
Altitude	120K	130K	120K	130K
Config.	OT	OT	OT	OT
α	0	0	0	0
ψ	+7	+7	-7	-7
501	.0421	.0297	.0244	.0214
502	.0721	.1026	.0290	.0549
503	.0123	.00922	.00928	.00944
504	.0104	.00922	.00912	.00796
505	.0115	.00946	.00815	.00716
506	.0113	.00922	.00960	.00812
507	.00989	.00898	.00847	.00764
508	.0105	.00991	.00960	.00944
509	.00957	.00777	.00815	.00699
510	.0105	.00874	.00734	.00603
511	.0102	.00850	.00815	.00716
512	.0101	.00825	.00817	.00651
513	.0102	.00850	.00890	.00748
514	.00957	.00801	.00831	.00716
515	.00957	.00825	.00815	.00726
516	.00957	.00777	.00831	.00651